



Virginia Commonwealth University  
VCU Scholars Compass

---

Theses and Dissertations

Graduate School


---

2020

**Recovery from visual dysfunction following mild traumatic brain injury is associated with adaptive reorganization of retinal inputs to lateral geniculate nucleus in the mouse model utilizing central fluid percussion injury.**

Vishal C. Patel  
*Virginia Commonwealth University*

Follow this and additional works at: <https://scholarscompass.vcu.edu/etd>

 Part of the [Nervous System Commons](#), [Nervous System Diseases Commons](#), and the [Neurosciences Commons](#)

© The Author

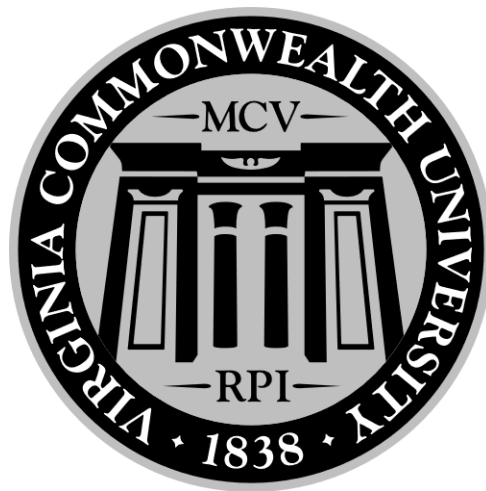
---

Downloaded from

<https://scholarscompass.vcu.edu/etd/6430>

This Dissertation is brought to you for free and open access by the Graduate School at VCU Scholars Compass. It has been accepted for inclusion in Theses and Dissertations by an authorized administrator of VCU Scholars Compass. For more information, please contact [libcompass@vcu.edu](mailto:libcompass@vcu.edu).

**Recovery from visual dysfunction following mild traumatic brain injury is associated with adaptive reorganization of retinal inputs to lateral geniculate nucleus in the mouse model utilizing central fluid percussion injury.**



Author: **Vishal C. Patel**

Lehigh University – Bachelor of Science 2006

Drexel University College of Medicine – Doctor of Medicine 2011

Thesis Advisor: **John T. Povlishock PhD**

Chairman

Department of Anatomy and Neurobiology

A dissertation submitted in partial fulfillment of the requirements for the degree of Doctor of Philosophy  
at Virginia Commonwealth University

Virginia Commonwealth University

Richmond, Virginia

August 2020

### **Acknowledgements**

The author would like to thank the many people who helped me with this work, both professionally and personally. My advisor, Dr. John Povlishock for continuing to support me in my efforts and providing me with the resources to succeed. Dr. Thomas Krahe who guided my understanding of visual neuroscience that became the basis for this work. Dr. Robert Scott Graham for giving the opportunity to complete my work while continuing in the neurosurgery residency program. Dr. Kathryn Holloway for giving me the opportunity at the McGuire VA to gain exposure to neurosurgery while providing the general surgery service with in-house coverage. My committee members Dr. William C. Broaddus, Dr. Kimberle Jacobs, Dr. Dong Sun, and Dr. Raymond Colello who provided guidance and reassurance where needed. My program director Dr. John Bigbee for his support and guidance through the entire process. Sue Walker and Lynn Davis who provided their help and logistic support in the laboratory. Dr. Christopher Jurgens and Dr. Michal Vascak who provided their friendship and guidance in the lab. My friends and family, my residency colleagues, and last but always first, my wife Dr. Bhavita Patel, who have all provided me with emotional support and encouragement throughout these years.

**Abstract**

Traumatic brain injury (TBI) is a leading cause of morbidity and mortality nationwide. Prevalence of mild TBI (mTBI) vastly outnumbers more severe forms however the associated morbidity has only recently gained public attention. Visual dysfunction is a significant component of mTBI associated morbidity with recovery of function linked with improvement in global outcomes. Examination of sensory and motor pathways in other brain injury paradigms support that recovery is largely dependent on adaptive plasticity of remaining connections. Current examinations of visual function recovery following mTBI is limited to identifying evidence for recovery and objective evidence for adaptive plasticity is limited. Therefore, to understand the mechanisms behind visual recovery in mTBI, we utilize a mouse model to examine the changes in the downstream target of retinal ganglion cells (RGC) in the formed vision pathway, the lateral geniculate nucleus (LGN). Using techniques designed to identify structural changes as well as electrophysiologic connectivity we aimed to identify if deafferentation due to experimental mTBI is met with adaptive structural and electrophysiologic reorganization of inputs to LGN relay cells, to determine if they may contribute to recovery of vision over time. Examination of ensuing deafferentation in LGN was performed using a combination of anterograde tract tracing with cholera toxin B conjugated fluorescent probes, immunohistochemistry targeting retinal ganglion cell axon terminals, and a transgenic mouse in which a subpopulation of retinal ganglion cells are labelled with green fluorescent protein. Our studies were designed to capture structural reorganization in specific subpopulations of retinal ganglion cells and determine if ensuing reorganization violated projection patterns established during normal development and refinement of the retinal geniculate pathway. Additionally, our studies examined the electrophysiologic responses of relay neurons in the lateral geniculate nucleus to stimulation of the optic tract as a function of time following injury. Using ex-vivo patch clamp recording of LGN relay neurons, we examined responses of these cells to stimulation of the optic tract following mTBI. Our findings demonstrated intact short-term depression at the retinal geniculate synapse following injury, which is a mechanism through which LGN relay neurons establish functional connectivity from retinal inputs. This

innate mechanism of short-term plasticity likely uncovers latent connectivity between the remaining retinal inputs and LGN relay neurons to provide new connectivity for functional recovery. These studies support the premise that recovery of function in the visual axis following mild TBI is dependent on adaptive structural and electrophysiologic reorganization within the lateral geniculate nucleus.

**Table of Contents**

	Page
List of abbreviations	6
Vita	8
Chapter 1 – Introduction	9
Chapter 2 – Adaptive Reorganization of Retinogeniculate Axon Terminals in Dorsal Lateral Geniculate Nucleus Following Experimental Mild Traumatic Brain Injury	31
Chapter 2B – Supplemental Evidence Regarding Adaptive Plasticity within the Dorsal Shell of dLGN using DRD4-GFP transgenic mouse.	64
Chapter 3 – Electrophysiologic connectivity between retinogeniculate projections and dLGN relay neurons following mTBI induced reorganization demonstrates intact fiber volley and normal paired-pulse depression across time points.	72
Chapter 4 – Discussion – Review of data	88
Bibliography	102

**List of abbreviations**

TBI	Traumatic brain injury
mTBI	Mild traumatic brain injury
TAI	Traumatic axonal injury
DAI	Diffuse axonal injury
MRI	Magnetic resonance imaging
DTI	Diffusion tensor magnetic resonance imaging
fMRI	Functional MRI
BOLD	Blood oxygenation level-dependent
DMN	Default mode network
GABA	$\gamma$ -aminobutyric acid
TMS	Transcranial magnetic stimulation
MEP	Motor evoked potential
rCBF	regional cerebral blood flow
PET	Positron emission tomography
EMG	Electromyography
bic	Bicuculine methobromide
LPZ	Lesion projection zone
GFP	Green fluorescent protein
Thy-1	Thymocyte differentiation antigen 1
AAV	adenoviral vector
RGC	Retinal ganglion cell
LGN	Lateral geniculate nucleus
dLGN	Dorsal lateral geniculate nucleus
vLGN	Ventral lateral geniculate nucleus
DSGC	Directionally selective retinal ganglion cells

TG	Tectogeniculate projections
SC	Superior colliculus
VEP	Visually evoked potential
cFPI	Central fluid percussion injury
CTB	Recombinant cholera toxin subunit $\beta$
VGLUT1	Vesicular glutamate transporter 1
VGLUT2	Vesicular glutamate transporter 2
ATM	Atmospheres
PBS	Phosphate buffered saline
DAPI	4',6-diamidino-2-phenylindole
UV LED	Ultraviolet light emitting diode
EtOH	Ethanol
EM	Electron microscopy
AP	Anterior-posterior
ANOVA	Analysis of variance
EGFP	Enhanced green fluorescent protein
DRD4	Dopamine receptor D4
BAC	Bacterial artificial chromosome
qPCR	Quantitative polymerase chain reaction
APP	Amyloid precursor protein
AMPA	$\alpha$ -amino-3-hydroxy-5-methyl-4-isoxazolepropionic acid
NMDA	N-Methyl-d-aspartate
EPSC	Excitatory post-synaptic current
aCSF	Artificial cerebrospinal fluid
SEM	Standard error mean
CNS	Central nervous system



### **Vita**

Vishal Chandulal Patel was born June 17, 1985 in London, UK. He moved to Brooklyn, NY in 1990 and graduated with honors from Stuyvesant High School in New York City before matriculating at Lehigh University as part of the combined BS/MD program with Drexel University College of Medicine in 2003. He graduated Lehigh University in 2006 with honors and Bachelor of Science in molecular biology before graduating with his Doctor of Medicine in 2011. He completed his internship and PGY2 in general surgery at Virginia Commonwealth University Hospital in 2013 before joining the graduate neuroscience program at the School of Medicine the same year. He joined the neurosurgery residency program also at VCU in 2017 where he continues his training in both neuroscience and neurosurgery.

## Chapter 1 - Introduction

### 1.1 Traumatic Brain Injury Epidemiology and Impact

Traumatic brain injury (TBI) describes the incidence of external mechanical force on the brain that induces a temporary or permanent alteration in brain function (Menon, Schwab, Wright, & Maas, 2010). The external force may be blunt force trauma to the head, blast overpressure wave, or rapid acceleration and deceleration that is linear or rotational (Thurman, Alverson, & Dunn, 1999). Evidence of brain pathology following TBI can be demonstrated using laboratory studies and radiographic or visual examination (CDC, *Traumatic Brain Injury—Injury Center*, 2015, <http://www.cdc.gov/traumaticbraininjury/>). The severity of brain injury can vary in response to these forces with mild injury producing temporary changes in cognitive and executive function to severe injury resulting in disability and death.

An average of 1.4 to 1.7 million TBI patients are seen by emergency departments annually in the United States with many sources estimating the true incidence of TBI to be more than twice this rate (Corrigan, Selassie, & Orman, 2010; Faul, Xu, Wald, Coronado, & Dellinger, 2010; Finkelstein, Corso, & Miller, 2006; Langlois, Rutland-Brown, & Wald, 2006; Leibson et al., 2011; McMahon et al., 2014). Brain injury accounts for approximately a third of all injury-related deaths in the United States, with adolescents and the elderly at greatest risk (Faul et al., 2010; Thurman et al., 1999). The most common cause of TBI in developed countries continues to be motor vehicle collisions but as the elderly population in these countries continues to grow, fall injury has increased at a dramatic rate and in the United States, has overtaken motor vehicle collision as the most common cause of TBI (Roozenbeek, Maas, & Menon, 2013; Salottolo, Carrick, Levy, & Morgan, 2017). The elderly are also particularly vulnerable to TBI related morbidity and mortality and thus represent a growing high-risk population (Thompson & McCormick, 2006).

Despite advances in TBI treatment paradigm in the United States, improvements in outcomes have predominantly occurred within the patient population suffering from moderate to severe TBI. Most of these outcome improvements are due to prevention of secondary ischemic damage by controlling brain edema following the initial insult (Eker, Asgeirsson, Grände, Schalén, & Nordström, 1998; Ghajar, 2000; Murray et al., 2007; Robertson, Valadka, & Hannay, 1999). Mild TBI (mTBI), however, does not present with these clinically modifiable cofactors (Jünger, Newell, Grant, & Avellino, 1997; Strebel, Lam, Matta, & Newell, 1997). Epidemiologic studies estimate that up to 80% of individuals with brain injury fall into the mild TBI category, highlighting the importance of understanding the impact and pathology involved (Bazarian, Blyth, & Cimpello, 2006; Cassidy, Carroll, Peloso, & Borg, 2004).

Mild TBI is a complex and heterogeneous disease process defined to be comprised by the following clinical criteria; alteration of consciousness less than 30 minutes duration or post-traumatic amnesia less than 24 hrs, Glasgow Coma Scale score of 13-15, absence of skull fractures, and non-focal neurologic exam (Cushman, Agarwal, & Fabian, 2001; T. Kay, Newman, Cavallo, & Ezrachi, 1992; Vos, Battistin, & Birbamer, 2002). This definition encompasses most of the literature on mTBI and focuses on the patient population that does not require medical intensive care or hospitalization (Belanger & Kretzmer, 2009). Symptoms in mTBI are not life threatening. Many patients do not seek medical attention or are discharged home soon after medical examination, however, patients do experience short term disability which can have profound and lasting effects (Humphreys, Wood, Phillips, & Macey, 2013; King, 1997; Rimel, Giordani, Barth, Boll, & Jane, 1981).

Symptoms in mTBI can vary greatly. Patients may describe a broad range of complaints including fatigue, restlessness, sensory changes that include vision, balance, and hearing, sleep

disturbance, mood disorders, and cognitive or memory dysfunction (Rosenbaum & Lipton, 2012). Most of these symptoms resolve with time, however, there are long standing quality of life changes which can occur despite resolution of symptoms (King, 1997; Rimel et al., 1981). Previous reports suggest a minority of patients (5-15%) do not recover or have incomplete recovery up to a year after injury, however, more a recent review suggests that mTBI may be associated with some degree of chronic cognitive impairment in up to 85% of individuals long after injury (Bazarian et al., 2006; Cassidy et al., 2004; Corrigan et al., 2010; Dean, Sato, Vieira, McNamara, & Sterr, 2015; McInnes, Friesen, MacKenzie, Westwood, & Boe, 2017).

The current consensus on treatment for mTBI recommends patient education, graduated return to activity, medication to treat associated headaches or resulting depression, and/or adjuvant therapies such as physical or cognitive therapy (Mittenberg, Canary, Condit, & Patton, 2010; Schneider et al., 2013). Unfortunately, very few studies provide strong evidence for any intervention modifying outcomes in a significant manner (Andersson, Emanuelson, Björklund, & Stålhammar, 2007; Borg, Holm, Peloso, & Cassidy, 2004; Comper, Bisschop, Carnide, & Tricco, 2005). It is clear from both past and recent literature that mTBI impacts a large and growing population and warrants continued investigation. The uncertainty regarding chronic persistence of symptoms highlights the importance of studying both injury and recovery mechanisms associated with mTBI in further detail. The prevalence and inability to improve outcomes in mTBI has led multiple authors, to describe mTBI as a ‘silent’ or ‘hidden’ epidemic across the last 30 years (Feinstein & Rapoport, 2000; Gordon, Brown, Sliwinski, & Patti, 1998; McMahon et al., 2014).

## **1.2 Anatomic source of clinical symptoms in mTBI.**

The human brain has a low modulus of elasticity and is easily deformable in response to external force. The forces imparted in trauma can induce a high degree of shear and strain forces within the white and grey matter of the brain (Bayly et al., 2005; Shabet, Christoforou, Zatlun, Genin, & Bayly, 2008). These forces produce widespread brain pathology impacting all the structural components of the brain including neuroglia, extracellular matrix, and vascular structures, but impact neuronal axons most dramatically (Andriessen, Jacobs, & Vos, 2010; Barkhoudarian, Hovda, & Giza, 2011; Hadanny & Efrati, 2016). The heterogeneous neuropathology is associated with broad long-term consequences but the most significant pathology in mild TBI thought to impart clinical manifestations is traumatic axonal injury (McGinn & Povlishock, 2016; J. Povlishock, 1992, 1993; J. Povlishock, Becker, Cheng, & Vaughan, 1983; John T Povlishock & Katz, 2005; Wolf, Stys, Lusardi, Meaney, & Smith, 2001).

Initial efforts focused on study of axon integrity in TBI however anatomic cohorts were small and represented older individuals (Blumbergs et al., 1994; Oppenheimer, 1968). Experimental studies in animal models have yielded significant information to help us understand the pathology involved in traumatic axonal injury. Over several decades of study in both human and animal models utilizing rodents, cats, and pigs, we have learned that despite the diffuse force of injury, axonal injury occurs in a scattered focal pattern throughout the brain (Blumbergs et al., 1994; Smith, Hicks, & Povlishock, 2013; Stone, Singleton, & Povlishock, 2001). Injured axons demonstrate structural perturbation which leads to focal swelling over a period of several hours prior to disconnection from the downstream segment (Christman, Grady, Walker, Holloway, & Povlishock, 1994; J. Povlishock & Christman, 1995). Downstream segments then undergo Wallerian degeneration. Both clinical studies and animal models have demonstrated that the degeneration leading to disconnection may start in the first few hours following injury but may potentially

progress over the course of several months following injury (J. Povlishock, 1992; John T Povlishock & Katz, 2005).

Importantly, the loss of these downstream axons means that all the distal axon terminals are lost as inputs to their post-synaptic targets. Each neuron in the human brain is estimated to synapse with up to 10,000 other neurons (Schüz & Palm, 1989). The consequence of the deafferentation is more apparent when comparing the cortical neuropil between injured and uninjured brains. Using magnetic resonance imaging (MRI) to examine the brain in vivo, there is persistent thinning and decreased functional as well as structural connectivity following mTBI even when accounting for age (Cohen et al., 2007; Dean et al., 2015; Govindarajan et al., 2016). MRI is an imaging technique which can build a three-dimensional model of soft tissue using the differences in signal attenuation created by hydrogen molecules in water, lipids, and proteins when placed in a uniform magnetic field and struck by an orthogonal radiofrequency burst. The change in attenuation of radio frequency signal is measured and fast Fourier transformation used to isolate the signal for individual voxels in a 3D space to create a model representation of the brain.

Clinical studies utilized diffusion tensor magnetic resonance imaging (DTI) as well as functional magnetic resonance imaging (fMRI) to study correlates of white matter injury burden also demonstrate axonal injury following mTBI. Diffusion tensor MRI is an MRI technique which measures diffusion restriction of water molecules in vivo to estimate the orientation and anisotropy of brain white matter (Shenton et al., 2012). The lipid bilayer of axons restricts diffusion of water molecules to the longitudinal axis of the axon and bundles of axons in white matter tracts typically run parallel. The technique allows quantitative analysis of a white matter tract along a particular axis and assign a scalar value between 0 (unrestricted diffusion) and 1

which denotes diffusion is restricted in a specific direction. Mean diffusivity of water molecules is another technique of quantification which summarizes the average diffusion in each direction for every voxel in an MRI image set. Increase in mean diffusivity or decrease in fractional anisotropy in white matter tracts correlated with TBI severity.(Ewing-Cobbs, Hasan, Prasad, Kramer, & Bachevalier, 2006; Kumar et al., 2009; Lipton et al., 2008; Wozniak et al., 2007).

Importantly, clinical manifestations of mild TBI were specifically confirmed to be associated with disruption in white matter integrity (Kraus et al., 2007; Messé, Caplain, & Péligrini-Issac, 2012; Scheid, Walther, Guthke, Preul, & Cramon, 2006; Zhang et al., 2010)). Severity of chronic memory deficits after TBI have been correlated with degree of in structural integrity of the fornix, a white matter tract which connects the right and left hippocampi (Kinnunen et al., 2010; Sugiyama et al., 2007). Impaired executive function after mTBI was also linked to DAI in the dorsolateral prefrontal cortex as measured using DTI (Lipton et al., 2008).

While many of the studies mentioned study white matter tracts, axon pathology in mTBI is not limited to white matter. Mounting evidence suggests that cortico-cortical axonal injury is an important contributor to clinical symptoms as well. fMRI studies over the last several years have demonstrated mTBI associated with grey matter changes in activity as well as functional connectivity(McDonald, Saykin, & McAllister, 2012). Functional MRI studies in mTBI using the blood oxygenation level-dependent (BOLD) signal to probe the spontaneous coherence of activity in different regions of the brain in the resting state, colloquially referred to as resting state networks (RSN), have been instrumental in helping understand some of the consequences of axonal injury in mTBI (Zhang et al., 2010)). Li et al. demonstrated alteration following mTBI in the default mode network (DMN), a resting state network responsible in part for intrinsic awareness (Li et al., 2011). The default mode network encompasses the posterior and anterior

cortical midline structures, with major hubs being located in the posterior cingulate cortex and precuneus, the medial prefrontal cortex, and the angular gyrus (Andrews-Hanna, Saxe, & Yarkoni, 2014; B. Johnson et al., 2012).

Predictive modeling of network dysfunction in mTBI support previous clinical and animal studies which examine if disruption of inhibitory and excitatory communication within local cortical networks of the grey matter contributes to global network dysfunction (Sharp, Scott, & Leech, 2014; Wolf & Koch, 2016). Animal studies of mTBI have demonstrated that loss of inputs to cortical pyramidal cells can impact their response to remaining inputs (Greer, Povlishock, & Jacobs, 2012; Hånell, Greer, McGinn, & Povlishock, 2015; Vascak, Jin, Jacobs, & Povlishock, 2017). Importantly, the loss of both excitatory and inhibitory inputs to cortical pyramidal cells following diffuse axonal injury results in axon initial segment structural modification which in turn modifies pyramidal cell firing patterns (Greer et al., 2012; Vascak, Sun, Baer, Jacobs, & Povlishock, 2017). Inhibitory inputs within the cortex predominate from GABAergic interneurons which despite remaining local, have been demonstrated to be susceptible to diffuse axonal injury (Vascak, Jin, et al., 2017). Traumatic axonal injury in mTBI thus causes disruption of both local cortical circuits and global connectivity to produce clinical symptoms in mTBI.

### **1.3 Consequences of deafferentation following injury.**

Axon loss in traumatic diffuse axonal injury is well established to result in loss of input to downstream neurons. Through recent works, we understand changes in electrophysiologic properties of downstream neurons occur as a result of loss of inputs, both excitatory and inhibitory. Studies examining cortex, deep grey structures, as well as the retina, have all demonstrated that once an injured axon undergoes Wallerian degeneration, the remaining soma



of the neuron to which the axon is lost, atrophies and fails to mount a successful repair response (Greer, McGinn, & Povlishock, 2011; Lifshitz, Kelley, & Povlishock, 2007; J. Wang, Hamm, & Povlishock, 2011).

Clinically, most cases of mTBI are thought to be associated with recovery. Indirect data utilizing functional MRI and MRI based tractography (diffuse tensor MRI) has established that improvement in cognitive decline and memory following mTBI correlate with improvement in functional connectivity and recovery of fractional anisotropy as far out as 6 months following injury related symptoms (Arfanakis et al., 2002; Bharath et al., 2015). While we understand that endogenous reparative processes maintain trophic support following injury, in the diffusely injured brain, recovery must be associated with a response to circuit disruption (Christman, Jr., Walker, & Povlishock, 1997; Emery, Royo, Fischer, Saatman, & McIntosh, 2003; Johansen-Berg, 2007). Reorganization following deafferentation has been noted in the cortex as well as the thalamus in the past, however these studies have involved stroke, nerve injury, or focal cortical lesion.

Using focal transcranial magnetic stimulation (TMS), mapping of the motor cortex somatotopy has demonstrated that following unilateral hemispheric ischemic injury, patients have heavily reduced or abolished amplitude in motor evoked potentials (MEP, Cicinelli, Traversa, & Rossini, 1997; Macdonell, Donnan, & Bladin, 1989). Focal TMS utilizes a hand-held figure-of-eight coil which produces a magnetic field inducing a focused local eddy current in the cortex of the brain in a non-invasive manner to induce neuronal activity. The output is measured using electrodes in the muscle groups of interest to record MEPs. Stroke patients have been noted to have reduction of motor excitability and decrease in cortical representation of paretic muscle groups which can be normalized over a period of 8-10 weeks (Cicinelli et al., 1997). Changes in cortical excitability and connectivity have also been measured using TMS in patients with central motor disorders that do not involve stroke. Caramia et al. demonstrated that excitability

and conduction of TMS signal are altered in patients with multiple sclerosis, amyotrophic lateral sclerosis, spinocerebellar ataxia, primary lateral sclerosis, and brain metastatic lesions (Caramia et al., 1991).

In subcortical stroke patients who have recovery of function, there is increase connectivity between corresponding cortical representation mapped using TMS and MEPs in the affected limb after neurorehabilitation (Cicinelli et al., 1997). Several groups have also demonstrated the recovery is associated with significant increase in regional cerebral blood flow (rCBF) in areas of the brain corresponding to the motor deficit as well as potential sites for recovery. The studies measured rCBF using positron emission tomography (PET) in conjunction with an administered radionuclide (usually inhaled  $C^{15}O_2$ ) and used rCBF as an index of synaptic activity (Chollet et al., 1991; Kanno et al., 1984; Roland, Meyer, Shibasaki, Yamamoto, & Thompson, 1982). Chollet et al. further demonstrated in a cohort of patients with recovery of function following unilateral upper extremity deficits that additional areas of activity on PET scan may correspond with cortical plasticity (Chollet et al., 1991).

Activity dependent interventions have demonstrated enlargement of the upper limb representation area in the affected hemisphere following stroke confirmed using multiple modalities including TMS, rCBF measurement via PET, as well as fMRI (Richards, Stewart, Woodbury, Senesac, & Cauraugh, 2008). Training-induced changes of the motor cortex in stroke patients have demonstrated that recovery is both possible, and potentiated through activity, supporting clinical rehabilitation (Liepert et al., 1998; Romero, Babikian, Katz, & Finklestein, 2006).

It has been postulated that injury to the motor cortex following stroke forces surviving neurons in motor associated areas, including corresponding ipsilateral areas, to create alternative neural ensembles to regain function via unmasking of latent synaptic connections or changes in

inhibitory GABAergic input to remaining neurons (Rossini & Pauri, 2000). In animal studies, plasticity in the adult brain can occur rapidly following nerve lesion or sensory deprivation supporting this hypothesis. Sanes et al. demonstrated dynamic reorganization of the motor cortex in rats occurs rapidly following facial nerve transection (J. Sanes, Suner, & Donoghue, 1990; J. Sanes, Suner, Lando, & Donoghue, 1988). Immediately following ligation of the nerves innervating facial vibrissae, cortical stimulation in the M1 cortex corresponding to facial vibrissae did not elicit any EMG activity however within hours following nerve transection, the same region of cortex elicited EMG responses in the forelimb. The boundary of cortical representation of the forelimb had rapidly remapped to the cortex that previously corresponded to facial vibrissae (Donoghue, Suner, & Sanes, 1990). These changes were found to be stable months following reorganization (Donoghue & Sanes, 1988). GABAergic modulation was later demonstrated to play a role in this rapid functional cortical reorganization via studies using the GABA antagonist bicuculine methobromide (bic). In cortical representation of the vibrissae musculature, injection of bic followed by electrical stimulation elicited EMG recorded activity in the forelimb which terminated after the bic injection was discontinued. At the same injection sites in the vibrissae related cortex, glutamate and acetylcholine injections failed to modulate activity related to the forelimb (Jacobs & Donoghue, 1991).

While these studies supported the premise that reorganization following nerve injury involves unmasking of latent connections and changes in GABAergic inhibitory input in the cortex, there was also mounting evidence more large-scale reorganization is also involved in deafferentation of the somatosensory system. Studies in primates by Florence and Kaas demonstrated that large scale reorganization occurs in the somatosensory system years following veterinary amputation of the forelimb for traumatic injury. Central projections of peripheral

nerve afferents were found to expand into denervated parts of the spinal cord and brainstem in primates using tract tracing following amputation (Florence & Kaas, 1995; Wu & Kaas, 1999).

Interpretation of these results are limited by the lack of evidence for axonal reorganization of afferents originating from the central nervous system.

Studies in cats and primates using retinal lesion to examine how the visual cortex responds to input loss also demonstrated function connectivity to non-injured retina after initially being unresponsive (Kaas et al., 1990). Optic chiasm sectioning in cats which removes activation from the ipsilateral temporal retina also resulted in visual cortex reorganization of remaining receptive fields over a period of weeks, suggesting unmasking of latent connections and changes to inhibitory input are likely augmented by largescale reorganization of inputs in the cortex (Milleret & Buser, 1984). Studies in the lateral geniculate nucleus of cats following small lesions in the retina have also demonstrated expansion of functional receptive fields after a period of a month however these studies did not provide structural evidence for axonal reorganization (Ulf Th Eysel, 1982; Ulf Th Eysel, Gonzalez-Aguilar, & Mayer, 1980; U. T. Eysel, Gonzalez-Aguilar, & Mayer, 1981).

More recent studies in transgenic mice by Keck et al., studied the structural correlates of functional plasticity in the visual cortex following retinal lesion using intrinsic signal imaging, which utilizes infrared light source to illuminate the cortex and aide visualization of rCBF with high detail as a correlate of synaptic activity, as well as two-photon confocal microscopy to visualize dendrites in the lesion projection zone (LPZ) of the visual cortex. The dendrites were visualized in vivo by using a cranial window in transgenic mice that express green fluorescent protein (GFP) in layer 5 pyramidal cells using the Thy-1 promoter. They noted that the initially unresponsive cortical region became responsive to visual stimulus in the weeks and months following retinal lesion and that this correlated with a turnover in dendritic spines within cortical

pyramidal cells. Completely abolishing retinal activity, however, only led to a modest increase in spine dynamics with turnover being much lower (Keck et al., 2008). The authors concluded that reorganization was likely dependent on activity in neighboring synapses, however, they were unable to comment on axonal reorganization as a limitation of their technique.

Investigation of corticocortical projections using biocytin injection into the cortex surrounding the LPZ following retinal lesions in cats demonstrated some evidence that reorganization of axons occurs in horizontally projecting neurons of the visual cortex. These axons demonstrated greater exuberance of terminal branching than seen in prior published examples of horizontally projecting neurons (Darian-Smith & Gilbert, 1994; Gilbert & Wiesel, 1992). Yamahachi et al. confirmed that rapid axonal sprouting and pruning accompanied the functional reorganization in visual cortex following retinal lesions using a macaque animal model (Yamahachi, Marik, McManus, Denk, & Gilbert, 2009). They reported horizontal connections from layer 2/3 pyramidal cells in adjacent receptive fields reorganize and innervate neurons in the LPZ. They used adeno-associated virus (AAV) vectors to label neurons and their projections with GFP using a cytomegalovirus promoter and examined their projections up to 1 year out following retinal lesion through a bone window using two-photon microscopy. They found exuberant outgrowth following retinal injury followed by a concomitant process of pruning reminiscent of transient overproduction of axons and synapses followed by refinement that occurs during development for formation of ocular dominance columns (Kasthuri & Lichtman, 2004; LeVay & Ferster, 1977; Vay, Wiesel, & Hubel, 1980).

Studying if collateral axon sprouting in the cortex is responsible for recovery following mTBI is complicated by the diffuse and scattered axon pathology resulting in subtle changes to produce local and long-distance cortical circuit dysfunction when compared to stroke or focal

injury. On the contrary, collateral axon sprouting may in fact, play a role in maladaptive plasticity following mTBI. In a cohort study examining 5 patients with mTBI and memory impairment, DTI tractography demonstrated unusual neural tracts from the fornix not observed in normal subjects, suggesting that collateral sprouting may be associated with maladaptive changes in the limbic circuitry (Jang & Lee, 2017). Experimentally, rodent studies using a behavioral assay to examine sensitivity to whisker stimulation has identified late-onset persistent sensory sensitivity following TBI (McNamara, Lisembee, & Lifshitz, 2010). The maladaptive behavioral response to whisker stimulation was correlated with maladaptive circuit reorganization (Hall & Lifshitz, 2010; Lifshitz, Witgen, & Grady, 2007). Interestingly, enrichment of the environment with novel objects, an enlarged enclosure, and housing with multiple cage mates, has been found to have no impact on the response to whisker stimulation of rodents following TBI compared to conventionally housed peers (McNamara et al., 2010). Enrichment of the environment has been demonstrated in several studies to improve motor performance as well as acquisition of spatial learning after TBI, suggesting differences in how plasticity may be adaptive in some neural circuits while being maladaptive in others (Bondi, Klitsch, Leary, & Kline, 2014).

#### **1.4 Studies in visual connectivity and development of mouse provide an ideal model to study functional plasticity and reorganization**

Studying the development of the retinal ganglion cell pathway has proved to be an excellent model to understand how individual neurons form complete neural networks (Dhande & Huberman, 2014; Huberman & Feller, 2008). Evolution of primate brains has produced a significant volume of cortex to process visual stimulus which supports the importance of

studying how injury impacts this neural network within the brain (Hubel & Wiesel, 1979; of, 1998; Wilkinson et al., 2000). The development of novel cell labeling techniques such as transgenic mouse lines, brain slice electrophysiology, and modern tract tracing techniques has further advanced our ability to peer into the visual network of the brain. By comparing how the brain responds in instances of injury to findings of developmental scientists who have focused how visual circuit connections are formed and mature, we can develop an understanding of whether post-injury changes are adaptive vs maladaptive, and in the future also determine if the system may be modulated in a specific manner to induce improved outcomes in mild TBI.

Reorganization of neural connections in the mature visual axis is a particularly good example of how innate homeostatic mechanisms can remodel in response to changes in connectivity. During development, the retinal ganglion cells (RGC) which receive and consolidate information from the rest of the retina, transmit visual stimulus to the lateral geniculate nucleus (LGN) via axons that travel down the optic nerve and through the optic chiasm to innervate LGN relay neurons on both sides. Early wiring in the visual axis between the retina and LGN is dependent on molecular cues such as ephrins/Ephs, major histocompatibility complex class I molecules, and other receptor-ligand signaling systems (Barallobre, Pascual, Río, & Soriano, 2005; Brose & Tessier-Lavigne, 2000; Datwani et al., 2009; Huberman, Murray, Warland, Feldheim, & Chapman, 2005; Huberman & Feller, 2008). In mouse, inputs to the ventral LGN and the intergeniculate leaflet synapse on neurons that project to subthalamic nuclei involved in image stabilization, oculocephalic and vestibulo-ocular reflexes while inputs projecting to dLGN innervate relay cells that project to the primary visual cortex (V1). Further refinement occurs in the dLGN pathway based on RGC subtype and is based on spontaneous

retinal activity along with experience-dependent plasticity during a critical period after eye opening (Pfeiffenberger, Yamada, & Feldheim, 2006; Rose & Bonhoeffer, 2018).

Studies regarding the development of the optic pathway in different organisms demonstrate a high degree of conservation in the underlying guidance mechanisms despite the differences in overall organization (Erskine & Herrera, 2007; Herrera et al., 2003; Nakagawa et al., 2000). Early during this process, the axons form numerous redundant connections to LGN relay neurons and there is significant overlap between axon terminal fields between RGCs originating from different parts of the retina, different subtypes of retinal ganglion cells, as well as the ipsilateral or contralateral retina across species. Unlike in primate, the LGN in mouse is not classically laminated and segregates inputs to the formed vision pathway predominantly based on ipsilateral or contralateral retinal origin. Over the 2-week period following birth, the axon terminals from either retina in right and left dorsal LGN (dLGN) segregate from each other until there is less than 10% of overlap between ipsilateral and contralateral retinogeniculate inputs to dLGN relay neurons (Jaubert-miazza, Green, Lo, Bui, & Guido, 2005). During postnatal development, axonal arbors have a critical period during which time the connections between thalamocortical neurons and cortical columns become defined and set into patterns which persist into adulthood based on activity dependent plasticity (Crair & Malenka, 1995). Monocular deprivation studies demonstrate that the critical period closes before 6 weeks with respect to the visual axis in mice, however closure of the critical period does not mean that no plasticity is possible afterward (Whitt, Petrus, & Lee, 2014). The degree of plasticity is more limited after closure of the critical period; however, cortical responses demonstrate plasticity following deafferentation as described in other injury paradigms.



### **1.5 Using the mouse model of the visual axis can aide in understanding the visual axis in higher order mammals.**

The advantage in studying projections specifically to dLGN allows for objective measurement of change with respect to the formed vision pathway. Axon plasticity can be evaluated to be adaptive verses maladaptive based on both structural and electrophysiologic changes using techniques well established in the developmental neurobiology fields.

In recent years, studies utilizing molecular tools and transgenic mouse lines, groups have demonstrated that retinal ganglion cells have molecular diversity which correlates with their response to different light stimulus (Guido, 2018). Murine studies in the primary visual cortex were initially delayed due to concerns that mouse dLGN organization differed greatly from primate LGN organization. Primate LGN transmits information to the visual cortex in three discrete parallel pathways which are structurally well defined, the magnocellular layer, the parvocellular layer, and the koniocellular layers between the two. Magnocellular cells receive input from rapid and transiently firing RGCs and mostly receive input from rod cells in the retina. This pathway allows for the perception of movement, depth, and small differences in contrast. Parvocellular cells receive input mostly from cones and are necessary for the perception of color and fine details (DeYoe & Essen, 1988; Nassi & Callaway, 2009). Koniocellular cells are less well defined in their role but their preferential projection to layers III to I suggest they provide modulatory inputs rather than major driver inputs to layer IV like the parvocellular and magnocellular cells (Xu et al., 2001). Studies using mouse models have helped establish the function and connectivity of the koniocellular pathway present in primates.

Mouse dLGN is known now to have specific segregation of pathways that closely approximates the pathway between primate LGN to visual cortex for contrast and spatial

information. In a large scale experiment examining single unit recordings in V1 in response to varying visual stimulus, Gao et al. found that, like primates, mouse V1 have neurons with short response latencies have lower spatial acuity, high contrast and temporal frequency sensitivity, while neurons with long latencies have high spatial acuity and lower contrast, speed, and temporal frequency sensitivity (Gao, DeAngelis, & Burkhalter, 2010). Structural studies of mouse LGN relay cells support that there are discrete parallel pathways to V1 and have helped further understand how structural connectivity relates with function. For example, examination of the morphology of dLGN relay cells have demonstrated that there are three morphologically distinct classes of relay cells which exhibit regional preferences and is suggestive of ‘hidden layering’ of the mouse dLGN. Using quantification of dendritic architecture and electrophysiology, cells which morphologically and physiologically resemble ‘W’ relay cells in the of cat LGN have been found to have regional preferences to a shell in mouse dLGN and resemble koniocellular cells in the primate pathway (Bickford, Zhou, Krahe, Govindaiah, & Guido, 2015; Hendry & Reid, 2000; Kerschensteiner & Guido, 2017; Krahe, El-Danaf, Dilger, Henderson, & Guido, 2011).

Bickford et al. demonstrated convergence of inputs in the dorsolateral margin of dLGN from directionally selective retinal ganglion cells (DSGC) and tectogeniculate projections (TG) from the superior colliculus (referred to as the optic tectum in higher order animals) onto ‘W’-like relay cells. Directionally selective retinal ganglion cells are a specific subtype of RGCs which respond to light stimulus only moving in a specific direction across their center-surround receptor field. Using transgenic mice along with viral vector injections to elicit expression of channel rhodopsin in TG projections, electrophysiology using patch-clamp recording of the LGN relay cells in the dorsolateral shell demonstrated that these ‘W’-like relay cells are driven through glutamatergic signaling from both DSGC projections as well as TG projections (Bickford

et al., 2015). These studies, along with confirmatory electron microscopy, and immunohistochemistry studies have advanced our understanding of the functional connectivity of the koniocellular layer in primates as a distinct third pathway to the visual cortex in conjunction with the magnocellular and parvocellular pathways, and help to establish the LGN as a complex computational center in addition to relaying sensory signal to the visual cortex.

### **1.6 Using the visual axis to study network disruption following mTBI**

Study of the clinical relevance of the changes that occur secondary to axon injury can be challenging, particularly when considering what variables within the injury paradigm will correlate with function deficit. Mild TBI (mTBI) is associated with cognitive, emotional, and behavioral manifestations which can be difficult to quantify. Persistent headaches, sensitivity to light, and oculomotor deficits that some mTBI patients experience long after injury may be secondary to a chronic maladaptive response to injury. Thalamic studies of mTBI have demonstrated that hypersensitivity to stimulus can be correlated with maladaptive changes in the rodent thalamocortical wiring following recovery, however, evidence for adaptive recovery is limited and the neurophysiologic substrate for recovery versus maladaptive change is poorly understood and requires further evaluation(Thomas, Hinzman, Gerhardt, & Lifshitz, 2012).

Fortunately, some visual complaints in patients following mTBI can be objectively measured and correlated with physiologic dysfunction along with disruption of brain connectivity. Visual dysfunction following mTBI has been well documented in reports by optometrists and ophthalmologists since the 1980s supporting that connectivity disruption in the visual axis can be objectively measured and quantified(Padula, Argyris, & Ray, 1994; Tierney, 1988). Reports since then that have focused on mTBI patients demonstrated that even mild injury

induces visual complaints in up to 60% of TBI (Alvarez et al., 2012). The large cohort of veterans returning from recent foreign conflicts demonstrated a large patient base with visual symptoms due to blast induced TBI even when accounting for ocular injury (Hoge et al., 2008). These papers highlight pervasive symptoms in the visual system along with the cognitive and memory disturbances; the latter two of which have previously received significantly more attention.

More importantly, since visual dysfunction can be measured and quantified, the impact of intervention following TBI can also objectively measured. The first such large scale report was produced in 1993 by Schlageter et al. who reported deficiency following TBI in visual acuity, oculomotor dysfunction including impaired pursuits and saccades, and impaired vergence in a mixed TBI population. Though their study was limited by their patient selection, it provided evidence that outcomes after rehabilitation and recovery in TBI patients can be objectively measured using the visual axis (Schlageter, Gray, Hall, Shaw, & Sammet, 1993). Several groups have since demonstrated a link between axonal injury and visual acuity loss using scalp based electrical recordings in post-mTBI patients. Specifically, they demonstrate changes in timing and amplitude of scalp recorded potentials evoked by visual stimulus of increasing complexity as well as decreased luminosity (Fimreite, Ciuffreda, & Yadav, 2015; Lachapelle, Bolduc-Teasdale, Ptitto, & McKerral, 2008; N. K. Yadav & Ciuffreda, 2014).

Studies utilizing animal models to examine the visual axis in TBI have also started to become more common. Study of the impact of repetitive mild TBI in an animal model by Tzekov et al. demonstrated that the visual axis provides a robust model to study mTBI. Due to the optic nerve being subject to DAI following mechanical insult, the health of retinogeniculate neurons in the eye can be directly studied utilizing optical coherence tomography which measures thickness of the nerve fiber layer, ganglion cell layer, inner and outer plexiform and

nuclear layers. (Tzekov et al., 2014). Further electrophysiologic studies can be performed utilizing visually evoked potentials (VEPs) to understand how DAI can interfere with cortical response to light input in the injury and recovery period. Visually evoked potentials are typically used clinically to identify functional integrity of the visual pathway from retina to the visual cortex and can be abnormal following optic nerve or axon injury such as demyelinating process of multiple sclerosis as well as recovery following remyelination (Brusa, Jones, & Plant, 2001; Jones & Brusa, 2003; Zeneroli et al., 1984). The demyelination in multiple sclerosis cause slowing of conduction of VEP signal to the cortex as well as disruption in amplitude secondary to axon dysfunction. Additional studies using the visual axis can utilize the unconscious visual pathways such as oculomotor reflex testing to further characterize network disruption following TBI as well as recovery (Ciuffreda et al., 2007, 2008; N. Yadav, Thiagarajan, & Ciuffreda, 2011).

### **1.7 Adaptive Plasticity Following Deafferentation in Experimental Injury**

While considerable evidence exists regarding the pathogenesis and progression of DAI to clinical symptoms, there is limited data available on how the remaining intact axons respond to injury. Studying effects of deafferentation experimentally following traumatic DAI through traditional techniques is difficult, as downstream targets are not completely devoid of intact and functional axonal projections. Publications by our group demonstrate that neurons sustaining DAI either undergo axotomy or repair however both populations demonstrate electrophysiological change as there are additional changes to interneuron connectivity (Greer et al., 2012; Vascak, Jin, et al., 2017). Using the same injury model, we also observed DAI preferentially distributed within the optic nerve and that the injured axons do not mount a successful axon regeneration attempt (J. Wang, Fox, & Povlishock, 2013; J. Wang et al., 2011). This

suggests that any recovery that may occur following experimental TBI, is likely occurring through changes in remaining intact connections. While it is well established that the ability of cortical neurons to adapt to change in afferent input persists in adulthood, studies involving deeper brain structures such as the thalamus had been historically sparse (Brainard & Knudsen, 1998; Darian-Smith & Gilbert, 1994; Guggenmos et al., 2013; Ziemann, Hallett, & Cohen, 1998). The determination of whether changes in the remaining intact connections are adaptive or maladaptive is also understudied with current opinions favoring maladaptive change (Hall & Lifshitz, 2010; Thomas et al., 2012).

Study of visual function following mTBI measured at the cortical level utilizing behavioral studies and examination of the visual cortex have identified initial dysfunction preceding recovery but studies on the role of the LGN, an important thalamic input to the visual cortex, in recovery of visual function is sparse. Previous studies have demonstrated that this recovery is not associated with regeneration of lost inputs through axon regrowth and not associated with repair of injured axons between the retina and the LGN. However, as an important structure in the processing of visual input, it is unlikely that ensuing recovery is completely dependent on cortical plasticity. **We hypothesize that recovery of visual function following deafferentation in mTBI is associated with structural and electrophysiologic adaptive plasticity in remaining retinal geniculate projections to the lateral geniculate nucleus.** The following studies were thus designed to identify the response of optic nerve axons to injury by examination of the downstream target in the formed vision pathway. Specific goals were to determine if the structural and electrophysiologic changes following injury are adaptive or maladaptive and to determine if specific subpopulations of retinal ganglion cells respond in a divergent pattern from other subpopulations. Identification of adaptive reorganization in the

visual axis to surviving retinal inputs to the lateral geniculate nucleus would expand our understanding on how recovery occurs in mTBI by demonstrating that adaptive reorganization in the subcortical structures such as LGN constitutes an important contribution to recovery of function. Our animal model of mild traumatic diffuse axonal injury is well designed to utilize the visual axis to answer questions regarding injury and plasticity using the visual axis as a correlate of how a large cortical network responds to the changes that follow diffuse traumatic axonal injury, and allows study of dysfunction as well as recovery in a manner not performed previously.

## **Chapter 2 - Adaptive Reorganization of Retinogeniculate Axon Terminals in Dorsal Lateral Geniculate Nucleus Following Experimental Mild Traumatic Brain Injury**

### **Abstract**

The pathologic process in traumatic brain injury (TBI) marked by delayed axonal loss, known as diffuse axonal injury (DAI), leads to partial deafferentation of neurons downstream of injured axons. This process is linked to persistent visual dysfunction following mild traumatic brain injury (mTBI), however, examination of deafferentation in humans is impossible with current technology. To investigate potential reorganization in the visual system following TBI, we utilized the central fluid percussion injury (cFPI) mouse model of mTBI. We report that in the optic nerve of adult male C57BL/6J mice, axonal projections of retinal ganglion cells (RGC) from the retina to the downstream thalamic target, dorsal lateral geniculate nucleus (dLGN), undergo injury followed by scattered widespread loss of axon terminals at 4 days post-injury. However, at 10 days post-injury, we observed reorganization of RGC axon terminals suggestive of an adaptive neuroplastic response. Further, while these changes persist at 20 days post-injury, recovery in RGC axon terminal distribution does not reach sham-injury levels. Additionally, our experiments in dLGN revealed segregation of axon terminals from ipsilateral and contralateral eye projections remained consistent with normal adult mouse distribution. Lastly, our examination of the shell and core of dLGN suggests different RGC subpopulations may vary in their susceptibility to injury or in their contribution to reorganization following injury. Collectively, these findings suggest subcortical axon terminal reorganization may contribute to recovery following mild TBI, and that different neural phenotypes may vary in their contribution to axon terminal reorganization despite exposure to the same injury.



## 2.1 Introduction

Traumatic brain injury (TBI) is an important public health issue which continues to be a major source of death and disability for healthy adults despite strides in education, prevention, and safety. The prevalence of concussion, also known as mild TBI (mTBI), comprises up to 80% of all TBI cases and many of these patients take up to 6 months to recover from associated disability, with a minority of patients (5-10%) never recovering (Bazarian et al., 2006; Cassidy et al., 2004; Corrigan et al., 2010; Dean et al., 2015). Through several studies, the morbidity associated with mTBI has been associated with presence and extent of diffuse axonal injury (DAI) found throughout the subcortical white matter and callosal projections (Christman et al., 1994; Farkas, Lifshitz, & Povlishock, 2006; V. E. Johnson et al., 2015; Kelley, Farkas, Lifshitz, & Povlishock, 2006; King, 1997). Of particular note in the pathogenesis of DAI, is that following axonal injury, the length distal to the injury undergoes degeneration and distal target neurons lose part of their excitatory or inhibitory input. This loss of input is hypothesized to lead to dramatic remodeling in surviving connections, however, literature supporting this premise following TBI is sparse because of the technical challenges associated with following terminal loss and recovery in a diffusely deafferented network (Büki & Povlishock, 2006; Leunissen et al., 2014; John T Povlishock & Katz, 2005).

While multiple brain loci have been linked to the morbidity associated with mTBI, visual circuit dysfunction has been recognized to be a significant contributor to morbidity in the context of mild TBI or concussion (Alvarez et al., 2012; Fimreite et al., 2015; Kapoor, Ciuffreda, & Han, 2004; Lachapelle et al., 2008; Lutkenhoff et al., 2013; Schlageter et al., 1993). Veterans returning from recent foreign conflicts contain a large cohort of patients with visual symptoms due to blast induced TBI (Hoge et al., 2008). Scalp recordings in post-concussive patients have also

demonstrated changes in timing and amplitude of electrical potentials evoked by visual stimulus of increasing complexity as well as decreased luminosity (Fimreite et al., 2015; Papathanasopoulos et al., 2008; N. K. Yadav & Ciuffreda, 2014; N. K. Yadav, Thiagarajan, & Ciuffreda, 2014). Collectively, these reports highlight pervasive symptoms in the visual system along with cognitive and memory disturbances associated with mTBI; the latter two of which have previously received significantly more attention (Dymowski, Owens, Ponsford, & Willmott, 2015; Finnanger et al., 2013).

Because the detailed analysis of DAI and its correlation to morbidity and recovery are impossible to evaluate in humans using current techniques, in the current communication, we move to an animal model of mTBI to study this question, exploiting the well-characterized visual axis of the mouse to assess deafferentation and recovery following DAI (Bickford, 2016; Bickford et al., 2010; Guido, 2008; Huberman & Feller, 2008). Using the mouse central fluid percussion injury (cFPI) model of mild TBI to induce diffuse axonal injury, we have previously reported that the optic nerve reveals a predilection for diffuse axonal injury based on identification of scattered axonal swellings as well as disconnected axonal segments (J. Wang et al., 2011). Distinct from other modes of optic nerve injury such as cutting, crushing, or stretching, the cFPI model induces only scattered DAI pathology with the sparing of a large fraction of axons, closely approximating the situation found in most cases of concussion and mild TBI (Marklund, 2016; Maxwell, Bartlett, & Morgan, 2015). In the experiments described here, we exploit this model to evaluate the downstream changes evoked by injury of the optic nerve and conduct analysis of deafferentation as well as potential reorganization of retinogeniculate axon projections to the dorsal lateral geniculate nucleus (dLGN), a critical structure in the formed vision pathway of mouse.

Through the implementation of anterograde tract tracing of retinal ganglion cells (RGCs) using Alexa fluorescent dyes conjugated to recombinant cholera toxin subunit  $\beta$  (CTB) as well as

immunohistochemistry against a well described marker for retinorecipient axon terminals, vesicular glutamate transporter 2 (VGLUT2), we examined deafferentation of dLGN relay neurons through identification of reduction in retinogeniculate axon terminals. Following cFPI induced DAI in the adult mouse optic nerve, we found axon terminal loss occurs in its downstream target, the dorsal lateral geniculate nucleus (dLGN). However, over time, the remaining intact axon fiber population undergoes structural reorganization of pre-synaptic terminals in a manner suggestive of axon terminal sprouting and adaptive recovery. Our findings support the hypothesis that in the adult mammalian brain, surviving subcortical axons and their axon terminals are capable of dramatic reorganization following mTBI induced DAI. We believe these findings to have important implications on our understanding of DAI in humans along with major implications with respect to study of repair and restoration of function following mTBI.

## **Materials and Methods**

### **2.2 Experimental Design**

Adult male C57BL/6J mice (9-12 weeks) were sourced directly from Jackson Laboratory (Bar Harbor, ME) or bred and maintained in house. Animals obtained directly were kept in house for 48 hours to habituate to our vivarium prior to experiments. Animals were then subjected to mild central fluid percussion injury ( $1.40 \text{ ATM} \pm 0.05$ ), as previously described (Greer, Hånell, McGinn, & Povlishock, 2013; Hånell et al., 2015; J. Wang et al., 2013, 2011). In brief, the fluid pressure pulse in this model results in a brief deformation of the brain through an intact dura and induces diffuse traumatic axonal injury in the optic nerve approximately 1mm proximal to the chiasm as well as other neocortical and subcortical sites not addressed in the current study.

As employed, the model involved the induction of general anesthesia in adult male mice with inhaled isoflurane (<5%) before placing their head in a stereotactic frame. Toe pinch reflexes were monitored during surgery and isoflurane concentration adjusted to maintain depth of anesthesia. The skin was opened over the skull and retracted to allow for a 3mm wide craniotomy midway between lambdoid and bregma cranial sutures. Care was taken to keep the underlying dura intact and a dissecting microscope was used to ensure dural integrity as well as prevention of injury to the large sagittal vascular structures. A luer hub was fixed in place over the craniotomy with dental cement and the animal was allowed to recovery from anesthesia for approximately 1 hour. The animal was then anesthetized (4% isoflurane) again prior to mounting to the fluid percussion device and the impulse delivered to the intact dura of the mouse brain. Sham-injured animals received the same surgeries including, craniotomy, the mounting of the luer hub and attaching the animal to the fluid percussion device, with the absence of the injury that results from release of the pendulum. During surgery to perform craniotomy and implant the luer hub, each mouse was monitored using a pulse oximeter sensor to collect blood oxygen saturation, heart rate, and respiratory rate. Post-injury or sham procedure, return of toe pinch reflex as well as righting reflex were recorded.

The animals were prepared for histologic analysis at 4, 10, and 20 days after injury. The early time point of 4 days was selected to allow axonal disconnection to reach its apogee prior to evaluation of deafferentation based on our previous report (J. Wang et al., 2011). We previously examined mTBI retinas for RGC death induced by DAI and demonstrated that the injured/axotomized RGCs continue to survive up to 28 days after injury (J. Wang et al., 2013). The time points of 10 and 20 days were chosen based on mouse studies evaluating deafferentation and recovery in the visual axis (Benowitz & Yin, 2008; Lima et al., 2012). For the

histological analyses, the animals were prepared in three different fashions for either immunohistochemistry, CTB, or routine histopathology. Animals prepared for CTB fluorophore visualization or VGLUT2 immunohistochemistry were sacrificed via intraperitoneal overdose of sodium pentobarbital. Those prepared for CTB visualization were transcardially perfused with 25mL of heparinized 0.9% saline (1u/mL) followed by 200mL of 4% paraformaldehyde dissolved and filtered into Millonig's buffer (pH 7.4). Animals undergoing VGLUT2 immunohistochemistry or standard histologic preparation in plastic sections were perfused in a similar fashion with the addition of 0.2% glutaraldehyde to the fixative perfusion solution. The brain, optic nerves, and eyes of each animal were post-fixed in their respective fixative for 24 hours and stored at 4 degrees Celsius in Millonig's buffer until sectioning. All protocols used in this study were approved by the Institutional Animal Care and Use Committee of Virginia Commonwealth University.

### **2.3 Examination of mTBI induced retinogeniculate axon terminal loss via VGLUT2 immunohistochemistry.**

For analysis of VGLUT2 immunoreactive axon terminal loss and recovery, animals were prepared as described above for mTBI (1.4  $\pm$ 0.05 ATM) or sham injury. Sham animals were prepared from littermates of mTBI animals and were sacrificed at similar time points following surgery. Our inclusion criteria were the absence of dural injury during surgical procedures, adequate wound healing following injury or sham-injury, normal feeding and drinking, and normal grooming in days following surgery. All animals prepared for VGLUT2 immunohistochemistry met inclusion criteria and therefore none were excluded from analysis. A total of 6 sham animals together with 4-5 mTBI animals for each post-injury time point were used to generate sections for analysis (Sham N = 6, 4 day mTBI N = 4, 10 day mTBI N = 5, 20

day mTBI N = 5). Free floating coronal sections (40 $\mu$ m) were obtained using a vibrating blade microtome (Leica VT1000 S). We determined a randomized start point and collected alternating sections through the entire left and right dLGN for each animal. Immunohistochemistry was performed on all collected sections by a blinded investigator. Sections were serial washed in phosphate buffered saline (PBS) before incubating for 1 hour at room temperature in blocking solution containing; 0.3M glycine (Sigma-Aldrich), 2.5% bovine serum albumin (Electron Microscopy Sciences), 2.5% normal goat serum (S1000, Vector Labs), in phosphate buffered saline (pH 7.2). Sections were then incubated overnight at room temperature on oscillating stage with 1:2000 dilution of affinity purified rabbit anti-VGLUT2 polyclonal IgG antibody (Synaptic Systems, Cat. No. 135 303) diluted into solution containing; 2.5% BSA, 2.5% NGS, 0.5% triton X-100 (Sigma-Aldrich), in PBS (pH 7.2). Following serial washes in antibody free blocking solution, sections were incubated in poly-clonal goat anti-rabbit IgG antibody conjugated to Alexa 568 (Life Technologies, Cat. No. A-11036) at 1:500 dilution in above blocking solution for 2 hours. Sections were serial washed in PBS, then phosphate buffer, followed by mounting with anti-fade mountant (Life Technologies, Cat. No. P-36931) and cover slipped. Slides were allowed to cure protected from light overnight and edges sealed with nail varnish prior to imaging.

Confocal microscopy was performed for qualitative examination of VGLUT2 positive axon terminals using a Zeiss LSM 700 scanning laser microscope with a Nikon Plan-Apochromat 63x/1.57 objective. The derived Z-stack images were obtained with consideration of Nyquist sampling and saved in CZI format for later examination. Images were processed using Zen Black (Carl Zeiss) to produce maximum intensity projections from Z-stacks.

Quantitative assessment of images obtained from immunohistochemistry for VGLUT2 was performed on sections through dLGN that receive projections from both eyes due to report of potential for reorganization between ipsilateral and contralateral projections following monocular sensory deprivation in adult mice (Coleman, Law, & Bear, 2009; Feldman, 2003). This region is well described as the anterior-posterior (AP) midline of dLGN and can be identified through anatomic landmarks of its borders (Godement, Saillour, & Imbert, 1980). Sections with anatomic or processing artifacts such as large perforating vessels or bubbles in the mountant which could bias analysis were excluded by a blinded investigator. Sections identified in a blinded fashion as containing the anterior-posterior midline of dLGN were imaged using monochromatic mode on a digital camera (Olympus DP 71) mounted to an epifluorescent upright microscope (Nikon E800) and illuminated using LED light source passed through a dichroic filter for 568nm and magnified with a 10x primary objective (Nikon Plan Fluor 10x/0.30). Background fluorescence was removed using background subtraction tool in ImageJ (NIH) with rolling ball radius set to 100. The area surrounding dLGN was cropped out using the polygonal lasso tool in Photoshop CS6 (Adobe) by a blinded investigator and images were converted from greyscale using the threshold function set to 20% such that in the final image, the area around dLGN was white, the area of dLGN was black, and the signal from the immunofluorescent marker was red. Using a custom software module, the number of red pixels were compared to the number of red or black pixels to derive a percent value for the area of each section through dLGN with VGLUT2 immunoreactivity. Sham animals sacrificed and perfused at different time points following surgery were pooled for analysis. Statistical comparisons between sham and each of the three time points following mTBI were performed as described below in image analysis and statistical methods sections.

## **2.4 Examination of retinogeniculate axon terminal loss following mTBI through anterograde tract tracing.**

In a separate experiment, mice subject to sham or mTBI were then subject to intravitreal injection of recombinant cholera toxin subunit  $\beta$  (CTB) conjugated to Alexa 488 or Alexa 594 fluorescent dye (ThermoFisher Scientific, Cat. No. C34775 and C34777). This tracer allows visualization of axonal projections and axon terminals without reliance on immunohistochemistry and also allows separation of projections from either eye based on the Alexa dye conjugated to the CTB molecule (Demas et al., 2006; Fort & Jouvett, 1990).

Mice were anesthetized with intraperitoneal injection of Ketamine (10mg/mL) and Xylazine (0.5mg/ml) solution diluted in sterile phosphate buffered saline with delivered volume based on weight of animal (0.01mL/g). A puncture 1mm behind the limbus at the superior temporal aspect of the eye was made using a 30 gauge sterile needle and approximately 3  $\mu$ l of vitreous fluid aspirated using a pulled borosilicate glass pipet. Using a separate clean pulled glass pipet, 3  $\mu$ l of 1% CTB reconstituted in sterile phosphate buffered saline was injected using a picospritzer into each eye with CTB conjugated to Alexa 488 injected into the right eye and CTB conjugated to Alexa 594 injected into the left eye for each animal. The pipet is left in place for approximately 30 seconds prior to removal. Body temperature is maintained with a heating pad (Harvard Homeothermic Blanket) during eye injection as well as recovery period before being returned to the vivarium. Animals were sacrificed and perfused with heparinized saline and 4% paraformaldehyde fixative 72 hours following eye injection and post-fixed for 24 hours in 4% paraformaldehyde.

The retinas of all animals were dissected from the remainder of the orbit and flat mounted to glass slides with 0.15 mm thick cover slips superglued in place to either side of the retina



before being mounted with Prolong Gold (Life Technologies, Cat. No. P-36931). A larger coverslip was laid to rest on the smaller cover slips to cover the flattened retina and the edges sealed with clear nail varnish prior to imaging on Nikon E800 epifluorescent microscope. A total of 4 animals per mTBI time point or sham cohort were selected for eye injections and projection analysis however animals were rejected and replaced if examination of the retinas post-fixation revealed dural injury, retinal injury, or non-uniform RGC labeling. One animal in the 4 day TBI group was rejected after image acquisition due to high background fluorescence which when subtracted, would also obscure the fluorescent signal such that the result severely under-represented signal from CTB labeled axon terminals. The final number of animals used in analysis is as follows; sham N = 4, 4 day post-mTBI N = 3, 10 day post-mTBI N = 4, 20 day post-mTBI N = 4.

The brains were blocked and free floating coronal sections were obtained at 70 $\mu$ m through the entire length of dLGN on a vibratome and serial mounted to glass slides with Prolong Gold containing DAPI. Slides were allowed to cure protected from light overnight and edges sealed with nail varnish prior to storage at -20 degrees Celsius until imaging. We noted differences in signal to background fluorescence for each of the two fluorophores used as well as between different batches of fluorophores obtained from Thermofisher scientific. This potential confound was obviated by processing sham and mTBI groups simultaneously and also accounted for by sampling both sides of each brain equally.

For imaging of sections from CTB injected animals, adjustment to exposure time made during imaging due to animal to animal variability in background fluorescence and Alexa signal intensity were kept constant between sections from the same animal. The exposure settings were recorded for each animal and comparable between sham and injury groups. Each fluorophore

was imaged using monochromatic mode on the Olympus DP 71 camera attached to a Nikon E800 epifluorescent microscope. Illumination was performed using UV LED light source passed through dichroic filters for Alexa 488 or Alexa 594 depending on the fluorescent channel being captured. Images of all sections through dLGN were examined and all sections through the AP midline for each dLGN were identified by recognition of ipsilateral and contralateral projections by a blinded investigator. Samples were excluded, however, if they contained large anatomic or processing artifacts that obscure the region of interest.

On images of dLGN containing both CTB conjugated Alexa dyes, corresponding to the AP midline of dLGN, the area representing dLGN was cropped out from the surrounding structures using the polygonal lasso tool in Photoshop CS6 (Adobe) by a blinded investigator. The same investigator removed background fluorescence by adjusting the level function in Photoshop for each fluorophore until the fluorescent signal in the adjacent thalamus was no longer present in each sample. Threshold percentage used for conversion of signal images to binary images were also determined by the blinded investigator who used the threshold percent value that best represented the observed signal from the fluorophores (Gianna Muir-Robinson, Hwang, & Feller, 2002; Torborg & Feller, 2004). Threshold percentage ranged from 16% to 63% for both red and green channels with a mean threshold of 30% (+- 7.8% std dev) for the green channel and a mean threshold of 38% (+- 10.0% std dev) for the red channel. The resulting image labeled ipsilateral or contralateral axon terminal projections red or green, the overlap between the two projections as yellow, and the remaining area of dLGN as black. Using again the custom software module, a percentage value was derived for percent of dLGN section area covered by ipsilateral or contralateral projections as well as overlap between ipsilateral and contralateral projections. Statistical comparisons were performed using parametric or non-

parametric comparisons between data from sham animals and animals from each time point following mTBI.

## **2.5 Examination of CTB fluorescent signal within contralateral zone of dLGN.**

Within the contralateral region of dLGN, which only receives input from the contralateral eye, there are anatomical subgroups of axon terminals that segregate between projecting to the dorsal shell of dLGN and projecting to the inner core (Huberman et al., 2008, 2009; Rivlin-Etzion et al., 2011; J. R. Sanes & Masland, 2015). To identify changes within the shell and core, we compared Alexa dye fluorescent signal in images of CTB injected mice after background fluorescence has been removed using the level adjustment tool in Photoshop. Animals prepared for CTB analysis above were re-analyzed through the grey scale images of only contralateral projections in dLGN (Sham N = 4, 4 day mTBI N = 3, 10 day mTBI N = 4, 20 day mTBI N = 4). Using all the sections we collected through the CTB labeled dLGN, a blinded investigator selected, using ImageJ (NIH), a vertical plot profile through the patch of contralateral projections for each section of dLGN. The optic tract where it enters dLGN was used as the top border while the bottom border was defined by the beginning of the thalamocortical tract in each section (Figure 5A). Sections with anatomic artifact that may bias results were excluded by the investigator. The plot profile values were then normalized to the selected region by subtracting the minimum value from each raw value and dividing the result by the difference between the minimum and maximum fluorescence. The results were then binned at 5% intervals of the depth from surface of the optic tract to derive a final percentage of average fluorescent intensity for each bin (Huberman et al., 2009) (Huberman et al., 2009). Values for each binned width were compared between the three time points and sham animals as seen in Figure 5B.

$$F_{\text{value}} = (F_{\text{raw}} - F_{\text{min}}) / (F_{\text{max}} - F_{\text{min}})$$

## **2.6 Routine histologic screening to assess the presence of DAI in the optic nerve**

The eyes and optic nerves of a sham-injured mouse and a 4 day post-mTBI mouse used for immunohistochemistry were dissected free from surrounding structures up to the level of the optic chiasm and removed from the surrounding brain by transection of the optic tract. The orbits of the eyes as well as the associated musculature were removed with sharp dissection from the optic nerves. The remaining optic nerve, chiasm, and beginning optic tract were placed en bloc in 2% osmium tetroxide in 0.1 M phosphate buffer (pH 7.2) for 90 minutes. After serial rinses in 0.1 M Millonig's buffer (pH 7.4), the tissue was then dehydrated with 15 minute incubations in a gradient of cold EtOH dilutions ranging from 30% to 95% in 10% increments. Dilutions stronger than 50% contained 1% uranyl acetate. Finally, tissue is dehydrated with 100% EtOH through 3 incubations before incubating with propylene oxide. Tissue is then incubated with propylene oxide and EM resin (Electron Microscopy Sciences) overnight. Next day, tissue is changed into new EM resin for embedding and placed in oven at 55° C. Resin molds containing both the right and left optic nerves were sectioned longitudinally on an ultramicrotome (Carl Zeiss) to produce sections with 1 µm thickness. Sections were then counterstained with toluidine blue before cover slipping with Permount mounting media (Fisher Scientific). Qualitative analysis of optic nerve sections is performed through multiple longitudinal sections to identify DAI pathology as well as intact axons. Images were taken using routine light microscopy with a DP71 digital camera attached to Nikon E800 and 100x oil immersion objective (NA 0.72).

## 2.7 Image Analysis and Statistical Methods

As reported previously, our injury model induces diffuse axonal injury symmetrically throughout the brain and optic nerves (Greer et al., 2013; J. Wang et al., 2011). The dLGN on both sides of each animal were treated as internal replicates. Brain sections representing the entire rostrocaudal length of dLGN were identified and all sections through the AP midline of each dLGN were pulled for analysis unless specifically stated otherwise. All sections through the dLGN were treated as independent observations for each group analyzed. Images were analyzed by a blinded investigator to remove background fluorescent signal and/or convert 8-bit images to binary thresholded images. Percentage of dLGN covered by CTB signal or VGLUT2 signal was determined using a custom software module courtesy of lab of Dr. William Guido. The software used the binary threshold images to compare the number of pixels coinciding with either CTB fluorophores or VGLUT2 fluorescent signal with the number of pixels coinciding with area of dLGN to derive a value for the percentage of dLGN covered by each CTB fluorophore or VGLUT2 fluorescent signal.

Statistical analysis was performed using JMP Pro 11 (SAS Institute Inc.). Determination of whether to use parametric or non-parametric inferential statistics was assessed using Levene's test to compare variance of groups in each dataset. For datasets with equal variance between groups, one-way analysis of variance (ANOVA) was performed, followed by pair-wise comparison utilizing Tukey-Kramer HSD to account for multiple comparisons. For datasets where Levene's test demonstrated unequal distribution of variance, variance was analyzed utilizing the Kruskal-Wallis non-parametric test, followed by Steel-Dwass post-hoc analysis to account for multiple pair-wise comparisons. Statistical significance was set at a  $p < 0.05$  for all datasets and all comparisons.

## Results

### 2.8 Physiological assessment of animals undergoing craniotomy and mild traumatic brain injury

To establish validity of comparison between animal groups, several assessments were made to address potential of experimental variability. Animals weighed prior to surgery showed no significant differences in weight between groups (Sham = 23.23 $\pm$  1.55g, 4 day mTBI = 25.82 $\pm$  0.94g, 10 day mTBI = 24.44  $\pm$  2.82g, 20 day mTBI = 24.54  $\pm$  2.26g; ANOVA  $F(3, 30) = 2.024$ ,  $p = 0.132$ ). Through the use of pulse oximetry during surgery, we found no incidence of hypoxia and no differences with respect to mean arterial blood oxygen saturation (Sham = 96.87  $\pm$  2.74%, 4 day mTBI = 96.66 $\pm$  1.97%, 10 day mTBI = 96.65 $\pm$ 2.84%, 20 day mTBI = 97.20  $\pm$  1.38%; ANOVA  $F(3, 30) = 0.093$ ,  $p = 0.963$ ) or mean respiratory rate between groups (Sham = 56.34  $\pm$  10.11, 4 day mTBI = 65.79  $\pm$  14.96, 10 day mTBI = 59.21  $\pm$  6.58, 20 day mTBI = 60.24  $\pm$  11.67; ANOVA  $F(3, 30) = 1.031$ ,  $p = 0.393$ ). Length of anesthesia used for each animal was also comparable (Sham = 38.92  $\pm$  2.88 min, 4 day mTBI = 39.05  $\pm$  4.40 min, 10 day mTBI = 47.17  $\pm$  3.68 min, 20 day mTBI = 43.86  $\pm$  4.11 min; ANOVA  $F(3, 30) = 1.06$ ,  $p = 0.380$ ). Examination of variation in the severity of injury between injury groups as measured in ATM also reveal no differences (4 day mTBI mean = 1.42  $\pm$  0.02 ATM, 10 day mTBI mean = 1.41  $\pm$  0.03, 20 day mTBI mean = 1.42  $\pm$  0.02; ANOVA  $F(2, 22) = 0.437$ ,  $p = 0.651$ ).

Following sham-injury or mTBI, animals were assessed for toe pinch reflex as well as righting reflex, a correlate of the return of consciousness in rodent models. We noted no death, apneic periods, or epileptiform motor movement in any animals following sham-injury or mTBI. While there was no statistical difference in return of toe pinch reflex between groups (Sham mean = 37.8 $\pm$ 11.6 sec, 4 day mTBI mean = 33.6 $\pm$ 13.1 sec, 10 day mTBI mean = 60.2  $\pm$  10.9

sec, 20 day mTBI mean = 46.3 +- 12.3 sec; ANOVA  $F(3, 30) = 1.03$ ,  $p = 0.394$ ), with respect to return of righting reflex, we noted a clear delineation between Sham and mTBI animals (Sham mean = 50.0 +- 12.3 sec, 4 day mTBI 244.3 +- 14.0 sec, 10 day mTBI 252.5+- 11.7 sec, 20 day mTBI 257.5 +- 13.1). Due to unequal variance based on Levene's test ( $F(3, 30) = 3.089$ ,  $p = 0.042$ ), nonparametric comparison using Kruskal-Wallis was performed and found to be significant ( $X^2 = 19.945$ ,  $p = 0.0002$ ). Steel-Dwass post-hoc analysis demonstrated sham righting reflex time was significantly different from each mTBI group (Sham vs 4 day mTBI  $p = 0.005$ , Sham vs 10 day mTBI  $p = 0.002$ , Sham vs 20 day mTBI  $p = 0.004$ ).

## **2.9 Basic pathological response to mTBI: I. Macroscopic change**

To confirm the reproducibility of our model, we performed qualitative assessment of brain tissue following sham-injury or mTBI. Consistent with mild TBI, no areas of macroscopic necrosis, contusion, subdural or subarachnoid hemorrhage were found in any of the animals studied. Epidural hematoma were found in both sham and injured animals however no volume assessments were performed as the hematoma was always restricted to the craniectomy site and peeled away during removal of the skull or removal of the dural membrane. The underlying brain was always visibly free of hematoma or hemorrhage after dissecting off the meninges.

The optic nerves were intact and non-hemorrhagic, although, at all post-injury time points, bilateral thinning was observed in the optic nerve segments just rostral to the optic chiasm. In contrast, the optic nerves in sham animals maintained a constant thickness along their length. Upon brain sectioning of sham and mTBI animals, no signs of hemorrhage were noted within the ventricles or parenchyma of either group. The mTBI sections did not exhibit any petechial hemorrhages within the cortex, thalamus, or along white matter tracts which is also consistent with the mild nature of our injury model.

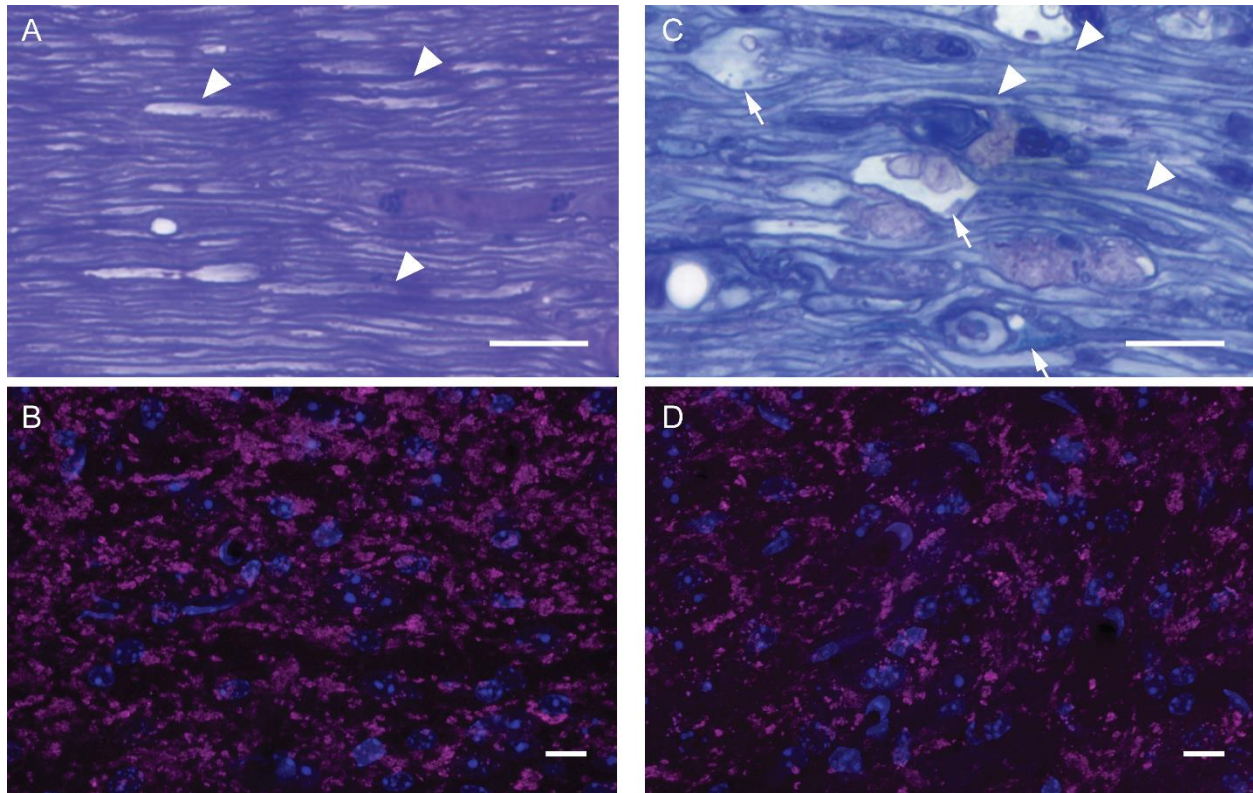


Figure 2.1 - Microscopic evaluation of longitudinal sections through the optic nerves from sham and 4 day post-mTBI mice (A & C) and confocal microscopic evaluation of the downstream axon terminals in dLGN through VGLUT2 immunohistochemistry (B & D). Sham-injured mouse optic nerve revealed normal histology with numerous thinly myelinated axons identifiable (arrowheads). The downstream axon terminals form scattered large clusters visualized in magenta with surrounding cell nuclei visualized in blue (B). By comparison, 4 days after injury, the optic nerve reveals axonal swellings (arrows) with pathologic accumulation of intracellular components and vesicles adjacent to normal appearing thinly myelinated axons (C). Downstream of the injured optic nerve was diffuse reduction in the large clusters of axon terminals visualized in magenta with surrounding nuclei in blue (D). Scale bars = 10  $\mu$ m.

## 2.10 Basic pathological response to diffuse axonal injury: II. Microscopic change

As seen in Figure 2.1A, plastic embedded thick sections of optic nerve from sham animals demonstrated many thinly myelinated axons as well as their supporting glia and vasculature consistent with previous studies (Inman, Sappington, Horner, & Calkins, 2006; Joos, Li, & Sappington, 2010; Mabuchi, Aihara, Mackey, Lindsey, & Weinreb, 2003; Mikelberg, Drance, Schulzer, & Yidegiligne, 1989). At 4 days post-injury, as seen in Figure 2.1C, microscopy revealed scattered diffuse axonal damage found among numerous intact axons within the optic nerve segments



rostral to the chiasm which is consistent with our previous descriptions in this model (J. Wang et al., 2013, 2011)(Wang et al., 2013, 2011). Examination of VGLUT2 immunoreactivity within dLGN allowed for identification of the retinogeniculate axon terminals downstream of the injured optic nerve. Assessment of this immunoreactivity in our sham-injured animals was consistent with previous reports of normal VGLUT2 immunoreactivity by others (El-Danaf et al., 2015; Hammer et al., 2014; Hammer, Monavarfeshani, Lemon, Su, & Fox, 2015). Within sham animals, the distribution of VGLUT2 immunoreactivity occurred in large clusters of variable size, likely composed of multiple axon terminals as they synapse on proximal dendrites of relay neurons. These axon terminal clusters appeared evenly distributed throughout dLGN, a finding consistent with reports on the normal ultrastructure of retinogeniculate synapses upon relay neurons within dLGN (Bickford et al., 2010, 2015; Guido, 2018; Hammer et al., 2014, 2015; Morgan, Berger, Wetzel, & Lichtman, 2016). Comparison of VGLUT2 immunoreactivity in mTBI animals 4 days post-injury to sham demonstrated the persistence of clusters (Figure 2.1B & D), however, the clusters in dLGN were more widely separated from each other, suggestive of axon terminal loss.

Further analysis of the optic nerve using CTB conjugated with Alexa fluorescent dyes demonstrated homogeneous filling in sham-injured animals. Coronal cross sections of the optic nerve from the optic disc to the chiasm demonstrated uniform labeling of right and left RGC axon tracts using epifluorescent microscopy (Figure 2.2B). The right and left RGC axon tracts remained identifiable as they decussated within the optic chiasm into ipsilateral and contralateral fibers for each side of the optic tract. While homogeneous filling was also seen in proximal coronal sections of both optic nerves in mTBI animals, we also noted scattered bright puncta within the injured segment of both optic nerves and drop in fluorescence in sections closer to the

chiasm. These findings are correlates of the DAI described above and in previous publications from our lab (J. Wang et al., 2011). Although not critically evaluated in the current study, it is of note that in both the sham and injured animals the fluorescence was not only homogenously distributed in the optic nerve, but also homogenously distributed in its established downstream projections, including the olivary pretectal nucleus, superior colliculus and LGN.

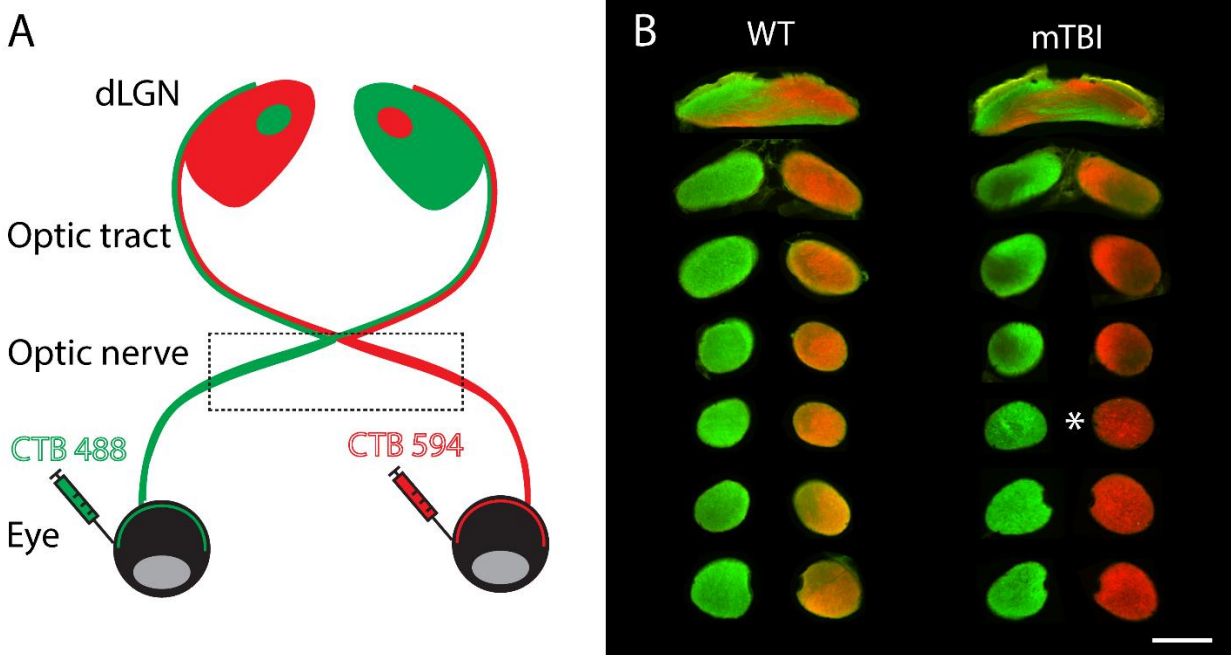


Figure 2.2 - Schematic representation of eye injections and visualization of tracer in the optic nerve. Recombinant cholera toxin  $\beta$  (CTB) conjugated to Alexa fluorescent dyes with two different excitation/emission profiles allow visualization of dLGN projections from the retinal ganglion cells labeled by eye injection of CTB. The projections outlined by the box in panel A are visualized in coronal sections of the optic nerve in panel B from uninjured mouse and 16 day post-injury mouse. Note the loss of fluorescent signal in mTBI sections downstream of the sections with bright puncta (marked with asterisk). Scale bar = 100  $\mu$ m.

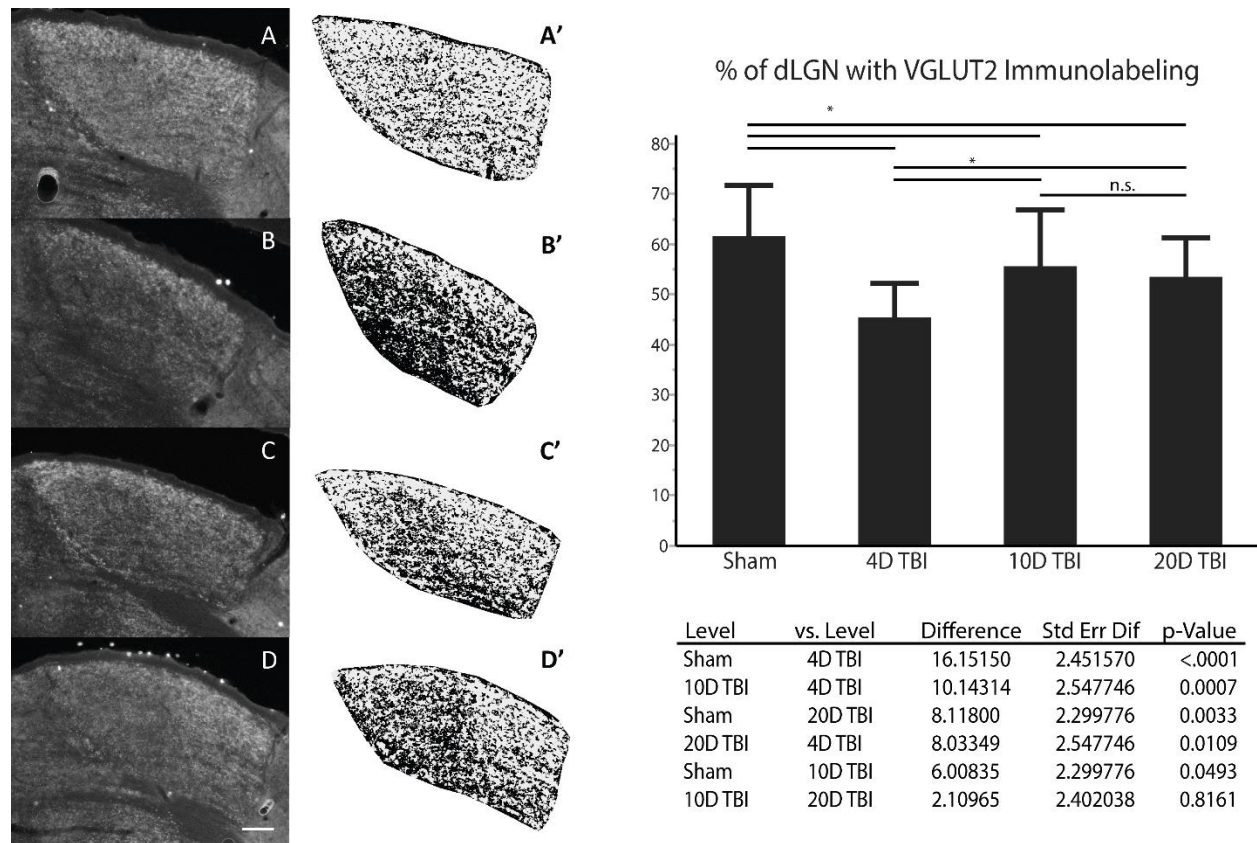


Figure 2.3 - VGLUT2 immunohistochemistry used to identify reorganization in dLGN following mTBI. Representative sections through anterior-posterior midline of dLGN in Sham (A), 4 day post-mTBI (B), 10 day post-mTBI (C), 20 day post-mTBI (D) are shown in grey scale prior to cropping surrounding image and conversion to binary image using threshold of 20% of illuminance (A' - D'); scale bar is 100 $\mu$ m. Data from each section is pooled by experimental group and the means compared using ANOVA with post-hoc pairwise comparison using Tukey-Kramer correction with p-values as shown in the table below graph. (Sham n = 36, 4D TBI n = 24, 10D TBI n = 30, 20D TBI n = 30; astrisk represents p-value < 0.05 for comparisons).

### 2.11 Evidence for mTBI/DAI induced deafferentation and reorganization in downstream target dLGN via VGLUT2 immunohistochemistry

To quantify the changes in VGLUT2 immunoreactivity within dLGN of animals at all three time points following mTBI or sham injury, we used an index based on the percentage of the dLGN area occupied by VGLUT2 immunostaining as detailed in the methods section and demonstrated in Figure 2.3. Specifically, the total area of dLGN that exhibited VGLUT2 immunoreactivity decreased at 4 days post-injury by approximately 26% compared to sham

animals (Sham = 61.6%, 4 day mTBI = 45.5%,  $p < 0.0001$ ). However, by 10 days post-injury, we noted a significant increase in area of dLGN demonstrating VGLUT2 immunoreactivity by approximately 22% compared to 4 day post-injury (10 day mTBI = 55.6%,  $p = 0.0007$ ). This increased distribution persisted at 20 days post-injury compared to 4 day post-injury (20 day mTBI = 53.5%,  $p = 0.0109$ ). Of note, neither the 10 day nor the 20 day post-injury group demonstrated full recovery of VGLUT2 immunoreactivity to sham levels and the difference on pairwise comparison was statistically significant for both pairs (10 day mTBI vs sham  $p = 0.0493$ , 20 day mTBI vs sham  $p = 0.0033$ ). Lastly, pairwise comparison of VGLUT2 immunoreactivity in 10 day and 20 day post-injury groups were found equivalent ( $p = 0.816$ ). Statistical analysis of the derived percentages were examined using Levene's test which demonstrated equal variances in the data from sham and all time points following mTBI ( $F(3, 116) = 2.397$ ,  $p = 0.072$ ). Analysis of variance (ANOVA) between samples from all four groups demonstrated significance of differences in variance ( $F(3, 116) = 14.767$ ,  $p < 0.0001$ ). Pair-wise comparisons between groups were performed utilizing Tukey-Kramer HSD to account for false discovery rate.

## **2.12 Confirmation of deafferentation and reorganization following DAI using anterograde tract tracing**

While VGLUT2 immunohistochemistry in dLGN is specific for retinogeniculate axon terminals in adult mice, it does not allow discrimination of whether the examined axon terminals originated from the ipsilateral or contralateral eye. We therefore performed anterograde tract tracing using fluorescent Alexa dyes conjugated to CTB to label axon terminals in mice that have undergone sham-injury or mTBI at the same time points addressed using VGLUT2 immunohistochemistry. By injecting recombinant cholera toxin subunit  $\beta$  (CTB) conjugated to

Alexa 488 or Alexa 594 into the right or left eye respectively after injury, we identified all retinorecipient brain regions connected to either retina through ipsilateral or contralateral projecting axons. Evaluation of all downstream targets of retinal ganglion cells in sham animals using epifluorescent microscopy demonstrated appropriate labeling of all subcortical targets including the superior colliculus, olivary pretectal nucleus, suprachiasmatic nucleus, ventral LGN, and intergeniculate body in addition to dorsal LGN. Additionally, through the use of the two fluorophores, we observed the distribution of ipsilateral and contralateral projections within these domains as reported by others (G Muir-Robinson & Hwang, 2002; Torborg & Feller, 2004). In contrast, the injured animals demonstrated decrease of CTB fluorescent signal in all subcortical targets mentioned above (not shown).

We quantitatively compared retinogeniculate axon terminals between the sham-injury group and the three time points following mTBI as we did using VGLUT2 immunohistochemistry. As noted previously, a percentage value for each section labeled through anterograde CTB labeling was derived as a percentage of dLGN area covered by CTB positive axon terminals from ipsilateral and contralateral projections. The measured overlap was then subtracted from the sum of ipsilateral and contralateral values to derive the percentage of dLGN labeled by axon terminals irrespective of the eye of origin. The derived percentages in each experimental group were then compared and presented in Figure 2.4. Statistical analysis demonstrated unequal variance between groups using Levene's test ( $F(3,97) = 3.927$ ,  $p = 0.0108$ ). We therefore used Kruskal-Wallis non-parametric comparison to demonstrate significance between groups ( $X^2 = 70.945$ ,  $p < 0.0001$ ). Using Steel-Dwass method to account for multiple pairwise post-hoc comparisons, we noted a 36% reduction in area of dLGN with fluorescent labeling at 4 day post-injury compared to sham-injury ( $Z = 6.182$ ,  $p < 0.0001$ ).

Mirroring our findings using VGLUT2 immunohistochemistry, we report that compared to 4 day post-injury, there is 23% increase in fluorescently labeled area at 10 day post-injury ( $Z = 3.650$ ,  $p = 0.0015$ ) and 26% increase at 20 day post-injury ( $Z = 4.097$ ,  $p = 0.0002$ ). Also, as noted for VGLUT2 immunohistochemistry, the partial recovery at 10 and 20 days post-injury did not reach sham values ( $Z = 6.223$ ,  $p < 0.0001$  and  $Z = 5.980$ ,  $p < 0.0001$  respectively). Moreover, no statistically significant change was witnessed from 10 day post-injury to 20 day post-injury ( $Z = 0.278$ ,  $p = 0.9925$ ), further suggesting that the axon terminal reorganization demonstrated through both VGLUT2 immunohistochemistry and CTB anterograde tracing did not recovery to sham levels by the time points chosen for this study.

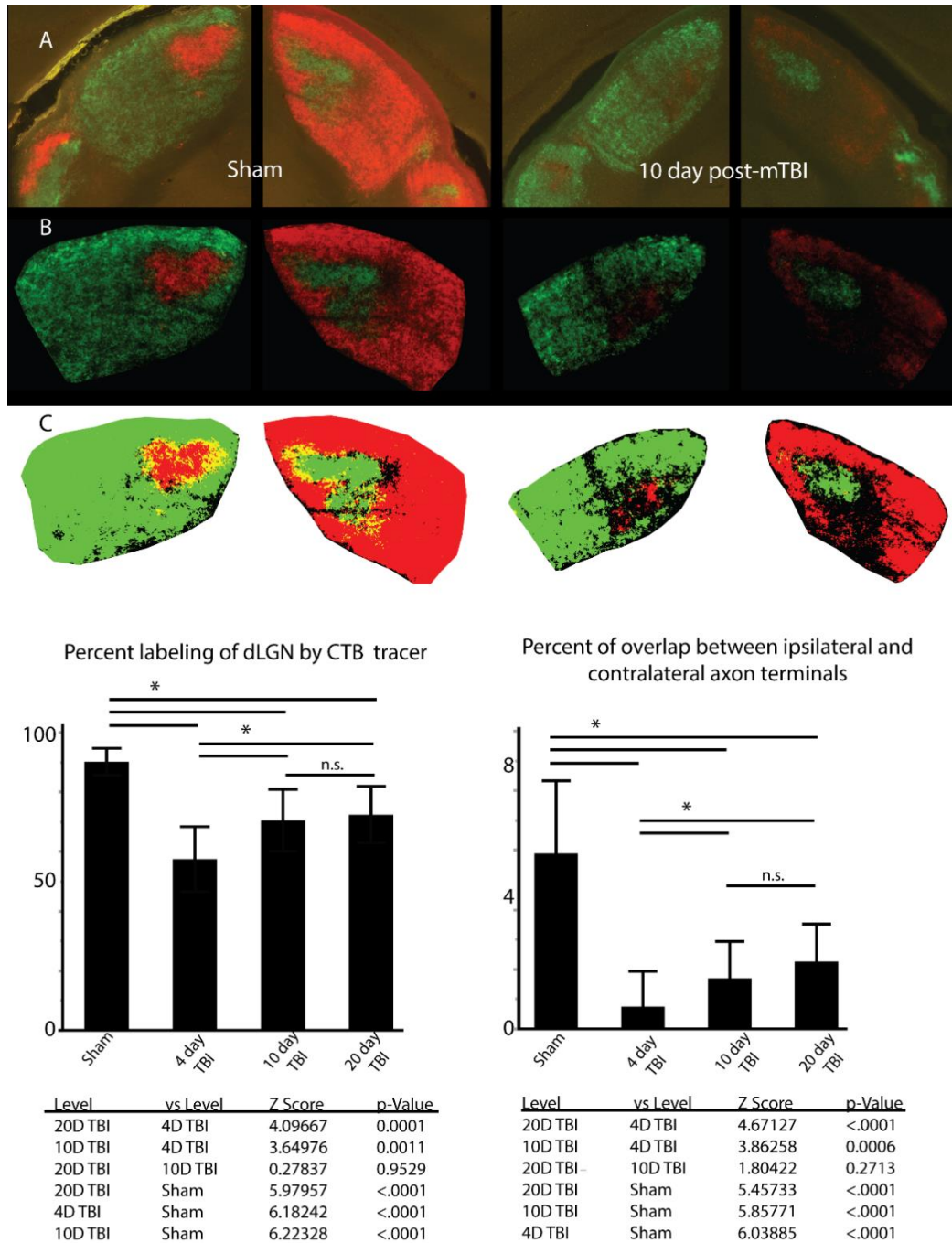


Figure 2.4 - Through the use of CTB conjugated to Alexa dyes to label retinogeniculate axon terminals, we find uniform labeling of ipsilateral and contralateral projecting axon terminals within both sides of dLGN (A). Images are adjusted for background fluorescence (B) before conversion to binary color scale images (C) for quantification of axon terminal reorganization. Examination of the percent of dLGN labeled by both ipsilateral and contralateral projecting axon terminals demonstrates a significant loss at 4 days post-injury which recovers at 10 days and 20 days post-injury. Examination of overlap between ipsilateral and contralateral projections demonstrates reorganization involves changes in the overlap between the two fiber populations however segregation is maintained relative to sham condition. Error bars derived from standard deviation. Asterisk over bars indicate comparison p value is < 0.05, n.s. = no significance.

### **2.13 Evaluation of eye specific axon terminals in dLGN following injury and reorganization in adult mouse.**

In addition to examination of dLGN area containing retinogeniculate axon terminals, we also examined the deafferentation and the subsequent reorganization response in relation to the overlap of ipsilateral and contralateral axon terminal fields within the AP midline of dLGN. Within this portion of dLGN, ipsilateral and contralateral axon terminals overlap significantly during the perinatal period and strongly segregate before adulthood (Guido, 2008; Huberman, Stellwagen, & Chapman, 2002). Due to the fact that all retinogeniculate axons express VGLUT2, our immunohistochemical analysis did not allow direct quantification of axon terminals based on retinal origin. This limitation was overcome by using recombinant CTB conjugated to different fluorescent Alexa dyes for each eye. In adult sham-injured animals, we demonstrated that the retinogeniculate axon terminal population maintained strong segregation of ipsilateral and contralateral inputs to the dLGN with average overlap measured 5.45%. By comparison, when comparing overlap between ipsilateral and contralateral projections in dLGN among TBI animals, there is even less overlap measured between the two axon terminal populations (4 day TBI = 0.68%, 10 day TBI = 1.56%, 20 day TBI = 2.08%) (Figure 2.4). Statistical analysis of the dataset demonstrated heteroscedasticity of data (Levene's test,  $F(3, 97) = 7.672$ ,  $p = 0.0001$ ) and thus non-parametric comparison using Kruskal-Wallis test was utilized to demonstrate significance between the percent of overlap of ipsilateral and contralateral projections in our comparison groups ( $X^2 = 68.4268$ ,  $p < 0.0001$ ). Each pair-wise comparison of differences using Steel-Dwass post-hoc analysis was found to be significant except for between 10 day vs 20 day post-injury ( $Z = 1.8042$ ,  $p = 0.271$ ). Despite the trend of increasing overlap over time following



injury, at 20 days post-injury, the measured overlap was still less than that present in our sham-injury group.

Analysis of only ipsilateral or only contralateral CTB labeled projections demonstrated the same pattern of loss at 4 days post-injury when compared to sham-injury animals, and similar reorganization at 10 days post-injury which persisted at 20 days post-injury. Analysis of variance of ipsilateral projecting retinogeniculate axon terminals demonstrated significance between Sham and TBI groups ( $F(3, 97) = 37.80, p < 0.0001$ ). Post-hoc analysis using Tukey-Kramer HSD confirmed significance of difference between Sham and all injury groups, as well as between 4 day post-injury group and both 10 and 20 day post-injury groups ( $p < 0.05$ ). Comparison between 10 day post-injury and 20 day post-injury again demonstrated no significance ( $p = 0.91$ ). Examination of contralateral projections yielded similar results. Due to the differences in variance between groups, non-parametric test was utilized for comparison and demonstrated differences between groups (Kruskal-Wallis,  $X^2 = 63.1948, p < 0.0001$ ). Pair-wise comparisons were all found to be significant (Steel-Dwass,  $p < 0.007$ ) except for 10 day post-injury vs 20 day post-injury ( $p = 0.999$ ). These considerations further suggest reorganization within dLGN following mTBI reaches equilibrium prior to reaching the distribution identified in sham animals at the chosen time points used.

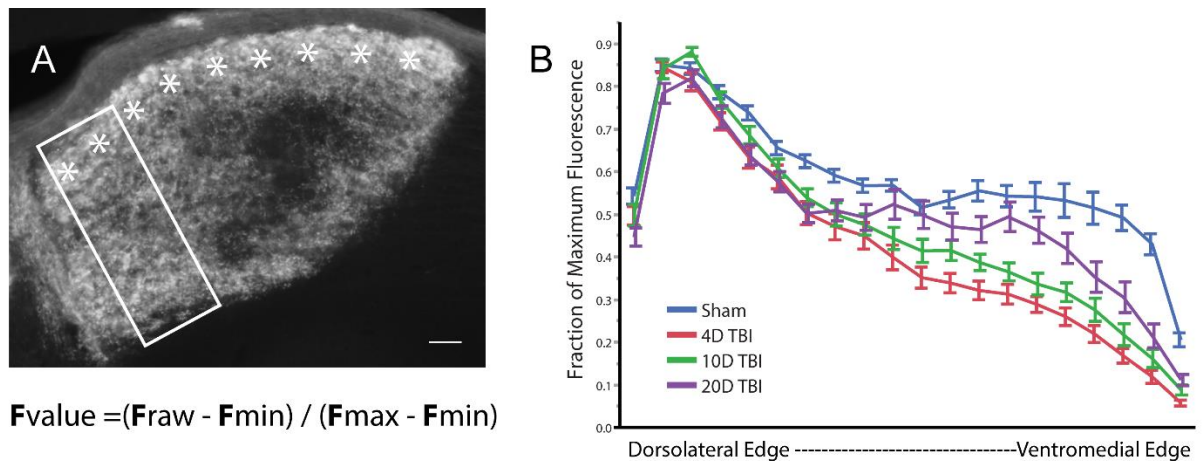


Figure 2.5 - In panel A, a section of dLGN from a sham mouse injected with CTB is shown. The shell is marked with asterisks. Using a rectangular window, we measured the plot profile of Alexa dye pixel intensity along the depth of the dLGN within the region receiving only contralateral inputs using methods described by Huberman et al. We normalized the values at each position along the depth using the formula above, where  $F_{min}$  is the minimum fluorescence value,  $F_{max}$  is the maximum fluorescence value, and  $F_{raw}$  is the signal intensity along each pixel width of the box for each given section. Normalized fluorescence values were binned at 5% intervals of the depth and averaged across all sections from all animals in each experimental group. Panel B demonstrates the change in fraction of max fluorescence as one moves from the dorsolateral edge to the ventromedial edge of dLGN for each group. Scale bar = 20um. Bars represent SEM. N = 3 to 4 animals per group with 3 to 4 samples per dLGN per animal.

#### 2.14 Evaluation of axon terminals from specific RGC subpopulations in the contralateral zone of dLGN following injury and reorganization in adult mouse.

In addition to dLGN being divided between regions which receive ipsilateral and contralateral visual input, the contralateral retinorecipient zone in dLGN is further organized into a dorsal shell and ventral core. Both the shell and core of this area in dLGN receive segregated inputs from specific unique subpopulations of retinal ganglion cells that only project to the contralateral dLGN and can be used to further differentiate changes in VGLUT2 immunolabeled as well as CTB labeled axon terminals within dLGN.

In sham animal sections that underwent immunohistochemistry for VGLUT2, there was no significant distinction found in axon terminal distribution between the shell and core of the

contralateral zone (Figure 2.3 – A). By contrast, at 4 days post-injury, we observed a marked drop in VGLUT2 immunolabeled axon terminal clusters in the core of dLGN while the shell appeared relatively spared of axon terminal cluster loss (Figure 2.3 – B). Moreover, while the distinction between the shell and core persisted at 10 days and 20 days post-injury, the difference in VGLUT2 labeling was less apparent (Figure 2.3 – C & D). Together, these changes in VGLUT2 expression within the shell and core of the contralateral zone are suggestive of reorganization. Efforts to quantify these differences in the shell and core through VGLUT2 immunohistochemistry were, however, unsuccessful due to narrow dynamic range of fluorescent signal intensity in examined sections.

In contrast to VGLUT2 immunohistochemistry, comparison of the relative fluorescent intensity in dLGN of axon terminals labeled by Alexa fluorophore in CTB injected animals demonstrated relatively stronger fluorescent signal in the shell compared to the core in both sham and mTBI animals (Figure 2.5B). When we compared the relative fluorescent signal of the shell to the core in sections from 4 day post-injured animals, the difference in relative fluorescence between the shell and core was larger, suggestive of vulnerability of the core to axon terminal loss or general sparing of axons which project preferentially to the dorsal shell. By 10 day post-injury, however, the core demonstrated more fluorescent signal intensity compared to 4 days post-injury and furthermore, at 20 day post-injury, the difference in signal between the shell and core continued to gradually approach the distribution pattern in sham animals. In conjunction with the results of the VGLUT2 immunohistochemistry data analysis, these findings support the premise that following DAI, a reactive response occurs in the intact axon population to repopulate lost input to dLGN relay neurons and that this response maintains eye specific segregation suggestive of adaptive structural plasticity.

## 2.15 Discussion

In this current study, we utilized the mouse central fluid percussion injury model of mild TBI to induce diffuse axonal injury in the optic nerve. Using with two independent methods to identify the downstream axon terminal fields of injured axons and by evaluating both the deafferentation and reorganization response among axon terminals in dLGN, we provide for the first time, insight into the potential consequences of mTBI induced DAI. One of the three vesicular glutamate transporters expressed in mammalian central nervous system, VGLUT2, is necessary for glutamatergic transmission in the diencephalon where dLGN forms and develops and is the specific isoform of VGLUT present in retinogeniculate axon terminals (El-Danaf et al., 2015; Hammer et al., 2015; Moechars et al., 2006) . In this regard, VGLUT2 immunohistochemistry provided us with a highly specific method to identify and compare retinogeniculate axon terminals in dLGN across each time point. As a result, we have high confidence in the quantification of our findings demonstrating axon terminal loss and subsequent reorganization through the analysis of dLGN area with VGLUT2 labeling.

Our use of anterograde axon terminal labeling with CTB conjugated to fluorescent dyes provided further insight into the reorganization of dLGN following DAI. Recombinant CTB labels neurons by irreversibly binding with GM1 gangliosides that diffuse along all fine projections of labeled neurons in both anterograde and retrograde fashion (Fort & Jouvett, 1990) . In contrast to immunohistochemistry, anterograde tracing assures that epitope masking or cross reactivity of antibodies is not a confounder, thus increasing sensitivity to find changes in axon terminal distribution. Additionally, by using two different fluorophores conjugated to CTB for right and left eyes in each animal, we were able to demonstrate that not only is there axon terminal loss following DAI and subsequent reorganization, but also that this reorganization

maintained the adult pattern of segregation between ipsilateral and contralateral axon terminals within dLGN. Use of an anterograde tracer such as CTB also provided confirmation that the dLGN axon terminals identified in our experiments remained contiguous with their soma of origin as the molecule does not diffuse across synapses or disassociate once it is bound to GM1 gangliosides (Fort & Jouvett, 1990). As CTB diffuses to all projections of labeled neurons, we are again reassured that the observed reorganization is not secondary to changes in strengthened latent connections but rather a structural reorganization among the intact retinogeniculate axon population.

In addition to demonstrating the potential for axon terminal reorganization within dLGN of adult mice following mTBI, we have also demonstrated the potential for different subpopulations of retinal ganglion cells to respond differently to DAI. Despite the homogeneous nature of injury within the optic nerve, we observed differences in reorganization between the shell and core of the dLGN contralateral zone. Specifically, axon terminals projecting to contralateral zone shell remained identifiable following injury compared to axon terminals projecting to the contralateral zone core. This finding suggests that RGCs and their axons that project to the shell of dLGN are more resilient than their counterparts projecting to the core. As an alternative hypothesis, the axon terminals within the shell may reorganize more rapidly compared to their counterparts in the core, however, this is less likely. Both possibilities, however, suggest that different RGC subpopulations respond differently to mTBI.

Through the methods employed in this report, we were unable to determine if the RGC subpopulations that innervated the shell and core of dLGN were the same subpopulations that contributed to axon terminal reorganization in those two regions. This issue can be addressed in future investigations using transgenic labeling of retinal subpopulations. Additionally, while we

report that retinogeniculate axon terminals reached equilibrium in reorganization prior to 20 days post-injury, we have not determined if this reorganization continues beyond 20 days. The apparent equivalence between our measurements at 10 days and 20 days post-injury may have masked a dynamic process in which axon terminal sprouting occurred concurrently with axon terminal pruning. Furthermore, the lack of functional or behavioral examination of the visual axis also leaves us without the ability to confirm if the observed reorganization was functionally adaptive or maladaptive. However, as the ventrotemporal retina dominates the contribution to ipsilateral input in dLGN, we believe determination of adaptive vs maladaptive plasticity may be tested through behavioral examination of recovery in central vision or function examination of the binocularly responsive portion of dLGN (Coleman et al., 2009; Howarth, Walmsley, & Brown, 2014; Young et al., 2013). While behavioral or functional examination of plasticity in RGC projections is beyond the scope of our current report, it remains of great importance to further understanding repair and recovery mechanisms following deafferentation within the adult mammalian brain.

Although current literature addressing mTBI demonstrates the occurrence of DAI as assessed via ultrastructure microscopy and histopathologic markers, the implications of deafferentation secondary to axonal injury has yet to be thoroughly addressed. Few have considered that diffusely damaged axons could result in extensive terminal loss which most likely contributes the morbidity associated with mTBI while also setting the stage for recovery via axonal plasticity. While other authors have demonstrated maladaptive axon plasticity in the rat thalamus following cFPI, the studies utilized a higher energy fluid pressure pulse of 1.9 ATM with the goal of modeling moderate TBI (Hall & Lifshitz, 2010; Thomas et al., 2012). The findings of maladaptive connections and stimulus hypersensitivity in these studies may be linked to the

extent of deafferentation in the thalamus, or the direct injury to the cortex which they demonstrate to also be significantly injured. Additionally, the interval between injury and maladaptive plasticity measured by the behavioral response to whisker stimulation in the rat was 1 month following injury. By contrast, in this study we used an impulse of 1.4 ATM to model mild TBI in mouse and do not see dramatic overlap between ipsilateral and contralateral retinal projections in dLGN up to 20 days following injury. The rapid reorganization shown in dLGN at 10 days following injury may highlight a period of plasticity following injury that can lead to maladaptive plasticity if meaningful connections are unsuccessful early in the post-injury period. While our examination of the overlap between ipsilateral and contralateral retinal projections suggests the axon plasticity is adaptive, future functional studies will be required to corroborate the structural findings.

Through the use of both VGLUT2 immunohistochemistry and CTB anterograde tracing of retinal ganglion cell axon terminals projecting from the retina to the dLGN, we believe our techniques have the sensitivity and specificity to support the claim that the visual system is capable of adaptive axon plasticity and provide new information on how the mammalian brain responds to mild diffuse axonal injury. In addition to our finding's general relevance to DAI and potential brain reorganization, we also believe that these studies provide critical insight into the visual symptoms and their course described in those who have sustained mild TBI. Specifically, while we do not reflect on how deafferentation of dLGN correlates with VEPs, the delayed and reduced amplitude of visually evoked potentials (VEP) in human studies following mTBI reflects disruption of axons between the retina and the visual cortex. Further, mTBI patients with visual symptoms that abated or returned to baseline with rehabilitation may also be explained by adaptive axon plasticity as presented in this report (Freed & Hellerstein, 1997; Kapoor et al., 2004;

N. K. Yadav et al., 2014) . These human studies suggest that the structural reorganization in the dLGN following mTBI may occur as an adaptive response rather than a maladaptive response but the consequences of reorganization in other brain regions and sensory modalities vulnerable to DAI will require continued investigation.

### **Acknowledgements**

This research was supported by the NICHD of the National Institutes of Health under award number R01 HD055813. Microscopy was performed at the VCU Microscopy Facility, supported, in part, by funding from NIH-NCI Cancer Center Support Grant P30 CA016059. The content is solely the responsibility of the authors and does not necessarily represent the official views of the National Institutes of Health. This chapter was accepted for publication 2016 and was printed in the March 2017 edition of *Experimental Neurology*, 289, p85–95.



## **Chapter 2B – Supplemental Evidence Regarding Adaptive Plasticity within the Dorsal Shell of dLGN using DRD4-GFP transgenic mouse.**

### **2.16 Introduction**

The availability of transgenic mice which selectively express fluorescent molecules has allowed for dramatic changes in the approach to identification of neurons and their efferent projections. Specifically, study of the retina and retinogeniculate projections has benefitted substantially from the development of transgenic mice along with fluorescent markers (Kerschensteiner & Guido, 2017). These studies have allowed for identification of specific subpopulations of retinal ganglion cells which have divergent electrophysiologic responses to light stimulus across their receptive field. Directionally selective retinal ganglion cells (DSGC) are one such subpopulation of neurons. Collectively, they respond to a center-ON stimulus moving in one of three cardinal directions across their receptor field (Huberman et al., 2009; J. Kay, Huerta, Kim, & Zhang, 2011; Kim, Zhang, & Meister, 2010; Rivlin-Etzion et al., 2011). They are expressed across the retina in a mosaic distribution pattern and have highly stereotyped pattern of projection to the dorsal shell of dLGN. Of particular interest, the localize of these projections specifically to the dorsolateral border of dLGN coincides with where a high degree of stability of retinogeniculate projections was noted in the previous results following mTBI (Patel, et al., 2016).

To probe whether the connections in the dorsolateral margin of dLGN played a role in adaptive vs maladaptive changes in the structural plasticity of projections to the core of dLGN, we utilized the DRD4-EGFP transgenic mouse line to identify a subpopulation of center-ON retinogeniculate cells tuned to respond to stimulus moving in the posterior direction across their retinal receptor field. Among retinal ganglion cell subpopulations of the DRD4-EGFP transgenic

mouse line, 5 to 9% of cells are tuned to light moving in the posterior direction across their receptor field and are labelled by production of green fluorescent protein (GFP) (Huberman et al., 2009). The projections of these RGCs within the dLGN have been demonstrated to exclusively localize to the dorsal lateral shell of the contralateral zone. Studies on the function of directionally tuned RGCs and their role in vision have demonstrated their downstream thalamic relay cells in the dorsal shell of dLGN are similar in function to the ‘W’ relay cells in cats and koniocellular cells in primates and involved in cortical processing of motion in layers 2-3 of V1 visual cortex of mice.

### **2.17 Supplemental Methods:**

DRD4-EGFP animals were obtained in the homozygous state from the lab of Dr. Andrew Huberman. This transgenic line was originally produced using bacterial artificial chromosome (BAC) vector insertion by the GENSAT projection (Gong et al., 2003). In accordance with current best practice protocols, we backcrossed the homozygous mice with C57Bl6-J mice from Jackson Labs to produce heterozygous carriers. Unfortunately, after determining the expression profile of heterozygous animals was inadequate for detailed histologic analysis, the animals were then bred back to be homozygous carriers. This increased the expression of GFP in the posteriorly tuned DSGCs to levels consistent with literature published with this line. Fluorescent immunohistochemistry against GFP was utilized to further strengthen the endogenous fluorescent signal and stabilize fluorescence for imaging purposes. This strategy was successful however a limitation is that future generations of homozygous breeding pairs have increased susceptibility to gene locus translocation as well as gene duplication. Pups from homozygous breeding parents were spot checked using qPCR based technique from Transnetyx (Cordova,

TN) using primers for the GFP gene to confirm gene copy number prior to experiments.

Additionally, it was noted that pups from different breeding pairs had variation in GFP expression and to ensure consistency, pups from the same litter were utilized for experiments.

Adult male homozygous DRD4-EGFP mice were exposed to sham or mild central fluid percussion injury (cFPI). Due to limited number of animals available at time of experiments, only 1 animal was prepared for analysis at 4 days and 20 days following injury. Animals were obtained from the same litter for further consistency in gene expression. The tissue was prepared for histologic analysis using 4% paraformaldehyde in millonig's buffer. Coronal free-floating sections were obtained using the vibrating blade microtome to create 40 $\mu$ m thick sections. Fluorescent immunohistochemistry was performed using Rabbit IgG Polyclonal Antibody from Thermo Fisher Scientific, catalog # A-6455, diluted 1:1000. Sections were incubated overnight at 4 degrees in primary antibody. Incubation with secondary antibody was performed using Goat anti-Rabbit antibody conjugated to Alexa 488 (Life Technologies, Cat #A11034) diluted 1:500 in blocking buffer for 2 hours to stabilize the GFP fluorescent signal. Sections were serial washed in PBS, then phosphate buffer, followed by mounting with anti-fade mountant (Life Technologies, Cat. No. P-36931) and cover slipped. Slides were cured overnight while protected from light and edges sealed with nail varnish prior to storage and imaging.

Confocal microscopy was performed for qualitative examination of GFP positive axon terminals using a Zeiss LSM 700 scanning laser microscope with a Nikon Plan-Apochromat 20x/1.57 objective. The derived Z-stack images were obtained with consideration of Nyquist sampling and saved in CZI format for later examination. Images were processed using Zen Black (Carl Zeiss) to produce maximum intensity projections from Z-stacks. Images were processed for localization of GFP positive axon terminals as a vertical plot profile through the contralateral

projection zone as performed for examination of CTB fluorescent signal within contralateral zone of dLGN.

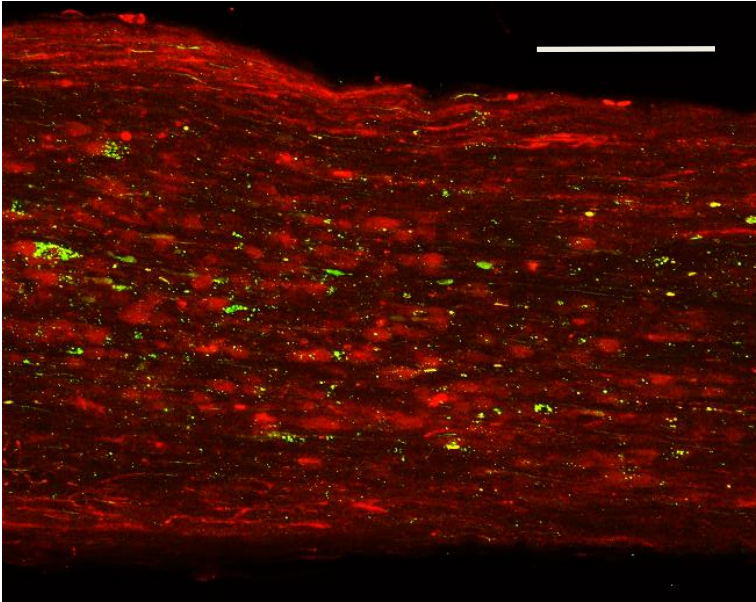


Figure 2B.1 – longitudinal section of optic nerve proximal to the site of disconnection in a DRD4-EGFP transgenic mouse exposed to mTBI 24hrs prior. APP, a marker for proximal axonal swellings following disconnection in traumatic axonal injury is visualized with immunohistochemistry using secondary antibody conjugated with red fluorescent marker. GFP expression marking DRD4 positive retinogeniculate axons are visible using green fluorescent marker to strength signal. Scale bar 100um.

### 2.18 Results:

Previous efforts examining axonal injury in the optic nerve demonstrated significant APP staining present at the 24hour time-point following injury (J. Wang et al., 2011). Using the DRD4-EGFP transgenic mouse, we examined the optic nerve after 24hrs following exposure to central fluid percussion injury. Following injury, we note axonal swelling consistent with axonal injury is present in the optic nerve after 24 hours. Qualitative assessment demonstrates some of the APP positive axonal swellings are also positive for GFP, denoting their origin from posteriorly-tuned

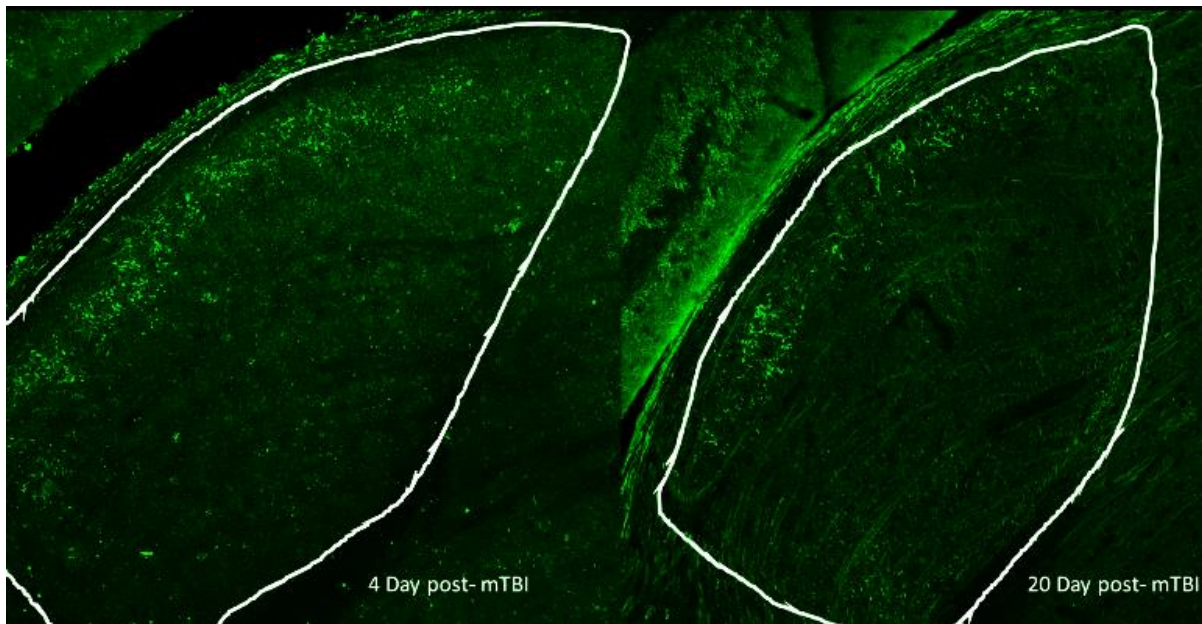


Figure 2B.2 – dLGN downstream from the site of optic nerve injury in DRD4-EGFP mice at 4 days and 20 days following exposure to mTBI. The GFP positive projections remain confined to the dorsolateral shell of dLGN despite widespread axon terminal reorganization seen in the anterograde labeling and VGlut2 immunohistochemistry studies. The borders of dLGN are outlined in both representative sections. Images were obtained using confocal microscopy (LSM 700 Carl Zeiss) to generate a Z-stack using a 20x primary objective and processed to generate a maximal-intensity projection using software from Carl Zeiss (Zen Lite Black).

ON-center directionally selective retinal ganglion cells in the DRD4-EGFP transgenic mouse line (Figure 2B.1). Downstream, qualitative examination of sections in dLGN demonstrated that at both 4 day and 20 day, retinogeniculate projections to the dorsolateral shell of dLGN did not demonstrate invasion of projections into the core of dLGN (Figure 2B.2). Quantification of the segregation of inputs to the shell of dLGN using methods described in methods section 2.5 demonstrates the projections remain segregated to the dorsolateral shell however the limited sample size does not allow for statistical examination (Figure 2B.3). These findings are consistent with what is seen during the development of directionally selective projections to the dorsal shell of dLGN without evidence for reorganization of these projections into the core of dLGN however broader question of how reorganization in this subset of retinal ganglion cells

reorganize following injury cannot be determined with the limited number of animals available to us for examination.

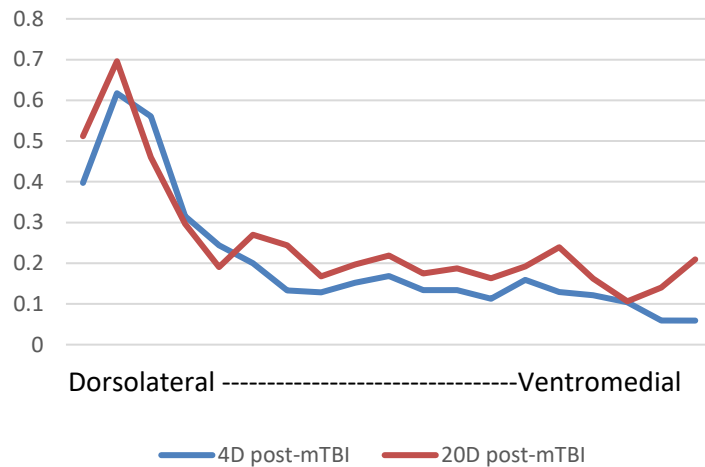


Figure 2B.3 – Using methods described by Huberman et al. to examine segregation of retinogeniculate projections to the dorsolateral shell of dLGN finds that the distal projections in the DRD4-EGFP transgenic mice remain confined to the shell and do not extend into the core of dLGN following central fluid percussion injury despite widespread reorganization demonstrated with anterograde tract tracing and VGlut2 immunohistochemistry.

## 2.19 Discussion

Directionally selective retinal ganglion cells represent a subset of ganglion cells with a very specific projection pattern to the dorsal shell of the contralateral retinorecipient LGN. With these characteristics in mind, the directionally selective population of retinal ganglion cells represented an opportunity to examine a unique subset of retinal ganglion cells with a highly specific projection pattern to LGN and note if their response to injury and recovery in mTBI involves maladaptive changes in this projection pattern. The DRD4-EGFP line is a well-established mouse transgenic line in which directionally selective retinal ganglion cells tuned to movement in the posterior direction across their receptive fields are labeled with GFP expression (J. Kay et al., 2011). Using this transgenic mouse, we identified that axons from posteriorly tuned retinal ganglion cells are vulnerable to injury as demonstrated by APP containing axon swellings. We further identified that subsequent reorganization in adult mouse LGN does not demonstrate maladaptive structural plasticity following injury. The lack of projections extending into the core

of dLGN despite the previously described expansion of retinogeniculate axon terminals throughout dLGN suggest the ensuing reorganization continues to remain confined to their expected downstream target relay cells.

Examination during development of specific subgroups of retinal ganglion cells and the fidelity with which they innervate their target relay cells during development have demonstrated that directionally selective cells are particularly accurate in their ability to target the dorsal shell of LGN without relying on refinement. This is in contrast to other subsets of retinal ganglion cells are more likely to have broad innervation crossing into neighboring regions of their usual projection patterns with subsequent refinement (Osterhout, El-Danaf, Nguyen, & Huberman, 2014). This distinction is due to the specific neural signal molecules or ligand binding cues that different RGC relay cells utilize during development for proper wiring, however, small molecule and ligand/receptor systems are not able to correctly result in functional wiring of the visual system alone. The development of function wiring from the retina to the visual cortex additionally relies on visual experience. Visual experience refers to the firing of retinal ganglion cells after development of the retina, both before and after eye opening. Spontaneous retinal activity is responsible for modification of The LGN relay cells targeted by directionally selective RGCs are similar in function to the W-like cells in cat and koniocellular layer of primate LGN (Denman & Contreras, 2016) (Denman & Contreras, 2016). Enucleation studies demonstrate the projections of these RGCs selectively innervate the contralateral LGN (J. Kay et al., 2011).

Utilization of transgenic mice that have been created using bacterial artificial chromosomes such as the DRD4-EFGP line in study of injury is confounded by variable expression of the reporter protein between litters of breeding pairs as well as over time as animals age. These limitations make side by side quantification of the effects of an intervention

difficult to statistically analyze. The directionally selective retinal ganglion population has also been found to express a neuropeptide called CART (cocaine- and amphetamine-regulated transcript). Future studies may benefit from cre-recombinase based cell labeling utilizing this gene to turn on transcription of a fluorescent reporter gene with higher fidelity rather than relying on bacterial artificial chromosome based transgenic mouse lines (J. Kay et al., 2011; J. R. Sanes & Masland, 2015).

Future studies may benefit from continued study of this subset of retinal geniculate projections to identify if the unique properties noted during development confer additional benefit to recovery following injury. For example, given the finding that retinal projections to LGN synapse onto one of three known subsets of LGN relay neurons (X-, Y-, W-like cells) and their roles in the formed vision pathway of higher order mammals, identifying if recovery of visual function is determined by recovery in one particular subset or by the recovery in innervation of all subsets of LGN relay neurons.



**Chapter 3 – Electrophysiologic connectivity between retinogeniculate projections and dLGN relay neurons following mTBI induced reorganization demonstrates intact fiber volley and normal paired-pulse depression across time points.**

Abstract:

Mild TBI is a pathology process resulting in diffuse axonal injury and deafferentation of downstream neurons. The process is linked with electrophysiologic dysfunction which can be objectively measured in both clinical and animal models. Studies in the structural and electrophysiologic properties of the visual pathway have provided significant insight into the connectivity of the retinogeniculate pathway during development and provide a foundation for study of recovery following axonal injury and deafferentation. Utilizing this experience to examine this pathway following TBI has identified that while we note structural adaptive recovery of axon terminals in the retinogeniculate pathway over a time scale of days, electrophysiologic connectivity between retinal inputs and LGN relay neurons is preserved following TBI. We find that relay neurons in the lateral geniculate nucleus demonstrate normal physiologic response to excitatory input from the optic tract and preserved fiber volley despite diffuse deafferentation following mild TBI. The preservation of normal electrophysiologic responses precedes the structural changes noted in our previous publication and suggests adaptive plasticity in the retinogeniculate pathway may rely on homeostatic mechanisms and unmasking of quiescent connectivity. We find that recovery of normal activity in the visual cortex following mild TBI over time is associated with both structural and electrophysiologic adaptive changes in the retinogeniculate pathway.

### **3.1 – Introduction: Visual complaints in mTBI coincide with objectively measured electrophysiology changes in both clinical reports and animal models.**

Mild traumatic brain injury (mTBI) is an acquired disease process in which physical force causes shear injury to the brain resulting in axon injury and loss, followed by deafferentation of downstream targets (Christman et al., 1994; J. Povlishock & Christman, 1995). The loss of connectivity between neurons results in cognitive, affective, and somatic sequela that typically resolve within 6 months following injury in most cases, however, some patients will continue to have a degree functional impairment that is long standing or permanent (Dean et al., 2015; McInnes et al., 2017). This dysfunction has been studied extensively via histologic and electrophysiologic analysis, however, the processes involved with recovery following mTBI remains a subjective of significant interest with ongoing coordinated efforts between multiple domestic and international agencies to support numerous clinical and laboratory research studies (NIH Publication No. 15-2478, ninds.nih.gov).

Visual complaints following mTBI are commonplace and found to be a significant source of morbidity by interfering with rehabilitation and recovery following injury (Alvarez et al., 2012)(Alvarez et al., 2012). Symptoms included photophobia, eyestrain, difficulty reading, decreased light, flicker, and pattern perception, and oculomotor dysfunction (Ciuffreda et al., 2007; Du, Ciuffreda, & Kapoor, 2005; Hellerstein, Freed, & Maples, 1995; Kapoor & Ciuffreda, 2002).

Recently, studying the visual axis using the central fluid percussion injury model, we have reported that following mTBI induced deafferentation of the lateral geniculate nucleus (LGN) in the mouse, structural plasticity of remaining retinogeniculate inputs leads to an adaptive structural reorganization over the course of several days (Patel et al., 2016). Using the central fluid percussion model, we induced partial axonal injury in the optic nerve, cortical, and

subcortical grey and white matter. Within the optic nerve, a proportion of axons undergo irreversible microtubule collapse and Wallerian degeneration (J. Wang et al., 2011). The retinal ganglion cells that project these injured axons atrophy and fail to mount a regenerative response (J. Wang et al., 2013). In a downstream target of the retinal ganglion cells, the LGN loses a significant number of inputs which we quantified as a decrease in density of axon terminals originating from the eyes targeting both ipsilateral and contralateral LGN. An initial loss of retinogeniculate axon terminal density noted at 4 days after injury was followed by reorganization and expansion of the retinogeniculate axon terminals when examined at 10 days following injury and noted to be stable at 20 days following injury. We demonstrated that the structural proliferation of axon terminals from different subgroups of retinal ganglion cells that survive following injury, also remained confined to their expected target areas in dLGN following partial axon loss in mTBI. The adaptive response was assessed using tract tracing using cholera toxin  $\beta$  (CTB) conjugated to Alexa fluorescent dyes and their terminal boutons were additionally examined using immunohistochemistry against VGLUT2, a marker for retinogeniculate axon terminals in dLGN (Land, Kyonka, & Shamalla-Hannah, 2004).

In addition to the structural changes noted in the retinogeniculate pathway, we have also seen adaptive changes in the cortical response in the visual axis following mTBI which match the time scale of the structural changes in dLGN (Krahe, E., Wang, & Povlishock, 2013). Using electrodes placed into right and left layer 4 of V1 visual cortex of mice after sham surgery or mTBI, visually evoked potentials (VEP) were recorded in response to full field 100% contrast sine wave gratings presented to the ipsilateral or contralateral eye separately. Visually evoked potentials were recorded every other day starting on day 4 after sham or mTBI surgery and carried out to greater than 10 days following surgery. Normal VEP waveform and amplitudes

were found in sham animals along with a preference for stimulus presented to the contralateral eye. Animals who underwent mTBI surgery initially demonstrated over 50% loss of amplitude and no preference for stimulus presented to either eye, however, amplitude returned to sham levels on recordings performed 8 or more days following injury and cortical responses again began favoring contralateral eye stimulus (Krahe et al., 2013).

Presented with evidence that the structural plasticity we noted in the visual axis occurs on a similar time scale with adaptive changes found in the cortical response to visual stimulus, we examine the electrophysiologic response of the retinogeniculate projections to dLGN relay neurons to determine if the structural adaptive reorganization we reported previously may contribute to the adaptive changes noted over time in the cortical response to visual stimulus. The retinogeniculate synapse is a well characterized system and has proven to be instrumental providing information on how synaptic plasticity contributes to the development of the mature central nervous system (Y. Hong & Chen, 2011). Furthermore, the retinogeniculate synapse has been instrumental in understanding how short-term plasticity contributes to temporal processing of information (Zucker & Regehr, 2002). Previous examination of the function and plasticity of retinogeniculate projections has relied on ex-vivo patch-clamp electrophysiology (C Chen & Neuron, 2000; C Chen & Regehr, 2003). Electrophysiologic study of VEP in sham and injured conditions can provide the ability to identify if connections are appropriately responsive to input or functioning in a maladaptive fashion through examination of their ability to participate in neural facilitation or depression, two basic mechanisms of short-term plasticity. These mechanisms act as dynamic filters for information transmission and are dependent on pre-synaptic and post-synaptic mechanisms. Simulation studies in which mechanisms of short-term plasticity are altered or removed demonstrate that deficits can arise in temporal processing of

information (Buonomano, 2000). Specifically, at the retinogeniculate synapse which relies on glutamate release, there is paired-pulse depression noted in response to a stimulus provided 100 to 120ms apart. This depression is attributed to a decreased release probability of neurotransmitter in response to the second stimulus as well as a decrease in the quanta of neurotransmitter released in response to the stimulus (Zucker & Regehr, 2002). Mechanism of this depression are related to pre-synaptic modulation via dopaminergic inputs onto the presynaptic membrane of retinogeniculate axon terminals as well as glutamate receptor modulation in the post-synaptic dLGN relay cell. Dopaminergic inputs onto retinogeniculate synapses have implicated in strongly depressing the amplitude of glutamate-mediated EPSCs in the post-synaptic dLGN relay neurons in paired-pulse stimulation via D2 receptors on the pre-synaptic membrane (Govindaiah & Cox, 2006). Additionally, the post-synaptic dLGN relay cell responds to glutamate release from retinogeniculate axon terminals via both AMPA and NMDA receptors (Hohnke, Oray, & Sur, 2000). The timing and tonicity of spike delivery has been attributed to the differential activation of the AMPA and NMDA receptors. The interaction between how these two receptors are activated on the post-synaptic membrane has been demonstrated to modulate the efficacy of activity transmission between retinogeniculate axon terminals and dLGN relay neurons (Blitz & Regehr, 2003).

Investigation of the electrophysiologic properties of retinogeniculate synapses have been generalized to other areas of the CNS including the somatosensory system, and brainstem (Kano & Hashimoto, 2009; Lu & Trussell, 2007; H. Wang & Zhang, 2008). The mechanisms of short-term plasticity are important for decoding information in a meaningful pattern. Deficits in temporal processing are seen in clinical studies of visually evoked-potentials (VEP) following mTBI where the timing and amplitude of scalp recorded potentials are altered and associated with

clinical changes in visual stimulus perception (Kapoor & Ciuffreda, 2002; Lachapelle et al., 2008; Lachapelle, Ouimet, Bach, Ptito, & McKerral, 2004; Spiegel et al., 2016). Changes in perception of visual stimulus following mTBI are usually transient and resolve with time further supporting the study of adaptive plasticity in the visual axis (Slobounov, Tutwiler, Sebastianelli, & Slobounov, 2006). To address if recovery of function at the level of the visual cortex following mTBI correlates with changes in functional connectivity of the retinogeniculate synapse, we used the mouse model of mild central fluid percussion injury to determine if changes in functional connectivity correlate with the adaptive structural change in retinogeniculate axon terminal density in dLGN following axon loss in the optic nerve.

### **3.2 Methods - Slice preparation for electrophysiologic assessment of dLGN relay neurons**

Using the techniques available to us to produce brain slices appropriate for electrophysiologic analysis of dLGN relay neurons, we estimated the number of inputs and performed paired pulse stimulation to identify if intact connections are also responding in the expected manner. Adult C57BL/6J mice (9-12 weeks of age) were sourced directly from Jackson Laboratory (Bar Harbor, ME) or bred and maintained in house. Animals obtained from Jackson Laboratory were kept in house at minimum 48 hours prior to experiments to habituate to our vivarium. Animals were evaluated at 4, 10, and 20 days after sham or mTBI surgery.

Surgery was performed using general anesthesia with inhaled isoflurane (<5%) before placing the animal in a stereotactic head holder. Toe pinch reflexes were monitored during surgery and anesthetic concentration adjusted to maintain anesthesia depth. The skin was opened over the skull and a 3mm craniotomy midway between lambdoid and bregma cranial sutures was performed using a hand trephine. Care was taken to keep the underlying dura intact and a

dissecting microscope was utilized to ensure dural integrity before gluing into place a luer hub over the craniotomy. The animal was placed in a warmed cage to recover from anesthesia before being re-anesthetized for sham or mTBI exposure. The luer hub was connected to the fluid percussion device which imparted a force of approximately 1.4 ATM in the injury group and 0 ATM in the sham group. Animals were monitored for return of righting reflex and toe pinch reflex following sham or mTBI. They recovered in a warmed cage before returning to the vivarium for a minimum of 24hr prior to electrophysiologic examination.

At time of electrophysiologic evaluation, animals were anesthetized using an overdose of inhaled isoflurane. Exsanguination and perfusion were performed using technique modified from Ting et al., 2014. Briefly, after incising the right atrium, the left heart was injected with 4 degree Celsius cold solution containing the following: N-methyl-D-glucamine 92mM, NaHCO<sub>3</sub> 30mM, Glucose 25mM, HEPES 20mM, MgSO<sub>4</sub>·7H<sub>2</sub>O 10mM, sodium ascorbate 5mM, sodium pyruvate 3mM, KCl 2.5mM, Thiourea 2mM, NaH<sub>2</sub>PO<sub>4</sub> 1.2mM, CaCl<sub>2</sub>·2H<sub>2</sub>O 0.5mM and titrated using 10N HCl to a pH of 7.3 to 7.4 after saturation with carbogen (95% O<sub>2</sub>, 5% CO<sub>2</sub> from Airgas, Radnor, PA) final osmolarity between 300 and 310 mOsm.

The brains were then dissected and blocked in the same cold solution. Using a razor, the brains were blocked at approximately a 15-degree angle offset to the sagittal axis and cyanoacrylate used to fix the tissue block to the cutting board. The tissue was submerged in cold perfusion solution and 350 μm thick brain slices preserving the optic tract as it enters dLGN were made by using a Leica VT1200 S sliding vibratome (Leica Biosystems, Nussloch, Germany). Typically, only one slice was obtained per animal.

Sections were incubated for 1 hour at 33 degrees Celsius prior to patching. Slices were then transferred to solution containing aCSF composed of NaCl 119mM, NaHCO<sub>3</sub> 24mM,

Glucose 12.5mM, KCl 2.5mM, MgSO<sub>4</sub>·7H<sub>2</sub>O 2mM, CaCl<sub>2</sub>·2H<sub>2</sub>O 2mM, NaH<sub>2</sub>PO<sub>4</sub> 1.2mM, pH adjusted to 7.3 to 7.4 with HCl or NaOH as needed and saturated with carbogen. Temperature was maintained at 33 degrees and slices were allowed to equilibrate for 15 minutes prior to transferring to patch clamp rig. Our patch clamp setup was composed of a microscope equipped with IR-DIC optics (900 nm IR filter) aligned for Kohler illumination using 100x water immersion lens and a recording chamber with a transparent glass base through which aCSF maintained at constant temperature. The aCSF was saturated with carbogen gas and continuously circulated. All solutions used were prepared with high purity Type 1 water using MilliQ system (Merck KGaA, Darmstadt, Germany).

Lateral geniculate relay neurons in the monocular zone of dLGN were identified using differential interference contrast phase microscopy and appropriate targets chosen based on morphology and feasibility within the target area. Compared to interneurons, the LGN relay neurons have smaller cell bodies. Whole-cell voltage and current-clamp recordings were made to assess intrinsic membrane properties and quantify EPSCs. Lateral geniculate relay neurons were distinguished from interneurons based both on morphology and intrinsic membrane properties. EPSCs were isolated utilizing the GABA antagonists, Bicuculline (25µM) and CGP 55845 (5µM). EPSCs were evoked by placing a bipolar stimulus electrode positioned in the optic tract. A constant current stimulus isolator was used to deliver stimuli of increasing intensity (0.2ms duration, 10-500µA). For paired-pulse stimulation, two consecutive stimuli (10Hz) were given 100ms apart. This was repeated 3-5 times (30s interval between trials) and traces were averaged.



### **3.3 – Results – Evaluation of retinal fiber inputs and paired-pulse depression using optic tract stimulation.**

Using increasing stimulus intensity to activate the optic tract leading into the dLGN, we monitored the number of EPSCs with discrete peaks in the post-synaptic dLGN relay neuron via whole cell patch clamp recording. Each discrete peak was attributed to a single retinal fiber contributing an excitatory input to the post-synaptic cell. Analyses of number of retinal fiber inputs to individual lateral geniculate relay neurons was performed by counting the number of discrete peaks produced by gradual increase in stimulus intensity to isolate discrete peaks though not in a systematic organized manner. A total of 28 animals were utilized (Sham 4 day N=6, Sham 10 day N=3, Sham 20 day N=2, TBI 4 day N=9, TBI 10 day N=4, TBI 20 day N=5). We recorded from 63 cells in total (Sham 4 day N=12, Sham 10 day N=12, Sham 20 day N=5, TBI 4 Day N=15, TBI 10 day N=10, TBI 20 day N=9). Utilizing a blinded investigator, we found no difference between TBI and Sham groups at any of the time points. Specifically, using ANOVA for comparison of all time points between TBI and Sham animals, no significant differences in estimate of inputs were found. At 4 day post-surgery, mean number of inputs in sham animals was  $3.833 \pm 1.749$  (SEM) while mean number of inputs in TBI animals was  $3.400 \pm 1.764$  (SEM) ( $F(1,25) = 0.405$ ,  $p = 0.5303$ ). At 10 day post-surgery, mean inputs in sham animals was estimated at  $2.167 \pm 1.115$  (SEM) while mean inputs in TBI animals was  $2.60 \pm 1.265$  (SEM) ( $F(1,20) = 0.729$ ,  $p = 0.403$ ). At 20 day mean inputs in sham animals was estimated at  $2.000 \pm 0.707$  while mean inputs in TBI animals was estimated at  $2.000 \pm 1.323$  (SEM) ( $F(1,12) = 0$ ,  $p = 1.0$ ). The decrease in number of inputs as time increased may be attributed to continued refinement and synaptic elimination with age and is consistent with findings from studies on the development and maturation of the retinogeniculate pathway (Chen and Regehr, 2000).

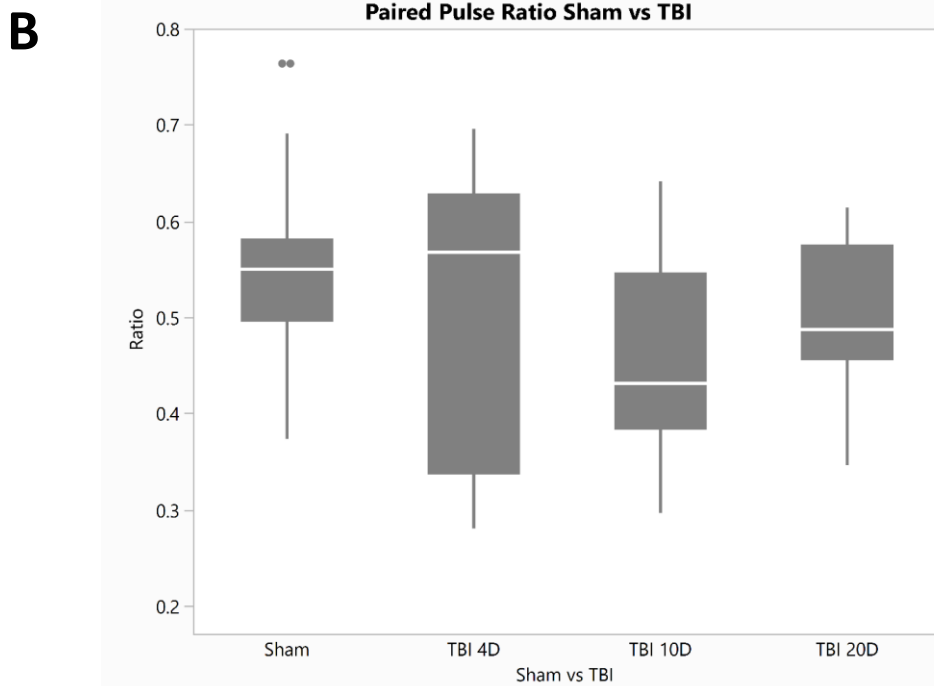
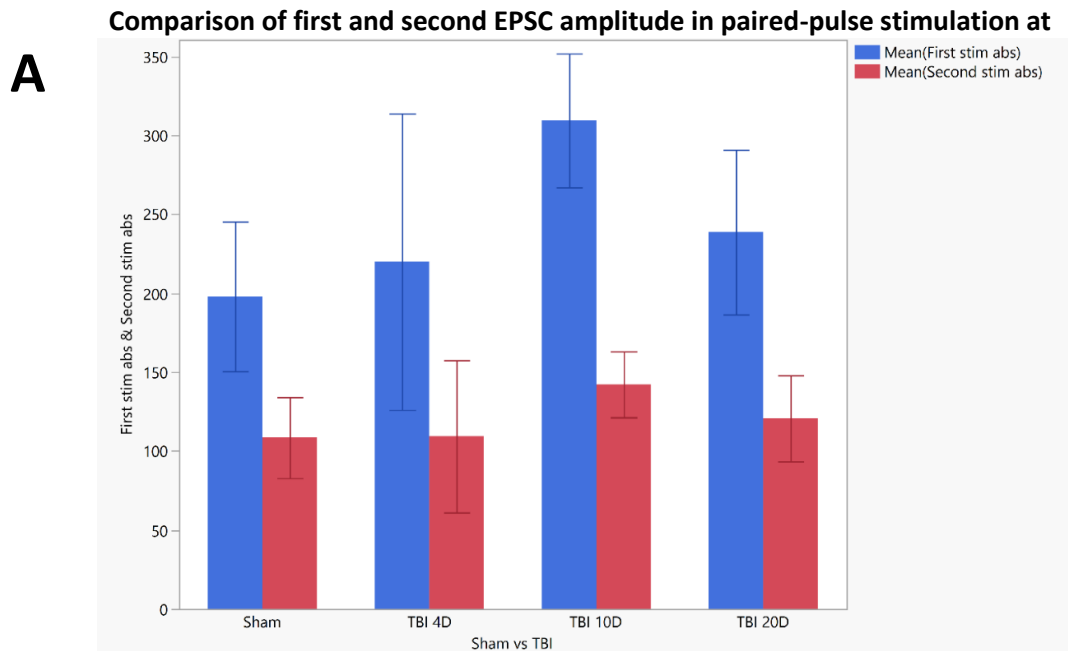


Figure 3.1 – A - Paired pulse stimulation demonstrated expected depression in the amplitude of the second EPSC in response to two consecutive 10Hz stimuli separated by 30 seconds between traces. Bipolar stimulator electrode placed in the optic tract well below the thalamus and whole cell patch clamp performed on LGN relay neurons. This was repeated 3-5 times and the traces averaged for each slice preparation (Sham n=20 cells from 17 mice; TBI 4 day n=7 cells from 7 mice; TBI 10 day n=17 cells from 13 mice; TBI 20 day n =12 from 8 mice). Blue represents first stim, red is second stim. Error bars represent SEM. B – Paired pulse ratio across groups demonstrated similar depression across all groups. Box plots demonstrate median (solid white line), quartiles (solid grey), and outliers (dots). ANOVA comparison of the paired pulse depression demonstrated no statistically significant differences between groups regardless of time after injury ( $F(3,55)$ ,  $p = 0.0639$ ).

Retinogeniculate transmission studied in-vitro in mice has been reported to elicit post-synaptic short-term depression in patch clamp studies of LGN relay neurons (Chinfei Chen, Blitz, & Regehr, 2002). The second of two impulses separated by a short interval produces a weaker response. Presynaptic mechanisms of this depression involve vesicle depletion, calcium sequestration, and dopaminergic input while post-synaptic mechanisms involve desensitization and saturation of the glutamate receptors AMPAR and NMDAR (Blitz, Foster, & Regehr, 2004; Blitz & Regehr, 2003; Budisantoso, Matsui, Kamasawa, Fukazawa, & Shigemoto, 2012; Govindaiah & Cox, 2006). When we examined paired-pulse stimulation of the optic tract leading into the dLGN following surgery, we noted intact paired-pulse depression of the retinogeniculate connection in both sham and TBI mice. We noted that TBI animals were not statistically different in the ratio between pulses compared to sham animals and that this did not change across time (Figure 3.1). Between all timepoints after sham or injury, statistical comparison using ANOVA ( $F(3,55) = 2.57, p=0.064$ ) demonstrated no statistical differences in the appropriate paired pulse depression following 10Hz stimulation averaged across 3-5 runs for each data point (Figure 3.1B). Statistical comparison using ANOVA was performed for 4 day and 10 day data with age matched sham controls as well and revealed no significant differences at 4 day ( $F(1,10) = 0.9612, p=0.35$ ) or 10 day ( $F(1,15) = 1.283, p = 0.275$ ) of the paired-pulse ratio between sham and TBI groups.

### **3.4 Discussion – Study of connectivity between retinogeniculate projections and LGN relay neurons continues to yield new information in relation to the synaptic reorganization occurring following mTBI.**

In our studies, we note no changes between the expected number of inputs to LGN relay neurons following sham or mTBI using the mouse model of mild central fluid percussion injury. When examining the paired-pulse depression ratio of LGN relay neurons, we noted depression of the amplitude in response to the second stimulus in both sham and mTBI groups. This is consistent with current literature on the response of retinogeniculate synapses on dLGN relay neurons in adult mouse which have reported that a paired-pulse stimulation with a 100ms interval between pulses produces a reduction in amplitude of the second EPSC to 60% of the first (Chen et al., 2002; Chen & Regehr, 2003). While this result is surprising in the context of the axotomy we have demonstrated in the optic nerve, it demonstrates that the remaining intact axons may continue to produce appropriate post-synaptic activity and demonstrate short-term mechanisms of plasticity. Additionally, the findings suggest that in the sham animal, there exists redundant axonal connections between retinogeniculate projections and dLGN relay neurons which remain quiescent until injury unmasks their connectivity. This has been demonstrated to occur in the cortex, particularly in limb loss and retinal lesion studies where afferent input loss will result in the corresponding cortex remapping to respond to adjacent inputs.

Electrophysiologic studies have been able to estimate functional inputs based on optic tract stimulation during patch clamp studies to be in the range of 4-5 inputs per dLGN relay neuron in mature mice (Gao et al., 2010; Hooks & Chen, 2006, 2008; Jaubert-miazza et al., 2005). This is consistent with our electrophysiologic findings demonstrating approximately 2 to 4 inputs per relay neuron in animals examined using optic tract electrical stimulation following mild central

fluid percussion injury and may represent the effects of homeostatic plasticity through activation of quiescent connections between RGCs and dLGN relay neurons. Studies utilizing optogenetics to stimulate pre-synaptic terminals in ex-vivo patch clamp studies of dLGN relay neurons have demonstrated that prior to closure of the critical period in mice, dLGN relay neurons may have functional connections with many more retinal ganglion cells than previously estimated and suggest less than a third of intact retinogeniculate connections dominate the post-synaptic activity in LGN relay neurons in adults (Litvina & Chen, 2017). This has been confirmed by Hammer et al. using the “Brainbow” technique to investigate structural connectivity between the retina and dLGN using adenoviral vectors injected into the eye of transgenic mice with RGCs expressing Cre recombinase to produce fluorescent proteins in varying ratios of each RGC. The unique ratio between the expression of the different fluorescent proteins in each RGC produced a fluorescent spectrum fingerprint which is uniquely matched to their thalamic projections. The technique also allows identification of synapses which originate from the same RGC as well as differentiate synapses originating from different RGCs and correlate the findings with serial electron microscopy to identify synapses (Hammer et al., 2015). This technique identified inputs to individual dLGN relay neurons in 6-week-old mice originate from 3 to 8 unique RGCs on most LGN relay neurons and potentially many more in a subset of LGN relay neurons. The finding by Hammer et al. in 6-week old mice likely represents the connectivity present in adult animals as most of the synaptic refinement concludes in the first 30 days in mice (Y. K. Hong et al., 2014). The number of inputs estimated by these two groups independently suggest redundant connectivity within the dLGN is present and our findings support that these connections may contributed to a rapid recovery of function at the retinogeniculate synapse.

Ex-vivo electrophysiologic analysis has limitations, however, it does allow reproducible comparison of changes in connectivity between animals undergoing sham and injury surgery (Hånell et al., 2015; Vascak, Sun, et al., 2017). In vivo, visual stimulus is constantly arriving to LGN relay neurons from RGCs while in the ex-vivo condition, stimulus is arriving very infrequently with large periods of quiescence between stimuli. Studies published more recently have suggested ex-vivo examination may be further limited by axotomy created by slice preparation, however, when comparing sham and mTBI mice, the artifacts produced by slice preparation and infrequent presynaptic input are applied equally to both groups (Litvina & Chen, 2017). Future studies can be performed regarding whether the AMPAR and NMDAR current at the postsynaptic membrane are preserved and contribute in the same manner following injury compared to sham as they may provide significant insight into changes in efficiency of synaptic transmission following injury. Additional limitations in our analysis stem from the large variance in the stimulus intensity as well as EPSCs recorded with paired-pulse stimulation. While using a bipolar electrode mitigates some of the current spreading into surrounding fiber tracts, we cannot rule out the possibility that some of the EPSCs recorded for estimation of inputs to LGN relay neurons as well as paired-pulse stimulation may be due to recruitment of alternative inputs to LGN relay neurons. The small sample size of also limits analysis of paired pulse depression due to the high variance we noted in our EPSC amplitudes. In examination of the paired-pulse data we did not find a statistical difference in the paired-pulse depression ratio at 10 day post-injury compared to sham and other injury groups, however, we did note a qualitative widening of the paired-pulse depression. This may be due to changes attributed to homeostatic plasticity mechanisms and not statistically significant due to the small sample size. While examining monocular deprivation in juvenile mice, Krahe and Guido demonstrated that homeostatic

plasticity in dLGN relay neurons resulted in increased mEPSC amplitude and frequency in parts of dLGN downstream to an eye deprived of visual stimulus (Krahe and Guido, 2011). In our studies, the qualitative increase in first stimulus EPSC amplitude we note at 10 day post-injury could also be explained by changes in release probability through modulation of pre-synaptic calcium and the subsequent dramatic drop in the second stimulus in paired-pulse stimulation could be explained by depletion of calcium stores or depletion of the pre-synaptic vesicles as a result of these changes. Alternatively, post-synaptic mechanism involving receptor internalization or modification may provide alternative means of modulation of paired-pulse depression.

The lack of any difference in the sham and TBI groups at any time point in our study suggests that while structural plasticity is present following injury and axon loss, changes are also occurring in the functional properties of relay neurons on a much faster time scale compared to the adaptive reorganization of retinogeniculate axon terminals we previously reported (Patel et al., 2016). These changes may be the result of the activation of quiescent connections through mechanisms which maintain homeostatic plasticity of the visual axis and may provide a substrate for ensuring that post-injury structural changes are adaptive rather than maladaptive. The role of LGN in processing of visual stimulus has only recently drawn rigorous interest (Piscopo, El-Danaf, Huberman, & Niell, 2013; Rivlin-Etzion et al., 2011). Studies on mechanisms of neuroplasticity continue to mold our understanding regarding how the brain codes information and responds to injury, however, previous consensus treating the geniculate nucleus and other thalamic structures as simple relay circuits had limited prior in-depth examination of how the retinogeniculate pathway processes and encodes visual stimulus (Guido, 2018). Our understanding of how innate homeostatic mechanisms contribute to structural changes and

recovery in mTBI will likely continue to grow as more information regarding communication of information from the eye to the visual cortex unfolds with continued investigation.

**Acknowledgement:**

I would like to acknowledge the contributions of Christopher W.D. Jurgens in aiding to perform the experiments and collect the electrophysiology data for chapter 3.



## **Chapter 4 – Discussion – Review of data**

### **4.1 Synopsis of findings**

In the studies presented we examined in significant detail the response of the mouse dorsal lateral geniculate nucleus (dLGN) to diffuse deafferentation following experimental mTBI. Our findings support previous studies which demonstrate diffuse mild injury causes partial retinal ganglion cell axon loss within the optic nerve and deafferentation of the downstream relay neurons within the dLGN. Importantly, we demonstrated the response to this injury and deafferentation is adaptive structural and electrophysiologic plasticity among the remaining intact axon terminals in the retinal geniculate pathway. Specifically, in chapter 2 we demonstrate that following an initial decrease in density of the retinal geniculate axon terminals in dLGN due to retinal ganglion cell axon loss, there is widescale reorganization and expansion of the remaining inputs between day 4 and day 10 following injury. The expansion of axon terminals remains stable at 20 days following injury. This was performed using both anterograde tract tracing using fluorescently tagged cholera toxin B introduced to the retinal ganglion cells and immunohistochemistry against VGLUT2, an axon terminal marker expressed predominantly by retinal geniculate projections. Anterograde tract tracing can potentially be limited by abnormal axon transport following injury, justifying confirmation of the results using the axon terminal marker VGLUT2. Though inputs to dLGN from the superior colliculus, another target of retinal ganglion cells, are also VGLUT 2 positive, they constitute a minority of inputs and project primarily to the dorsolateral shell.

Information collected using the two techniques separately provided robust reproduction of the data, strongly supporting the hypothesis that axon terminals undergo expansion and

reorganization following partial loss of inputs induced by mild fluid percussion injury. Additionally, we demonstrated normal structural segregation of inputs from the ipsilateral and contralateral eye remain segregated to their respective regions of dLGN after the expansion of retinal geniculate axon terminals at the 10- and 20-day time points following injury. Projections from directionally selective retinal ganglion cells (DSGC), a subset of retinal ganglion cells (RGC), normally segregate to the dorsolateral shell of dLGN. To examine if projections from this specific subgroup of RGCs undergo change in projection pattern, we utilized the transgenic mouse line DRD4-EGFP backcrossed with our C57B16 mouse line. Soma and projections from DSGCs in this transgenic line express GFP and within dLGN, we found that the projections remain segregated to the dorsolateral shell of dLGN, even after reorganization of inputs 10- and 20-days following injury which supports the premise that reorganization following injury is not associated with maladaptive changes in connectivity between injured axons in the optic nerve and dLGN relay neurons in this mTBI model. The changes observed are characterized as adaptive as despite the widescale reorganization and expansion of axon terminals in dLGN, there is preservation of the normal segregation patterns of axon terminals to distinct regions of dLGN. If we noted the ensuing reorganization and expansion to violate these normal bounds, we would have classified them as maladaptive. Hall et al. demonstrated previously that axonal sprouting in the thalamus of rats forming maladaptive circuits following TBI contributed to morbidity in the whisker circuit (Hall and Lifshitz, 2010).

While not critically examined in our experiments, there are some changes in the optic nerve that appear to localize at the site of the optic nerve entering the intracranial compartment. Specifically, in view of the coronal sections through the optic nerve, we note an area of signal loss in the CTB labeled optic nerves just prior to the chiasm. This same region was examined in

previous reports by Wang et al. and attributed to focal edema in the optic nerve, however, given the retinotopic organization of the optic nerve, an alternative hypothesis is that some retinal ganglion cell populations are particularly vulnerable to injury (Wang et al., 2011). Though the question remains outside of the scope of our report and would require significant investment to further examine, there are numerous transgenic mouse lines which label specific subsets of retinal ganglion cells and would allow for detailed examination of this hypothesis (Ivanova et al., 2010).

In Chapter 3, electrophysiologic examination of the function in the visual axis following injury recording visually evoked potentials (VEP) in the visual cortex also noted return of normal waveforms and amplitudes 8 to 10 days following injury. We examined retinal geniculate synapses and their electrophysiologic responses to stimulation of the optic tract. We identified that LGN relay neurons continued to respond appropriately to stimulation of the optic tract and no significant differences between injury and sham animals were noted in number of active inputs or in the paired pulse depression, a marker of short-term synaptic plasticity at 4 and 10 days after injury. Studies by other groups have demonstrated that while dLGN relay neurons typically only respond electrophysiologically to 2-4 axon inputs, structural studies demonstrate connections with up to 8 or more inputs. Together, these findings suggest that deafferentation of dLGN relay neurons may be associated with activation of quiescent inputs which are not electrophysiologically active until axon loss following injury provides a dearth of input to relay neurons. The ensuing proliferation of axon terminals identified in chapter 2 at 10- and 20-days following injury may contribute to recovery of VEP waveform and amplitude. Further, our findings that the mechanisms of short-term plasticity at the retinal geniculate synapse is not disturbed following injury in the intact axon population provides a pathway for short term

plasticity to rewire the functional connectivity of the visual pathway after injury. These finds are instrumental in understanding the brain's response to injury. We have demonstrated that adaptive plasticity following mTBI can occur in the visual thalamus and future studies are needed to determine if these correlations contribute to recovery in cortical processing of visual stimulus. Recent examination of the role of the thalamus in the natural recovery of cognitive impairment following mTBI reinforces this concept. MRI study of fractional anisotropy and mean diffusivity in the thalamus of individuals studied longitudinally have demonstrated correlation between improved cognitive test scores, increase in anisotropy, decrease in diffusivity, and increase in thalamus volume (Munivenkatappa & Agrawal, 2016). Functional studies utilizing fMRI have demonstrated clinical recovery in cognitive deficits correlated with functional connectivity of the thalamus to resting state networks in patients with mTBI (Banks et al., 2016).

#### **4.2 Neurobiological relevance of findings in animal studies of visual axis in human mTBI**

Features encountered in our animal studies of mild central fluid percussion injury (cFPI) underscores the relevance to dysfunction encountered in clinical mTBI. In study of the impact of external force on the human brain, we have noted the resulting shear forces impart changes to all the structural components of the brain, but impact axons more dramatically. The same features encountered in pathologic analysis of human brains following mTBI have been re-demonstrated in our animal model. The mechanical injury imparted in the cFPI model simulates the rapid acceleration/deceleration forces seen in human brain injury with correlate of transient behavioral suppression analogous to concussion in humans (Dixon, Lyeth, Povlishock, & Findling, 1987; Graham, Lawrence, Adams, Doyle, & McLellan, 1988; McGinn & Povlishock, 2016; J. Povlishock, 1992; J. Povlishock et al., 1983; J T Povlishock & Becker, 1985; Smith & Meaney, 2000).

The ensuing deafferentation has broad consequences on patient morbidity, however, most efforts to understand plasticity and recovery following mTBI have focused on white matter changes, cortical changes, and cognitive testing. The examination of the visual system has recently started to gain traction as more information regarding visual symptoms in mTBI comes to light (Greenwald, Kapoor, & Singh, 2012; Kapoor & Ciuffreda, 2002; Ventura, Balcer, & Galetta, 2014). Correlation between impairment of executive function, attention, and memory have been associated with concurrent impaired visual function (Marcus H Heitger et al., 2009; M H Heitger, Anderson, & Jones, 2002). Specifically, changes in scalp recorded visually evoked potentials (VEP) following mTBI have been demonstrated to correlate with cognitive symptoms. Resolution or lack of abnormalities in VEPs have correlated with ability for patients to return to work (Lachapelle et al., 2008). Our examination of VEPs in mice following mild cFPI also demonstrated changes in amplitude and timing of signal transmission to the visual cortex following injury and that the changes recover over a period of 8-10 days following injury. We exploited the similarities between the clinical condition and our animal model to identify the changes which may contributed to the recovery of VEPs in the visual cortex and noted over a similar time period a significant change in density of axon terminals in the dLGN which is upstream of the cortex in the visual axis.

Changes in synaptic density of retinal geniculate axon terminals in dLGN following injury is a novel finding in our model. The dLGN in the visual axis is analogous to the thalamus in the motor system. It acts to relay information from the retina to the visual cortex, however, it also regulates adaption to stimulus, signal gain, and modulation of receptive fields through retrograde connectivity with layer VI of the visual cortex (Monavarfeshani et al., 2017). Over 60% of all synapses on dLGN relay cells originate from cortical thalamic projections while only

10% originate from retinal ganglion cells (Bickford et al., 2010). In conjunction with the known plasticity of the visual cortex in response to retinal injury, we did not anticipate large-scale retinal input reorganization to contribute to recovery, however, the extent of the observed structural reorganization and timing with recovery of VEPs suggests a significant correlation. The expansion of retinal geniculate axon terminals we identified also preserved the expected segregation of axon terminals to the ipsilateral and contralateral eye fields as well as segregation of a specific subset of retinal ganglion cells, directionally selective On-Off ganglion cells, to the dorsolateral shell of dLGN, implicating an adaptive response driving the observed changes. While further studies need to be performed to establish causation, the findings have broad implications on how we examine recovery following injury in mTBI, particularly within the visual axis. Future studies will also need to reference changes in the corticogeniculate projection population. As up to 60% of synapses in dLGN originate from the visual cortex, it is likely that these retrograde projections aid in the adaptive response to input following injury. We are fortunate that the unique structural characteristics of retinal geniculate projections lend themselves to analysis using confocal and light microscopy. In comparison to corticogeniculate synapses which are typically 2-3um in size, demonstrate classic bouton on dendritic spine morphology, and are much more densely packed, retinogeniculate synapses are much larger, demonstrate a complex glomerular morphology, and are sparse, allowing clear identification of changes in density with light and confocal microscopy. Examination of corticogeniculate projections in dLGN will benefit greatly from innovation in microscopy as examination using techniques described in this project proved limited to identify meaningful changes.

### **4.3 Retinal geniculate axon plasticity and relation to previous findings**

Previous study of the visual axis has helped provide insight into mechanisms of recovery of function following injury of long-projection axons within the CNS, however, the majority of these studies employ the optic nerve crush animal model and study of the visual axis in animal models of mTBI is limited (de Lima et al., 2012; Tzekov et al., 2014, 2016; Wang et al., 2013; Evanson et al., 2018). Reports have noted changes in the optic nerve and retinal ganglion cell (RGC) loss after repeated mTBI injury models, however, the repeated injury model commonly described utilizes an impactor against the skull, thus the orbits as well as the brain are equally exposed to the injury force (Tzekov et al., 2014, 2016). Retinal ganglion cell loss is also present in the optic nerve crush injury model and attributed to glutamate induced excitotoxicity which is a potential confounder in the optic nerve crush model (Schuettauf et al., 2000; Yoles and Schwartz 1998). By comparison, in the central fluid percussion injury model, force is imparted to the brain through a central craniotomy and has demonstrated no RGC loss as far out as 28 days following injury, however, diffuse partial axotomy and atrophy of the associated RGCs does cause deafferentation of dLGN relay neurons (Wang et al., 2013, Patel et al., 2016).

Using the optic nerve crush injury model, several groups have demonstrated that intrinsic and extrinsic molecular mechanisms hinder initial attempts at regeneration in the optic nerve following crush injury, and that axon regrowth can occur when some of these molecular brakes are removed (Weber et al., 2010; Dai et al, 2009; Fukuda et al, 1998; Bei et al., 2016; Park et al., 2008; Sun et al., 2011). Early work by Keirstead et al. used a peripheral nerve interposition graft to induce axon regrowth following optic nerve transection (Keirstead et al., 1989). More recent efforts have demonstrated that deletion of Pten and Socs3 in retinal ganglion cells (RGCs) using Cre-expressing adeno-associated virus (AAV-Cre) eye injections in transgenic mice where the

Pten and Socs3 genes are flanked by lox P sites, promotes long-distance axonal regeneration and can target deep grey structures such as the suprachiasmatic nucleus after optic nerve crush injury (Li et al., 2015; Park et al., 2008; Sun et al., 2011). These efforts are important in understanding the molecular brakes associated with axon outgrowth and producing new connectivity in the visual axis, however, relying on optic nerve crush injury to cause axotomy results in most axons to be injured and disconnected. By comparison, the reorganization and electrophysiologic changes we note in our injury model associated with adaptive reorganization of intact connections is more likely to be associated with constitutively active mechanisms of homeostasis such as those that govern cortical plasticity (Nudo, 2013; Uesaka et al., 2006).

Study of the visual cortex and ocular dominance plasticity has provided significant insight to how Hebbian plasticity precedes structural changes (Fox and Stryker, 2017). Studies in the striate cortex of primates have demonstrated that deprived eye results in structural changes in geniculate cortical afferents to layer 4 (Hubel and Weisel, 1977; Hill & Zito, 2013; Wiegert & Oetner, 2013). Zenke & Gerstner recently published their interpretation of the interaction between Hebbian plasticity and homeostatic plasticity in understanding how the brain maintains homeostasis while also providing mechanisms for learning and memory (Zenke & Gerstner, 2017).

Interestingly, studies over the course of the last several decades examining plasticity in the visual axis all presume that following lesion of retinal afferents, projections from the dLGN to the cortex, do not undergo reorganization. Much of the examination of reorganization of structural afferents focused on cortical reorganization. Thalamocortical contribution to reorganization was thought to be insufficient based on examination of both visual and somatosensory systems (Gilbert and Wiesel, 1990, 1992; Rasmusson et al., 1985; Pons et al.,



1991). A retrograde labeling study of the cortex following retinal lesion in cats failed to demonstrate reorganization of cortical axonal projections originating from LGN further supported this opinion (Darian-Smith & Gilbert, 1995). This finding was likely due to the significant modulation of LGN activity by corticothalamic projections and associated plasticity. Despite LGN being a relay nucleus, modulatory corticothalamic inputs far outnumber retinogeniculate projections across rodents, cats, and primates (Hendrickson et al., 1978; Fitzpatrick et al., 1994; Guillery and Sherman, 2002; Briggs and Usrey, 2011; Bickford et al., 2010). Cortical feedback has been demonstrated to tune LGN relay neuron activity and suppression of this feedback has demonstrated unmasking of latent retinal drivers (Aguila, Cudeiro, Rivadulla, 2017).

Further hampering examination of reorganization in the retinal geniculate pathway in adult animals may be secondary to consensus opinion on the retinal geniculate synapse suggesting that subcortical regions of the brain such as the thalamus and dLGN were thought to develop earlier and be less sensitive to sensory experience. Early studies suggested retinal geniculate connectivity relied on spontaneously activity within the retinal and molecular signaling to establish an initial retinotopic map which refined after eye opening through pruning of excess retinal afferents to dLGN relay neurons (Feldheim et al., 1998; Pfeiffenberger et al., 2005; Chen and Regehr, 2000; Jaubert-Miazza et al., 2005; Ziburkus and Guido, 2006; Hooks and Chen, 2006, 2008). Butts et al., demonstrated in simulation using measurements of the pattern of facilitation and depression in lateral geniculate nucleus in the context of realistic activity patterns from retinal inputs that Hebbian rules govern activity based refinement and segregation from eye specific inputs during development (Butts et al., 2007). Based on examination of mechanisms of homeostasis responsible for cortical structural plasticity and

refinement of retinal inputs to LGN during development, it is reasonable to now consider that the same mechanisms may be present in thalamic structures such as the dLGN, and may not be observed until diffuse deafferentation sparing a subpopulation of inputs is encountered such as the condition present in the cFPI model of mTBI.

#### **4.4 Recommendations for futures studies and current limitations hampering application of specific novel techniques to further examine retinal geniculate reorganization.**

Through examination of the retinal geniculate synapse following mTBI, we have found significant structural reorganization following deafferentation of dLGN relay neurons. The structural reorganization occurs in conjunction with electrophysiologic changes in connectivity as measured using visually evoked potentials in the cortex. Our findings must be put into the context of evolving understanding of the mechanisms governing organization of dLGN and its retinal afferents as well as the mechanisms governing structural plasticity of the retinogeniculate synapse. Initial studies on plasticity within the visual cortex utilized monocular deprivation to identify how the absence of visual stimulus results in reorganization of functional and structural connectivity. Understanding of whether the retinal geniculate reorganization we identified is dependent on visual stimulus could be answered through monocular eye closure immediately after mTBI. These studies can be difficult, especially when monocular deprivation must occur over a period of up to 10 days for us to identify changes in the previously described reorganization of retinal inputs in dLGN. Through personal experience, these experiments are difficult due to the propensity of mice to repeatedly and successfully reopen sutured and glued eyelids over the course of several days.

Detailed examination of the axon terminals synapsing onto dLGN relay neurons has been undertaken to simply understand the connectivity of the retina to the organization of inputs in dLGN. Hammer et al. utilized the ‘Brainbow’ technique to investigate structural connectivity between the retina and dLGN using adenoviral vectors injected into the eye of transgenic mice with RGCs expressing Cre recombinase to produce fluorescent proteins in varying ratios of each RGC. The unique ratio between the expression of the different fluorescent proteins in each RGC produced a fluorescent spectrum fingerprint which is uniquely matched to their thalamic projections. The technique also allows identification of synapses which originate from the same RGC as well as differentiate synapses originating from different RGCs (Hammer et al., 2015). This technique identified inputs to dLGN relay neurons originate from 10 to 14 unique RGCs and allowed correlation between different locations on the retina and the specific localization of their axon terminals within dLGN. While the technique proves useful to investigate connectivity, variable and incomplete expression as well as uncertainty regarding validity in injury models hampers use of this technique to study connectivity in mTBI, a condition in which diffuse deafferentation and axon injury can hamper axon transport. Injection of adenoviral vectors could potentially increase the cytotoxic stress on RGCs following mTBI confounding results.

Morgan et al. used serial electron microscopy through the mouse dLGN to build a large high resolution 3D data set and combed through it to demonstrate conclusively that connections between individual RGC projections and thalamocortical neurons of dLGN are more numerous than the 4-5 inputs estimated electrophysiologically, thus confirming the findings of Hammer et al. The technique would retain the ability to estimate inputs following injury however the serial electron microscopy is prohibitively time consuming and resource intensive, hampering its use to

study effects of mTBI on connectivity where findings in a single or small number of tissue samples cannot reliably estimate the population as a whole (Morgan et al., 2016).

Examination of the electrophysiologic connectivity of retinal geniculate inputs to dLGN relay neurons in our study failed to yield significant differences across time between sham and injured animals. Litvina et al., provided an explanation for the low number of inputs estimated by electrophysiologic studies by expanding on prior work using optogenetics. The group used transgenic mice to express channel rhodopsin (ChR2) selectively in RGC presynaptic terminals and activated them using light while patch clamp recording from a single LGN relay neuron. They demonstrated that prior to closure of the critical period in mice, inputs are more numerous than estimated by optic tract electrical stimulation and prior estimates of 2-4 inputs per LGN relay neuron could potentially represent a result of severed axons in slice preparation (Litvina and Chen, 2017). Using optogenetics to stimulate pre-synaptic terminals in slice preparations of dLGN during patch clamp recording from relays cells suggested that up to 8 sources of input may synapse onto a single dLGN relay neuron however they conclude that thirty percent of inputs dominate post-synaptic activity in LGN relay neurons.. This technique may allow examination of the hypothesis that lack of differences in our patch clamp studies of dLGN relay neurons is due to activation of quiescent inputs following deafferentation. Alternatively, the studies by Litvina et al. examining connectivity in mouse dLGN are performed in juvenile mice and may represent connectivity prior to synaptic pruning which in mouse, continues until young adulthood (P60 days).

Consideration of sex differences in mTBI have been reported in several well characterized studies and reports (Attella et al., 1987; Espinoza and Wright, 2011; Gözl et al., 2019). Recent acknowledgement by the NIH that underlying biologic differences attributed to

gender can significantly impact disease and pathologic states. The studies presented here are preliminary and future work should include consideration of biologic differences associated with gender.

#### **4.5 Concluding remarks**

Clinical and animal model studies have supported the premise that mTBI induces dysfunction which is transient despite irreversible loss of axon terminals associated with axonal loss. The structural and functional mechanisms responsible for this recovery is poorly understood. Current evidence implicates cortical plasticity as the driving force behind recovery, however, emerging data has also implicated plasticity within deep grey structures such as the thalamus. Specifically, studies examining the role of the LGN in visual perception have demonstrated that it performs more than simply relaying retinal input to the visual cortex, but also modulate and processes visual information before transmission to the visual cortex. Our findings have demonstrated that following diffuse axonal injury in the retinal geniculate pathway, there is widespread loss of retinal inputs to dLGN relay neurons which then recovers over a period of time that correlates with recovery of function measured by studying visually evoked potentials in the visual cortex. Our electrophysiologic studies were unable to identify changes in number of inputs to dLGN relay neurons however our methods were limited in eliciting responses from quiescent inputs in sham animals and future studies will be required to verify that the lack of change in number of inputs to dLGN relay neurons is associated with adaptive changes potentially based on known mechanisms of homeostatic plasticity. The dLGN is the thalamic analogue within the visual axis. The expansive study of the visual axis in neuroscience provides a robust basis for examination of how thalamic plasticity impacts

functional change in behavior and recovery following dysfunction. Our observations additionally open the door to additional questions about the responds to diffuse deafferentation in other thalamic circuits and suggests the importance of studying reorganization in deep grey structures and their role in adaptive plasticity following traumatic brain injury in human studies.

## Bibliography

- Aguila, J., Cudeiro, F. J., & Rivadulla, C. (2017). Suppression of V1 feedback produces a shift in the topographic representation of receptive fields of LGN cells by unmasking latent retinal drives. *Cerebral Cortex*, 27(6), 3331-3345.
- Alvarez, T. L., Kim, E. H., Vicci, V. R., Dhar, S. K., Biswal, B. B., & Barrett, A. (2012). Concurrent Vision Dysfunctions in Convergence Insufficiency With Traumatic Brain Injury. *Optometry & Vision Science*, 89(12), 1740. Retrieved from <https://doi.org/10.1097/OPX.0b013e3182772dce>
- Andersson, E. E., Emanuelson, I., Björklund, R., & Stålhammar, D. (2007). Mild traumatic brain injuries: the impact of early intervention on late sequelae. A randomized controlled trial. *Acta Neurochirurgica*, 149(2), 151–160. Retrieved from <https://doi.org/10.1007/s00701-006-1082-0>
- Andrews-Hanna, J. R., Saxe, R., & Yarkoni, T. (2014). Contributions of episodic retrieval and mentalizing to autobiographical thought: evidence from functional neuroimaging, resting-state connectivity, and fMRI meta-analyses. *NeuroImage*, 91, 324–35. Retrieved from <https://doi.org/10.1016/j.neuroimage.2014.01.032>
- Andriessen, T. M., Jacobs, B., & Vos, P. E. (2010). Clinical characteristics and pathophysiological mechanisms of focal and diffuse traumatic brain injury. *Journal of Cellular and Molecular Medicine*, 14(10), 2381–2392. Retrieved from <https://doi.org/10.1111/j.1582-4934.2010.01164.x>
- Arfanakis, K., Haughton, V. M., Carew, J. D., Rogers, B. P., Dempsey, R. J., & Meyerand, E. M. (2002). Diffusion tensor MR imaging in diffuse axonal injury. *AJNR. American Journal of Neuroradiology*, 23(5), 794–802.
- Attella, M. J., Nattinville, A., & Stein, D. G. (1987). Hormonal state affects recovery from frontal cortex lesions in adult female rats. *Behavioral and Neural Biology*, 48(3), 352-367.
- Banks, S. D., Coronado, R. A., Clemons, L. R., Abraham, C. M., Pruthi, S., Conrad, B. N., ... Archer, K. R. (2016). Thalamic Functional Connectivity in Mild Traumatic Brain Injury: Longitudinal Associations With Patient-Reported Outcomes and Neuropsychological Tests. *Archives of Physical Medicine and Rehabilitation*, 97(8), 1254–1261. Retrieved from <https://doi.org/10.1016/j.apmr.2016.03.013>
- Barallobre, M. J., Pascual, M., Río, J. A. D., & Soriano, E. (2005). The Netrin family of guidance factors: emphasis on Netrin-1 signalling. *Brain Research Reviews*, 49(1), 22–47. Retrieved from <https://doi.org/10.1016/j.brainresrev.2004.11.003>

- Barkhoudarian, G., Hovda, D. A., & Giza, C. C. (2011). The Molecular Pathophysiology of Concussive Brain Injury. *Clinics in Sports Medicine*, 30(1), 33–48. Retrieved from <https://doi.org/10.1016/j.csm.2010.09.001>
- Barton, R. A. (1998). Visual specialization and brain evolution in primates. *Proceedings of the Royal Society of London. Series B: Biological Sciences*, 265(1409), 1933-1937.
- Bayly, P., Cohen, T., Leister, E., Ajo, D., Leuthardt, E., & Genin, G. (2005). Deformation of the Human Brain Induced by Mild Acceleration. *Journal of Neurotrauma*, 22(8), 845–856. Retrieved from <https://doi.org/10.1089/neu.2005.22.845>
- Bazarian, J. J., Blyth, B., & Cimpello, L. (2006). Bench to Bedside: Evidence for Brain Injury after Concussion—Looking beyond the Computed Tomography Scan. *Academic Emergency Medicine*, 13(2), 199–214. Retrieved from <https://doi.org/10.1197/j.aem.2005.07.031>
- Bei, F., Lee, H. H. C., Liu, X., Gunner, G., Jin, H., Ma, L., ... & Chen, C. (2016). Restoration of visual function by enhancing conduction in regenerated axons. *Cell*, 164(1-2), 219-232.
- Belanger, H. G., Kretzmer, T., Yoash-Gantz, R., Pickett, T., & Tupler, L. A. (2009). Cognitive sequelae of blast-related versus other mechanisms of brain trauma. *Journal of the International Neuropsychological Society*, 15(1), 1-8.
- Benowitz, L., & Yin, Y. (2008). Rewiring the injured CNS: Lessons from the optic nerve. *Experimental Neurology*, 209(2), 389–398. Retrieved from <https://doi.org/10.1016/j.expneurol.2007.05.025>
- Bharath, R. D., Munivenkatappa, A., Gohel, S., Panda, R., Saini, J., Rajeswaran, J., ... Biswal, B. B. (2015). Recovery of resting brain connectivity ensuing mild traumatic brain injury. *Frontiers in Human Neuroscience*, 9, 513. Retrieved from <https://doi.org/10.3389/fnhum.2015.00513>
- Bickford, M. E. (2016). Thalamic Circuit Diversity: Modulation of the Driver/Modulator Framework. *Frontiers in Neural Circuits*, 9, 86. Retrieved from <https://doi.org/10.3389/fncir.2015.00086>
- Bickford, M. E., Slusarczyk, A., Dilger, E. K., Krahe, T. E., Kucuk, C., & Guido, W. (2010). Synaptic development of the mouse dorsal lateral geniculate nucleus. *Journal of Comparative Neurology*, 518(5), 622–635. Retrieved from <https://doi.org/10.1002/cne.22223>
- Bickford, M. E., Zhou, N., Krahe, T. E., Govindaiah, G., & Guido, W. (2015). Retinal and Tectal ‘Driver-Like’ Inputs Converge in the Shell of the Mouse Dorsal Lateral Geniculate Nucleus. *The Journal of Neuroscience : The Official Journal of the Society for Neuroscience*, 35(29), 10523–34. Retrieved from <https://doi.org/10.1523/jneurosci.3375-14.2015>



- Blitz, D. M., Foster, K. A., & Regehr, W. G. (2004). Short-term synaptic plasticity: a comparison of two synapses. *Nature Reviews Neuroscience*, 5(8), 630–640. Retrieved from <https://doi.org/10.1038/nrn1475>
- Blitz, D. M., & Regehr, W. G. (2003). Retinogeniculate Synaptic Properties Controlling Spike Number and Timing in Relay Neurons. *Journal of Neurophysiology*, 90(4), 2438–2450. Retrieved from <https://doi.org/10.1152/jn.00562.2003>
- Blumbergs, P. C., Scott, G., Manavis, J., Wainwright, H., Simpson, D. A., & McLean, A. J. (1994). Staining of amyloid precursor protein to study axonal damage in mild head injury. *The Lancet*, 344(8929), 1055–1056. Retrieved from [https://doi.org/10.1016/s0140-6736\(94\)91712-4](https://doi.org/10.1016/s0140-6736(94)91712-4)
- Bondi, C. O., Klitsch, K. C., Leary, J. B., & Kline, A. E. (2014). Environmental Enrichment as a Viable Neurorehabilitation Strategy for Experimental Traumatic Brain Injury. *Journal of Neurotrauma*, 31(10), 873–888. Retrieved from <https://doi.org/10.1089/neu.2014.3328>
- Borg, J., Holm, L., Peloso, P., & Cassidy, J. (2004). Non-surgical intervention and cost for mild traumatic brain injury: results of the WHO Collaborating Centre Task Force on Mild Traumatic Brain Injury.
- Brainard, M. S., & Knudsen, E. I. (1998). Sensitive periods for visual calibration of the auditory space map in the barn owl optic tectum. *Journal of Neuroscience*, 18(10), 3929–3942.
- Briggs, F., & Usrey, W. M. (2011). Corticogeniculate feedback and visual processing in the primate. *The Journal of physiology*, 589(1), 33–40.
- Brose, K., & Tessier-Lavigne, M. (2000). Slit proteins: key regulators of axon guidance, axonal branching, and cell migration. *Current Opinion in Neurobiology*, 10(1), 95–102. Retrieved from [https://doi.org/10.1016/s0959-4388\(99\)00066-5](https://doi.org/10.1016/s0959-4388(99)00066-5)
- Brusa, A., Jones, S., & Plant, G. (2001). Long-term remyelination after optic neuritis: A 2-year visual evoked potential and psychophysical serial study. *Brain : A Journal of Neurology*, 124(Pt 3), 468–79.
- Budisantoso, T., Matsui, K., Kamasawa, N., Fukazawa, Y., & Shigemoto, R. (2012). Mechanisms underlying signal filtering at a multisynapse contact. *The Journal of Neuroscience : The Official Journal of the Society for Neuroscience*, 32(7), 2357–76. Retrieved from <https://doi.org/10.1523/jneurosci.5243-11.2012>
- Büki, A., & Povlishock, J. T. (2006). All roads lead to disconnection?--Traumatic axonal injury revisited. *Acta Neurochirurgica*, 148(2), 181–93; discussion 193–4. Retrieved from <https://doi.org/10.1007/s00701-005-0674-4>

- Buonomano, D. V. (2000). Decoding Temporal Information: A Model Based on Short-Term Synaptic Plasticity. *Journal of Neuroscience*, 20(3), 1129–1141. Retrieved from <https://doi.org/10.1523/jneurosci.20-03-01129.2000>
- Butts, D. A., Weng, C., Jin, J., Yeh, C. I., Lesica, N. A., Alonso, J. M., & Stanley, G. B. (2007). Temporal precision in the neural code and the timescales of natural vision. *Nature*, 449(7158), 92–95.
- Caramia, M. D., Cicinelli, P., Paradiso, C., Mariorenzi, R., Zarola, F., Bernardi, G., & Rossini, P. M. (1991). ‘Excitability’ changes of muscular responses to magnetic brain stimulation in patients with central motor disorders. *Electroencephalography and Clinical Neurophysiology/Evoked Potentials Section*, 81(4), 243–250. Retrieved from [https://doi.org/10.1016/0168-5597\(91\)90009-m](https://doi.org/10.1016/0168-5597(91)90009-m)
- Cassidy, J., Carroll, L., Peloso, P., & Borg, J. (2004). Incidence, risk factors and prevention of mild traumatic brain injury: results of the WHO Collaborating Centre Task Force on Mild Traumatic Brain Injury.
- Chen, Chinfai, Blitz, D. M., & Regehr, W. G. (2002). Contributions of Receptor Desensitization and Saturation to Plasticity at the Retinogeniculate Synapse. *Neuron*, 33(5), 779–788. Retrieved from [https://doi.org/10.1016/s0896-6273\(02\)00611-6](https://doi.org/10.1016/s0896-6273(02)00611-6)
- Chen, C., & Regehr, W. G. (2000). Developmental remodeling of the retinogeniculate synapse. *Neuron*, 28(3), 955–966.
- Chen, C., & Regehr, W. G. (2003). Presynaptic modulation of the retinogeniculate synapse. *Journal of Neuroscience*, 23(8), 3130–3135.
- Chollet, F., Dipiero, V., Wise, R., Brooks, D., Dolan, R., & Frackowiak, R. (1991). The functional anatomy of motor recovery after stroke in humans: A study with positron emission tomography. *Annals of Neurology*, 29(1), 63–71. Retrieved from <https://doi.org/10.1002/ana.410290112>
- Christman, C. W., Grady, S. M., Walker, S. A., Holloway, K. L., & Povlishock, J. T. (1994). Ultrastructural Studies of Diffuse Axonal Injury in Humans. *Journal of Neurotrauma*, 11(2), 173–186. Retrieved from <https://doi.org/10.1089/neu.1994.11.173>
- Christman, C. W., Jr., S. J., Walker, S. A., & Povlishock, J. (1997). Characterization of a prolonged regenerative attempt by diffusely injured axons following traumatic brain injury in adult cat: a light and electron microscopic immunocytochemical study. *Acta Neuropathologica*, 94(4), 329–337. Retrieved from <https://doi.org/10.1007/s004010050715>
- Cicinelli, P., Traversa, R., & Rossini, P. M. (1997). Post-stroke reorganization of brain motor output to the hand: a 2–4 month follow-up with focal magnetic transcranial stimulation. *Electroencephalography and Clinical Neurophysiology/Electromyography and Motor Control*, 105(6), 438–450. Retrieved from [https://doi.org/10.1016/s0924-980x\(97\)00052-0](https://doi.org/10.1016/s0924-980x(97)00052-0)

- Ciuffreda, K. J., Kapoor, N., Rutner, D., Suchoff, I. B., Han, M. E., & Craig, S. (2007). Occurrence of oculomotor dysfunctions in acquired brain injury: A retrospective analysis. *Optometry - Journal of the American Optometric Association*, 78(4), 155–161. Retrieved from <https://doi.org/10.1016/j.optm.2006.11.011>
- Ciuffreda, K. J., Rutner, D., Kapoor, N., Suchoff, I. B., Craig, S., & Han, M. E. (2008). Vision therapy for oculomotor dysfunctions in acquired brain injury: A retrospective analysis. *Optometry - Journal of the American Optometric Association*, 79(1), 18–22. Retrieved from <https://doi.org/10.1016/j.optm.2007.10.004>
- Cohen, A. S., Pfister, B. J., Schwarzbach, E., Grady, M. S., Goforth, P. B., & Satin, L. S. (2007). Progress in Brain Research. *Progress in Brain Research*, 161, 143–169. Retrieved from [https://doi.org/10.1016/s0079-6123\(06\)61010-8](https://doi.org/10.1016/s0079-6123(06)61010-8)
- Coleman, J., Law, K., & Bear, M. (2009). Anatomical origins of ocular dominance in mouse primary visual cortex. *Neuroscience*, 161(2). Retrieved from <https://doi.org/10.1016/j.neuroscience.2009.03.045>
- Comper, P., Bisschop, Carnide, N., & Tricco, A. (2005). A systematic review of treatments for mild traumatic brain injury. Retrieved from <https://doi.org/10.1080/02699050400025042>
- Corrigan, J. D., Selassie, A. W., & Orman, J. A. (2010). The Epidemiology of Traumatic Brain Injury. *The Journal of Head Trauma Rehabilitation*, 25(2), 72. Retrieved from <https://doi.org/10.1097/HTR.0b013e3181ccc8b4>
- Crair, M. C., & Malenka, R. C. (1995). A critical period for long-term potentiation at thalamocortical synapses. *Nature*, 375(6529), 325–328. Retrieved from <https://doi.org/10.1038/375325a0>
- Cushman, J., Agarwal, N., & Fabian, T. (2001). Practice management guidelines for the management of mild traumatic brain injury: the EAST practice management guidelines work group.
- Dai, Y., Sun, X., & Chen, Q. (2009). Differential induction of c-Fos and c-Jun in the lateral geniculate nucleus of rats following unilateral optic nerve injury with contralateral retinal blockade. *Experimental brain research*, 193(1), 9-18.
- Darian-Smith, C., & Gilbert, C. D. (1994). Axonal sprouting accompanies functional reorganization in adult cat striate cortex. *Nature*, 368(6473), 737-740.
- Darian-Smith, C., & Gilbert, C. D. (1995). Topographic reorganization in the striate cortex of the adult cat and monkey is cortically mediated. *Journal of Neuroscience*, 15(3), 1631-1647.
- Datwani, A., McConnell, M. J., Kanold, P. O., Micheva, K. D., Busse, B., Shamloo, M., ... Shatz, C. J. (2009). Classical MHCII Molecules Regulate Retinogeniculate Refinement and

- Limit Ocular Dominance Plasticity. *Neuron*, 64(4), 463–470. Retrieved from <https://doi.org/10.1016/j.neuron.2009.10.015>
- Dean, P. J., Sato, J., Vieira, G., McNamara, A., & Sterr, A. (2015). Long-term structural changes after mTBI and their relation to post-concussion symptoms. *Brain Injury*, 29(10), 1211–1218. Retrieved from <https://doi.org/10.3109/02699052.2015.1035334>
- Demas, J., Sagdullaev, B. T., Green, E., Jaubert-Miazza, L., McCall, M. A., Gregg, R. G., ... Guido, W. (2006). Failure to Maintain Eye-Specific Segregation in nob, a Mutant with Abnormally Patterned Retinal Activity. *Neuron*, 50(2). Retrieved from <https://doi.org/10.1016/j.neuron.2006.03.033>
- Denman, D. J., & Contreras, D. (2016). On Parallel Streams through the Mouse Dorsal Lateral Geniculate Nucleus. *Frontiers in Neural Circuits*, 10, 20. Retrieved from <https://doi.org/10.3389/fncir.2016.00020>
- DeYoe, E. A., & Essen, D. C. V. (1988). Concurrent processing streams in monkey visual cortex. *Trends in Neurosciences*, 11(5), 219–226. Retrieved from [https://doi.org/10.1016/0166-2236\(88\)90130-0](https://doi.org/10.1016/0166-2236(88)90130-0)
- Dhande, O. S., & Huberman, A. D. (2014). Visual Circuits: Mouse Retina No Longer a Level Playing Field. *Current Biology*, 24(4), R155–R156. Retrieved from <https://doi.org/10.1016/j.cub.2013.12.045>
- Dixon, C. E., Lyeth, B. G., Povlishock, J. T., Findling, R. L., Hamm, R. J., Marmarou, A., ... & Hayes, R. L. (1987). A fluid percussion model of experimental brain injury in the rat. *Journal of neurosurgery*, 67(1), 110-119.
- Donoghue, J. P., & Sanes, J. N. (1988). Organization of adult motor cortex representation patterns following neonatal forelimb nerve injury in rats. *Journal of Neuroscience*, 8(9), 3221-3232.
- Donoghue, J., Suner, S., & Sanes, J. (1990). Dynamic organization of primary motor cortex output to target muscles in adult rats II. Rapid reorganization following motor nerve lesions. *Experimental Brain Research*, 79(3), 492–503. Retrieved from <https://doi.org/10.1007/bf00229319>
- Du, T., Ciuffreda, K., & Kapoor, N. (2005). Elevated dark adaptation thresholds in traumatic brain injury. *Brain Injury*, 19(13), 1125–38. Retrieved from <https://doi.org/10.1080/02699050500149817>
- Dymowski, A., Owens, J., Ponsford, J., & Willmott, C. (2015). Speed of processing and strategic control of attention after traumatic brain injury. *Journal of Clinical and Experimental Neuropsychology*, 37(10), 1–12. Retrieved from <https://doi.org/10.1080/13803395.2015.1074663>

- Eker, C., Asgeirsson, B., Grände, P., Schalén, W., & Nordström, C. (1998). Improved outcome after severe head injury with a new therapy based on principles for brain volume regulation and preserved microcirculation. *Critical Care Medicine*, 26(11), 1881–6.
- El-Danaf, R. N., Krahe, T. E., Dilger, E. K., Bickford, M. E., Fox, M. A., & Guido, W. (2015). Developmental remodeling of relay cells in the dorsal lateral geniculate nucleus in the absence of retinal input. *Neural Development*, 10, 19. Retrieved from <https://doi.org/10.1186/s13064-015-0046-6>
- Emery, D. L., Royo, N. C., Fischer, I., Saatman, K. E., & McIntosh, T. K. (2003). Plasticity following Injury to the Adult Central Nervous System: Is Recapitulation of a Developmental State Worth Promoting? *Journal of Neurotrauma*, 20(12), 1271–1292. Retrieved from <https://doi.org/10.1089/089771503322686085>
- Erskine, L., & Herrera, E. (2007). The retinal ganglion cell axon's journey: Insights into molecular mechanisms of axon guidance. *Developmental Biology*, 308(1), 1–14. Retrieved from <https://doi.org/10.1016/j.ydbio.2007.05.013>
- Espinoza, T. R., & Wright, D. W. (2011). The role of progesterone in traumatic brain injury. *The Journal of head trauma rehabilitation*, 26(6), 497–499. <https://doi.org/10.1097/HTR.0b013e31823088fa>
- Evanson, N. K., Guilhaume-Correa, F., Herman, J. P., & Goodman, M. D. (2018). Optic tract injury after closed head traumatic brain injury in mice: A model of indirect traumatic optic neuropathy. *PloS one*, 13(5), e0197346.
- Ewing-Cobbs, L., Hasan, K., Prasad, M., Kramer, L., & Bachevalier, J. (2006). Corpus callosum diffusion anisotropy correlates with neuropsychological outcomes in twins discordant for traumatic brain injury. *AJNR. American Journal of Neuroradiology*, 27(4), 879–81.
- Eysel, Ulf Th. (1982). Functional reconnections without new axonal growth in a partially denervated visual relay nucleus. *Nature*, 299(5882), 442–444. Retrieved from <https://doi.org/10.1038/299442a0>
- Eysel, Ulf Th, Gonzalez-Aguilar, F., & Mayer, U. (1980). A functional sign of reorganization in the visual system of adult cats: Lateral geniculate neurons with displaced receptive fields after lesions of the nasal retina. *Brain Research*, 181(2), 285–300. Retrieved from [https://doi.org/10.1016/0006-8993\(80\)90613-7](https://doi.org/10.1016/0006-8993(80)90613-7)
- Eysel, U. T., Gonzalez-Aguilar, F., & Mayer, U. (1981). Time-dependent decrease in the extent of visual deafferentation in the lateral geniculate nucleus of adult cats with small retinal lesions. *Experimental Brain Research*, 41(3–4), 256–263. Retrieved from <https://doi.org/10.1007/bf00238882>

- Farkas, O., Lifshitz, J., & Povlishock, J. T. (2006). Mechanoporation Induced by Diffuse Traumatic Brain Injury: An Irreversible or Reversible Response to Injury? *The Journal of Neuroscience*. Retrieved from <https://doi.org/10.1523/jneurosci.5119-05.2006>
- Faul, M., Xu, L., Wald, M., Coronado, V., & Dellinger, A. M. (2010). Traumatic brain injury in the United States: national estimates of prevalence and incidence, 2002–2006. *Injury Prevention*, 16(Suppl 1), A268–A268.
- Feinstein, A., & Rapoport, M. (2000). Mild traumatic brain injury: the silent epidemic. *Canadian Journal of Public Health*, 91(5), 325-326.
- Feldheim, D. A., Vanderhaeghen, P., Hansen, M. J., Frisé, J., Lu, Q., Barbacid, M., & Flanagan, J. G. (1998). Topographic guidance labels in a sensory projection to the forebrain. *Neuron*, 21(6), 1303-1313.
- Feldman, D. (2003). Ocular dominance plasticity in mature mice. *Neuron*, 38(6), 846–8. Retrieved from [https://doi.org/10.1016/S0896-6273\(03\)00359-3](https://doi.org/10.1016/S0896-6273(03)00359-3)
- Fimreite, V., Ciuffreda, K. J., & Yadav, N. K. (2015). Effect of luminance on the visually-evoked potential in visually-normal individuals and in mTBI/concussion. *Brain Injury*, 29(10), 1199–1210. Retrieved from <https://doi.org/10.3109/02699052.2015.1035329>
- Finkelstein, E., Corso, P. S., & Miller, T. R. (2006). *The incidence and economic burden of injuries in the United States*. Oxford University Press, USA.
- Finnanger, T. G., Skandsen, T., Andersson, S., Lydersen, S., Vik, A., & Indredavik, M. (2013). Differentiated patterns of cognitive impairment 12 months after severe and moderate traumatic brain injury. *Brain Injury*, 27(13–14), 1606–16. Retrieved from <https://doi.org/10.3109/02699052.2013.831127>
- Fitzpatrick, D., Usrey, W. M., Schofield, B. R., & Einstein, G. (1994). The sublaminar organization of corticogeniculate neurons in layer 6 of macaque striate cortex. *Visual neuroscience*, 11(2), 307-315.
- Florence, S., & Kaas, J. (1995). Large-scale reorganization at multiple levels of the somatosensory pathway follows therapeutic amputation of the hand in monkeys. *Journal of Neuroscience*, 15(12), 8083–8095. Retrieved from <https://doi.org/10.1523/jneurosci.15-12-08083.1995>
- Fort, P., & Jouvét, M. (1990). Iontophoretic application of unconjugated cholera toxin B subunit (CTb) combined with immunohistochemistry of neurochemical substances: a method for transmitter identification of retrogradely labeled neurons. *Brain Research*, (534).
- Fox K, & Stryker M. (2017). Integrating Hebbian and homeostatic plasticity: introduction. *Phil. Trans. R. Soc. B* 372: 20160413. <http://dx.doi.org/10.1098/rstb.2016.0413>

- Freed, S., & Hellerstein, L. (1997). Visual electrodiagnostic findings in mild traumatic brain injury. *Brain Injury*, 11(1), 25–36. Retrieved from <https://doi.org/10.1080/026990597123782>
- Fukuda, Y., Watanabe, M., Sawai, H., & Miyoshi, T. (1998). Functional recovery of vision in regenerated optic nerve fibers. *Vision research*, 38(10), 1545-1553.
- Gao, E., DeAngelis, G. C., & Burkhalter, A. (2010). Parallel Input Channels to Mouse Primary Visual Cortex. *The Journal of Neuroscience*, 30(17), 5912–5926. Retrieved from <https://doi.org/10.1523/jneurosci.6456-09.2010>
- Ghajar, J. (2000). Traumatic brain injury. *The Lancet*, 356(9233), 923-929.
- Gilbert, C. D., & Wiesel, T. N. (1990). The influence of contextual stimuli on the orientation selectivity of cells in primary visual cortex of the cat. *Vision research*, 30(11), 1689-1701.
- Gilbert, C. D., & Wiesel, T. N. (1992). Receptive field dynamics in adult primary visual cortex. *Nature*, 356(6365), 150–152. Retrieved from <https://doi.org/10.1038/356150a0>
- Godement, P., Saillour, P., & Imbert, M. (1980). The ipsilateral optic pathway to the dorsal lateral geniculate nucleus and superior colliculus in mice with prenatal or postnatal loss of one eye. *The Journal of Comparative Neurology*, 190(4), 611–26. Retrieved from <https://doi.org/10.1002/cne.901900402>
- Gölz, C., Kirchhoff, F. P., Westerhorstmann, J., Schmidt, M., Hirnet, T., Rune, G. M., ... & Schäfer, M. K. (2019). Sex hormones modulate pathogenic processes in experimental traumatic brain injury. *Journal of neurochemistry*, 150(2), 173-187.
- Gong, S., Zheng, C., Doughty, M. L., Losos, K., Didkovsky, N., Schambra, U. B., ... Hatten, M. E. (2003). A gene expression atlas of the central nervous system based on bacterial artificial chromosomes. *Nature*, 425(6961), 917–925. Retrieved from <https://doi.org/10.1038/nature02033>
- Gordon, W. A., Brown, M., Sliwinski, M., Hibbard, M. R., Patti, N., Weiss, M. J., ... & Sheerer, M. (1998). The enigma of "hidden" traumatic brain injury. *The Journal of Head Trauma Rehabilitation*.
- Govindaiah, G., & Cox, C. L. (2006). Depression of retinogeniculate synaptic transmission by presynaptic D2-like dopamine receptors in rat lateral geniculate nucleus. *European Journal of Neuroscience*, 23(2), 423–434. Retrieved from <https://doi.org/10.1111/j.1460-9568.2005.04575.x>
- Govindarajan, K. A., Narayana, P. A., Hasan, K. M., Wilde, E. A., Levin, H. S., Hunter, J. V., ... McCarthy, J. J. (2016). Cortical Thickness in Mild Traumatic Brain Injury. *Journal of Neurotrauma*, 33(20), 1809–1817. Retrieved from <https://doi.org/10.1089/neu.2015.4253>

- Graham, D. I., Lawrence, A. E., Adams, J. H., Doyle, D., & McLellan, D. R. (1988). Brain damage in fatal non-missile head injury without high intracranial pressure. *Journal of Clinical Pathology*, 41(1), 34–37. Retrieved from <https://doi.org/10.1136/jcp.41.1.34>
- Greenwald, B. D., Kapoor, N., & Singh, A. D. (2012). Visual impairments in the first year after traumatic brain injury. *Brain Injury*, 26(11), 1338–59. Retrieved from <https://doi.org/10.3109/02699052.2012.706356>
- Greer, J. E., Hånell, A., McGinn, M. J., & Povlishock, J. T. (2013). Mild traumatic brain injury in the mouse induces axotomy primarily within the axon initial segment. *Acta Neuropathologica*, 126(1), 59–74. Retrieved from <https://doi.org/10.1007/s00401-013-1119-4>
- Greer, J. E., McGinn, M. J., & Povlishock, J. T. (2011). Diffuse traumatic axonal injury in the mouse induces atrophy, c-Jun activation, and axonal outgrowth in the axotomized neuronal population. *The Journal of Neuroscience : The Official Journal of the Society for Neuroscience*, 31(13), 5089–105. Retrieved from <https://doi.org/10.1523/JNEUROSCI.5103-10.2011>
- Greer, J. E., Povlishock, J. T., & Jacobs, K. M. (2012). Electrophysiological abnormalities in both axotomized and nonaxotomized pyramidal neurons following mild traumatic brain injury. *The Journal of Neuroscience : The Official Journal of the Society for Neuroscience*, 32(19), 6682–7. Retrieved from <https://doi.org/10.1523/jneurosci.0881-12.2012>
- Guggenmos, D. J., Azin, M., Barbay, S., Mahnken, J. D., Dunham, C., Mohseni, P., & Nudo, R. J. (2013). Restoration of function after brain damage using a neural prosthesis. *Proceedings of the National Academy of Sciences*, 110(52), 21177–21182. Retrieved from <https://doi.org/10.1073/pnas.1316885110>
- Guido, W. (2008). Refinement of the retinogeniculate pathway. *The Journal of Physiology*, 586(18), 4357–4362. Retrieved from <https://doi.org/10.1113/jphysiol.2008.157115>
- Guido, W. (2018). Development, form, and function of the mouse visual thalamus. *Journal of Neurophysiology*, 120(1), 211–225. Retrieved from <https://doi.org/10.1152/jn.00651.2017>
- Guillery, R. W., & Sherman, S. M. (2002). Thalamic relay functions and their role in corticocortical communication: generalizations from the visual system. *Neuron*, 33(2), 163–175.
- Hadanny, A., & Efrati, S. (2016). Treatment of persistent post-concussion syndrome due to mild traumatic brain injury: current status and future directions. *Expert Review of Neurotherapeutics*, 16(8), 875–887. Retrieved from <https://doi.org/10.1080/14737175.2016.1205487>
- Hall, K. D., & Lifshitz, J. (2010). Diffuse traumatic brain injury initially attenuates and later expands activation of the rat somatosensory whisker circuit concomitant with neuroplastic responses. *Brain Research*. Retrieved from <https://doi.org/10.1016/j.brainres.2010.01.067>



- Hammer, S., Carrillo, G. L., Govindaiah, G., Monavarfeshani, A., Bircher, J. S., Su, J., ... Fox, M. A. (2014). Nuclei-specific differences in nerve terminal distribution, morphology, and development in mouse visual thalamus. *Neural Development*, 9(1), 16. Retrieved from <https://doi.org/10.1186/1749-8104-9-16>
- Hammer, S., Monavarfeshani, A., Lemon, T., Su, J., & Fox, M. (2015). Multiple Retinal Axons Converge onto Relay Cells in the Adult Mouse Thalamus. *Cell Reports*, 12(10), 1575–1583. Retrieved from <https://doi.org/10.1016/j.celrep.2015.08.003>
- Hånell, A., Greer, J. E., McGinn, M. J., & Povlishock, J. T. (2015). Traumatic brain injury-induced axonal phenotypes react differently to treatment. *Acta Neuropathologica*, 129(2), 317–32. Retrieved from <https://doi.org/10.1007/s00401-014-1376-x>
- Heitger, Marcus H, Jones, R. D., Macleod, A., Snell, D. L., Frampton, C. M., & Anderson, T. J. (2009). Impaired eye movements in post-concussion syndrome indicate suboptimal brain function beyond the influence of depression, malingering or intellectual ability. *Brain*, 132(10), 2850–2870. Retrieved from <https://doi.org/10.1093/brain/awp181>
- Heitger, M H, Anderson, T. J., & Jones, R. D. (2002). Progress in Brain Research. *Progress in Brain Research*, 140, 433–448. Retrieved from [https://doi.org/10.1016/s0079-6123\(02\)40067-2](https://doi.org/10.1016/s0079-6123(02)40067-2)
- Hellerstein, L. F., Freed, S., & Maples, W. C. (1995). Vision profile of patients with mild brain injury. *Journal of the American Optometric Association*, 66(10), 634–9.
- Hendrickson, A. E., Wilson, J. R., & Ogren, M. P. (1978). The neuroanatomical organization of pathways between the dorsal lateral geniculate nucleus and visual cortex in Old World and New World primates. *The Journal of comparative neurology*, 182(1), 123-136.
- Hendry, S. H. C., & Reid, R. C. (2000). The Koniocellular Pathway in Primate Vision. *Annual Review of Neuroscience*, 23(1), 127–153. Retrieved from <https://doi.org/10.1146/annurev.neuro.23.1.127>
- Herrera, E., Brown, L., Aruga, J., Rachel, R. A., Dolen, G., Mikoshiba, K., ... Mason, C. A. (2003). Zic2 Patterns Binocular Vision by Specifying the Uncrossed Retinal Projection. *Cell*, 114(5), 545–557. Retrieved from [https://doi.org/10.1016/s0092-8674\(03\)00684-6](https://doi.org/10.1016/s0092-8674(03)00684-6)
- Hill, T. C., & Zito, K. (2013). LTP-induced long-term stabilization of individual nascent dendritic spines. *Journal of Neuroscience*, 33(2), 678-686.
- Hoge, C. W., McGurk, D., Thomas, J. L., Cox, A. L., Engel, C. C., & Castro, C. A. (2008). Mild traumatic brain injury in U.S. Soldiers returning from Iraq. *The New England Journal of Medicine*, 358(5), 453–63. Retrieved from <https://doi.org/10.1056/NEJMoa072972>
- Hohnke, C. D., Oray, S., & Sur, M. (2000). Activity-Dependent Patterning of Retinogeniculate Axons Proceeds with a Constant Contribution from AMPA and NMDA Receptors. *Journal of*

- Neuroscience*, 20(21), 8051–8060. Retrieved from <https://doi.org/10.1523/jneurosci.20-21-08051.2000>
- Hong, Y., & Chen, C. (2011). Wiring and rewiring of the retinogeniculate synapse. Retrieved from <https://doi.org/10.1016/j.conb.2011.02.007>
- Hong, Y. K., Park, S., Litvina, E. Y., Morales, J., Sanes, J. R., & Chen, C. (2014). Refinement of the retinogeniculate synapse by bouton clustering. *Neuron*, 84(2), 332–9. Retrieved from <https://doi.org/10.1016/j.neuron.2014.08.059>
- Hooks, B. M., & Chen, C. (2006). Distinct Roles for Spontaneous and Visual Activity in Remodeling of the Retinogeniculate Synapse. *Neuron*, 52(2), 281–291. Retrieved from <https://doi.org/10.1016/j.neuron.2006.07.007>
- Hooks, B. M., & Chen, C. (2008). Vision Triggers an Experience-Dependent Sensitive Period at the Retinogeniculate Synapse. *The Journal of Neuroscience*, 28(18), 4807–4817. Retrieved from <https://doi.org/10.1523/jneurosci.4667-07.2008>
- Howarth, M., Walmsley, L., & Brown, T. M. (2014). Binocular Integration in the Mouse Lateral Geniculate Nuclei. *Current Biology*, 24(11), 1241–1247. Retrieved from <https://doi.org/10.1016/j.cub.2014.04.014>
- Hubel, D. H., Wiesel, T. N., LeVay, S., Barlow, H. B., & Gaze, R. M. (1977). Plasticity of ocular dominance columns in monkey striate cortex. *Philosophical Transactions of the Royal Society of London. B, Biological Sciences*, 278(961), 377–409.
- Hubel, D. H., & Wiesel, T. N. (1979). Brain Mechanisms of Vision. *Scientific American*, 241(3), 150–162. Retrieved from <https://doi.org/10.1038/scientificamerican0979-150>
- Huberman, A. D., Manu, M., Koch, S. M., Susman, M. W., Lutz, A. B., Ullian, E. M., ... Barres, B. A. (2008). Architecture and activity-mediated refinement of axonal projections from a mosaic of genetically identified retinal ganglion cells. *Neuron*, 59(3), 425–38. Retrieved from <https://doi.org/10.1016/j.neuron.2008.07.018>
- Huberman, A. D., Murray, K. D., Warland, D. K., Feldheim, D. A., & Chapman, B. (2005). Ephrin-As mediate targeting of eye-specific projections to the lateral geniculate nucleus. *Nature Neuroscience*, 8(8), 1013–1021. Retrieved from <https://doi.org/10.1038/nn1505>
- Huberman, A. D., Stellwagen, D., & Chapman, B. (2002). Decoupling eye-specific segregation from lamination in the lateral geniculate nucleus. *The Journal of Neuroscience : The Official Journal of the Society for Neuroscience*, 22(21), 9419–29.
- Huberman, A. D., Wei, W., Elstrott, J., Stafford, B. K., Feller, M. B., & Barres, B. A. (2009). Genetic identification of an On-Off direction-selective retinal ganglion cell subtype reveals a layer-specific subcortical map of posterior motion. *Neuron*, 62(3), 327–34. Retrieved from <https://doi.org/10.1016/j.neuron.2009.04.014>

- Huberman, & Feller. (2008). Mechanisms underlying development of visual maps and receptive fields. Retrieved from <https://doi.org/10.1146/annurev.neuro.31.060407.125533>
- Humphreys, I., Wood, R. L., Phillips, C. J., & Macey, S. (2013). The costs of traumatic brain injury: a literature review. *ClinicoEconomics and Outcomes Research : CEOR*, 5, 281–7. Retrieved from <https://doi.org/10.2147/ceor.s44625>
- Inman, D. M., Sappington, R. M., Horner, P. J., & Calkins, D. J. (2006). Quantitative correlation of optic nerve pathology with ocular pressure and corneal thickness in the DBA/2 mouse model of glaucoma. *Investigative Ophthalmology & Visual Science*, 47(3), 986–96. Retrieved from <https://doi.org/10.1167/iovs.05-0925>
- Jacobs, K. M., & Donoghue, J. P. (1991). Reshaping the cortical motor map by unmasking latent intracortical connections. *Science*, 251(4996), 944–948.
- Jang, S. H., & Lee, H. D. (2017). Abundant unusual neural branches from the fornix in patients with mild traumatic brain injury: A diffusion tensor tractography study. *Brain Injury*, 31(11), 1–4. Retrieved from <https://doi.org/10.1080/02699052.2017.1350997>
- Jaubert-miazza, L., Green, E., Lo, F., Bui, K., & Visual ..., M. J. (2005). Structural and functional composition of the developing retinogeniculate pathway in the mouse. Retrieved from <https://doi.org/10.1017/S0952523805225154>
- Johansen-Berg, H. (2007). Structural Plasticity: Rewiring the Brain. *Current Biology*, 17(4), R141–R144. Retrieved from <https://doi.org/10.1016/j.cub.2006.12.022>
- Johnson, B., Zhang, K., Gay, M., Horovitz, S., Hallett, M., Sebastianelli, W., & Slobounov, S. (2012). Alteration of brain default network in subacute phase of injury in concussed individuals: Resting-state fMRI study. *NeuroImage*, 59(1), 511–518. Retrieved from <https://doi.org/10.1016/j.neuroimage.2011.07.081>
- Johnson, V. E., Stewart, W., Weber, M. T., Cullen, D., Siman, R., & Smith, D. H. (2015). SNTF immunostaining reveals previously undetected axonal pathology in traumatic brain injury. *Acta Neuropathologica*. Retrieved from <https://doi.org/10.1007/s00401-015-1506-0>
- Jones, S. J., & Brusa, A. (2003). Neurophysiological evidence for long-term repair of MS lesions: implications for axon protection. *Journal of the Neurological Sciences*, 206(2), 193–8.
- Joos, K. M., Li, C., & Sappington, R. M. (2010). Morphometric Changes in the Rat Optic Nerve Following Short-term Intermittent Elevations in Intraocular Pressure. *Investigative Ophthalmology & Visual Science*, 51(12), 6431–6440. Retrieved from <https://doi.org/10.1167/iovs.10-5212>
- Jünger, E., Newell, D., Grant, G., & Avellino, A. (1997). Cerebral autoregulation following minor head injury.

- Kaas, J., Krubitzer, L., Chino, Y., Langston, A., Polley, E., & Blair, N. (1990). Reorganization of retinotopic cortical maps in adult mammals after lesions of the retina. *Science*, 248(4952), 229–231. Retrieved from <https://doi.org/10.1126/science.2326637>
- Kanno, I., Lammertsma, A. A., Heather, J. D., Gibbs, J. M., Rhodes, C. G., Clark, J. C., & Jones, T. (1984). Measurement of Cerebral Blood Flow Using Bolus Inhalation of C15O2 and Positron Emission Tomography: Description of the Method and its Comparison with the C15O2 Continuous Inhalation Method. *Journal of Cerebral Blood Flow & Metabolism*, 4(2), 224–234. Retrieved from <https://doi.org/10.1038/jcbfm.1984.31>
- Kano, M., & Hashimoto, K. (2009). Synapse elimination in the central nervous system. *Current Opinion in Neurobiology*, 19(2), 154–161. Retrieved from <https://doi.org/10.1016/j.conb.2009.05.002>
- Kapoor, N., & Ciuffreda, K. J. (2002). Vision disturbances following traumatic brain injury. *Current Treatment Options in Neurology*, 4(4), 271–280.
- Kapoor, N., Ciuffreda, K. J., & Han, Y. (2004). Oculomotor rehabilitation in acquired brain injury: a case series. *Archives of Physical Medicine and Rehabilitation*, 85(10), 1667–78.
- Kasthuri, N., & Lichtman, J. W. (2004). Structural dynamics of synapses in living animals. *Current Opinion in Neurobiology*, 14(1), 105–111. Retrieved from <https://doi.org/10.1016/j.conb.2004.01.013>
- Kay, J., Huerta, D. I. la, Kim, I., & Zhang, Y. (2011). Retinal ganglion cells with distinct directional preferences differ in molecular identity, structure, and central projections. Retrieved from <https://doi.org/10.1523/JNEUROSCI.0907-11.2011>
- Kay, T., Newman, B., Cavallo, M., & Ezrachi, O. (1992). Toward a neuropsychological model of functional disability after mild traumatic brain injury. Retrieved from <https://doi.org/10.1037/0894-4105.6.4.371>
- Keck, T., Mrcic-Flogel, T. D., Afonso, M. V., Eysel, U. T., Bonhoeffer, T., & Hübener, M. (2008). Massive restructuring of neuronal circuits during functional reorganization of adult visual cortex. *Nature Neuroscience*, 11(10), 1162–1167. Retrieved from <https://doi.org/10.1038/nn.2181>
- Kelley, B. J., Farkas, O., Lifshitz, J., & Povlishock, J. T. (2006). Traumatic axonal injury in the perisomatic domain triggers ultrarapid secondary axotomy and Wallerian degeneration. *Experimental Neurology*, 198(2), 350–360. Retrieved from <https://doi.org/10.1016/j.expneurol.2005.12.017>
- Kerschensteiner, D., & Guido, W. (2017). Organization of the dorsal lateral geniculate nucleus in the mouse. *Visual Neuroscience*, 34, E008. Retrieved from <https://doi.org/10.1017/s0952523817000062>

- Kim, I., Zhang, Y., & Meister, M. (2010). Lamina restriction of retinal ganglion cell dendrites and axons: subtype-specific developmental patterns revealed with transgenic markers.
- King, N. (1997). Mild head injury: Neuropathology, sequelae, measurement and recovery. *British Journal of Clinical Psychology*, 36(2), 161–184. Retrieved from <https://doi.org/10.1111/j.2044-8260.1997.tb01405.x>
- Kinnunen, K. M., Greenwood, R., Powell, J. H., Leech, R., Hawkins, P. C., Bonnelle, V., ... Sharp, D. J. (2010). White matter damage and cognitive impairment after traumatic brain injury. *Brain: A Journal of Neurology*, 134(Pt 2), 449–63. Retrieved from <https://doi.org/10.1093/brain/awq347>
- Krahe, T. E., & Guido, W. (2011). Homeostatic plasticity in the visual thalamus by monocular deprivation. *Journal of Neuroscience*, 31(18), 6842–6849.
- Krahe, E., T., Wang, J., & Povlishock, and J. T. (2013). DIFFUSE AXONAL INJURY (DAI) FOUND WITHIN THE MOUSE VISUAL SYSTEM FOLLOWING MILD TRAUMATIC BRAIN INJURY (MTBI) COMPROMISES VISUAL CORTICAL PLASTICITY., 30.(15), A102–A103.
- Krahe, T. E., El-Danaf, R. N., Dilger, E. K., Henderson, S. C., & Guido, W. (2011). Morphologically Distinct Classes of Relay Cells Exhibit Regional Preferences in the Dorsal Lateral Geniculate Nucleus of the Mouse. *The Journal of Neuroscience*, 31(48), 17437–48. Retrieved from <https://doi.org/10.1523/JNEUROSCI.4370-11.2011>
- Kraus, M. F., Susmaras, T., Caughlin, B. P., Walker, C. J., Sweeney, J. A., & Little, D. M. (2007). White matter integrity and cognition in chronic traumatic brain injury: a diffusion tensor imaging study. *Brain*, 130(10), 2508–2519. Retrieved from <https://doi.org/10.1093/brain/awm216>
- Kumar, R., Gupta, R. K., Husain, M., Chaudhry, C., Srivastava, A., Saksena, S., & Rathore, R. K. (2009). Comparative evaluation of corpus callosum DTI metrics in acute mild and moderate traumatic brain injury: Its correlation with neuropsychometric tests. *Brain Injury*, 23(7–8), 675–685. Retrieved from <https://doi.org/10.1080/02699050903014915>
- Lachapelle, J., Bolduc-Teasdale, J., Ptito, A., & McKerral, M. (2008). Deficits in complex visual information processing after mild TBI: electrophysiological markers and vocational outcome prognosis. *Brain Injury*, 22(3), 265–74. Retrieved from <https://doi.org/10.1080/02699050801938983>
- Lachapelle, J., Ouimet, C., Bach, M., Ptito, A., & McKerral, M. (2004). Texture segregation in traumatic brain injury—a VEP study. *Vision Research*, 44(24), 2835–2842. Retrieved from <https://doi.org/10.1016/j.visres.2004.06.007>

- Land, P. W., Kyonka, E., & Shamalla-Hannah, L. (2004). Vesicular glutamate transporters in the lateral geniculate nucleus: expression of VGLUT2 by retinal terminals. *Brain Research*, 996(2), 251254. Retrieved from <https://doi.org/10.1016/j.brainres.2003.10.032>
- Langlois, J. A., Rutland-Brown, W., & Wald, M. M. (2006). The epidemiology and impact of traumatic brain injury: a brief overview. *The Journal of Head Trauma Rehabilitation*, 21(5), 375–8.
- Leibson, C., Brown, A., Ransom, J., Diehl, N., Perkins, P., Mandrekar, J., & Malec, J. (2011). Incidence of traumatic brain injury across the full disease spectrum: a population-based medical record review study. *Epidemiology (Cambridge, Mass.)*, 22(6), 836–44. Retrieved from <https://doi.org/10.1097/ede.0b013e318231d535>
- Leunissen, I., Coxon, J. P., Caeyenberghs, K., Michiels, K., Sunaert, S., & Swinnen, S. P. (2014). Subcortical volume analysis in traumatic brain injury: The importance of the fronto-striato-thalamic circuit in task switching. *Cortex*, 51, 67–81. Retrieved from <https://doi.org/10.1016/j.cortex.2013.10.009>
- LeVay, S., & Ferster, D. (1977). Relay cell classes in the lateral geniculate nucleus of the cat and the effects of visual deprivation. *The Journal of Comparative Neurology*, 172(4), 563–584. Retrieved from <https://doi.org/10.1002/cne.901720402>
- Liepert, J., Miltner, W. H. R., Bauder, H., Sommer, M., Dettmers, C., Taub, E., & Weiller, C. (1998). Motor cortex plasticity during constraint-induced movement therapy in stroke patients. *Neuroscience Letters*, 250(1), 5–8. Retrieved from [https://doi.org/10.1016/s0304-3940\(98\)00386-3](https://doi.org/10.1016/s0304-3940(98)00386-3)
- Lifshitz, J., Kelley, B. J., & Povlishock, J. T. (2007). Perisomatic thalamic axotomy after diffuse traumatic brain injury is associated with atrophy rather than cell death. *Journal of Neuropathology and Experimental Neurology*, 66(3), 218–29. Retrieved from <https://doi.org/10.1097/01.jnen.0000248558.75950.4d>
- Lifshitz, J., Witgen, B., & Grady, M. (2007). Acute cognitive impairment after lateral fluid percussion brain injury recovers by 1 month: Evaluation by conditioned fear response. *Behavioural Brain Research*, 177(2), 347–357. Retrieved from <https://doi.org/10.1016/j.bbr.2006.11.014>
- Lima, S., Koriyama, Y., Kurimoto, T., Oliveira, J., Yin, Y., Li, Y., ... Benowitz, L. (2012). Full-length axon regeneration in the adult mouse optic nerve and partial recovery of simple visual behaviors. *Proceedings of the National Academy of Sciences*, 109(23), 9149–9154. Retrieved from <https://doi.org/10.1073/pnas.1119449109>
- Lipton, M. L., Gellella, E., Lo, C., Gold, T., Ardekani, B. A., Shifteh, K., ... Branch, C. A. (2008). Multifocal White Matter Ultrastructural Abnormalities in Mild Traumatic Brain Injury with Cognitive Disability: A Voxel-Wise Analysis of Diffusion Tensor Imaging.

- Journal of Neurotrauma*, 25(11), 1335–1342. Retrieved from <https://doi.org/10.1089/neu.2008.0547>
- Li, R., Chen, K., Fleisher, A. S., Reiman, E. M., Yao, L., & Wu, X. (2011). Large-scale directional connections among multi resting-state neural networks in human brain: A functional MRI and Bayesian network modeling study. *NeuroImage*, 56(3), 1035–1042. Retrieved from <https://doi.org/10.1016/j.neuroimage.2011.03.010>
- Li, S., He, Q., Wang, H., Tang, X., Ho, K. W., Gao, X., ... & Wong, Y. H. (2015). Injured adult retinal axons with Pten and Socs3 co-deletion reform active synapses with suprachiasmatic neurons. *Neurobiology of disease*, 73, 366-376.
- Litvina, E. Y., & Chen, C. (2017). An evolving view of retinogeniculate transmission. *Visual Neuroscience*, 34, E013. Retrieved from <https://doi.org/10.1017/S0952523817000104>
- Lutkenhoff, E. S., McArthur, D. L., Hua, X., Thompson, P. M., Vespa, P. M., & Monti, M. M. (2013). Thalamic atrophy in antero-medial and dorsal nuclei correlates with six-month outcome after severe brain injury. *NeuroImage: Clinical*, 3. Retrieved from <https://doi.org/10.1016/j.nicl.2013.09.010>
- Lu, T., & Trussell, L. O. (2007). Development and Elimination of Endbulb Synapses in the Chick Cochlear Nucleus. *The Journal of Neuroscience*, 27(4), 808–817. Retrieved from <https://doi.org/10.1523/jneurosci.4871-06.2007>
- Mabuchi, F., Aihara, M., Mackey, M. R., Lindsey, J. D., & Weinreb, R. N. (2003). Optic nerve damage in experimental mouse ocular hypertension. *Investigative Ophthalmology & Visual Science*, 44(10), 4321–30.
- Macdonell, R., Donnan, G., & Bladin, P. (1989). A comparison of somatosensory evoked and motor evoked potentials in stroke. *Annals of Neurology*, 25(1), 68–73. Retrieved from <https://doi.org/10.1002/ana.410250111>
- Marklund, N. (2016). Rodent Models of Traumatic Brain Injury: Methods and Challenges. *Methods in Molecular Biology (Clifton, N.J.)*, 1462, 29–46. Retrieved from [https://doi.org/10.1007/978-1-4939-3816-2\\_3](https://doi.org/10.1007/978-1-4939-3816-2_3)
- Maxwell, W. L., Bartlett, E., & Morgan, H. (2015). Wallerian Degeneration in the Optic Nerve Stretch-Injury Model of Traumatic Brain Injury: A Stereological Analysis. *Journal of Neurotrauma*, 32(11), 780–790. Retrieved from <https://doi.org/10.1089/neu.2014.3369>
- McDonald, B. C., Saykin, A. J., & McAllister, T. W. (2012). Functional MRI of mild traumatic brain injury (mTBI): progress and perspectives from the first decade of studies. *Brain Imaging and Behavior*, 6(2), 193–207. Retrieved from <https://doi.org/10.1007/s11682-012-9173-4>

- McGinn, M. J., & Povlishock, J. T. (2016). Pathophysiology of Traumatic Brain Injury. *Neurosurgery Clinics of North America*, 27(4), 397–407. Retrieved from <https://doi.org/10.1016/j.nec.2016.06.002>
- McInnes, K., Friesen, C. L., MacKenzie, D. E., Westwood, D. A., & Boe, S. G. (2017). Mild Traumatic Brain Injury (mTBI) and chronic cognitive impairment: A scoping review. *PLOS ONE*, 12(4), e0174847. Retrieved from <https://doi.org/10.1371/journal.pone.0174847>
- McMahon, P. J., Hricik, A., Yue, J. K., Puccio, A. M., Inoue, T., Lingsma, H. F., ... Vassar, M. J. (2014). Symptomatology and Functional Outcome in Mild Traumatic Brain Injury: Results from the Prospective TRACK-TBI Study. *Journal of Neurotrauma*, 31(1), 26–33. Retrieved from <https://doi.org/10.1089/neu.2013.2984>
- McNamara, K. C. S., Lisembee, A. M., & Lifshitz, J. (2010). The whisker nuisance task identifies a late-onset, persistent sensory sensitivity in diffuse brain-injured rats. *Journal of Neurotrauma*, 27(4), 695–706. Retrieved from <https://doi.org/10.1089/neu.2009.1237>
- Menon, D., Schwab, K., Wright, D., & Maas, A. (2010). Position statement: definition of traumatic brain injury.
- Messé, A., Caplain, S., & Pélérini-Issac, M. (2012). Structural integrity and postconcussion syndrome in mild traumatic brain injury patients. Retrieved from <https://doi.org/10.1007/s11682-012-9159-2>
- Mikelberg, F., Drance, Schulzer, M., & Yidegiligne, H. (1989). The normal human optic nerve: axon count and axon diameter distribution.
- Milleret, C., & Buser, P. (1984). Receptive field sizes and responsiveness to light in area 18 of the adult cat after chiasmotomy. Postoperative evolution; role of visual experience. *Experimental Brain Research*, 57(1), 73–81. Retrieved from <https://doi.org/10.1007/bf00231133>
- Mittenberg, W., Canyock, E. M., Condit, D., & Patton, C. (2010). Treatment of Post-Concussion Syndrome Following Mild Head Injury. *Journal of Clinical and Experimental Neuropsychology*, 23(6), 829–836. Retrieved from <https://doi.org/10.1076/jcen.23.6.829.1022>
- Moechars, D., Weston, M. C., Leo, S., Callaerts-Vegh, Z., Goris, I., Daneels, G., ... Hampson, M. R. (2006). Vesicular Glutamate Transporter VGLUT2 Expression Levels Control Quantal Size and Neuropathic Pain. *The Journal of Neuroscience*, 26(46), 12055–12066. Retrieved from <https://doi.org/10.1523/JNEUROSCI.2556-06.2006>
- Monavarfeshani, A., Sabbagh, U., & Fox, M. A. (2017). Not a one-trick pony: Diverse connectivity and functions of the rodent lateral geniculate complex. *Visual neuroscience*, 34.



- Morgan, J., Berger, D., Wetzel, A., & Lichtman, J. (2016). The Fuzzy Logic of Network Connectivity in Mouse Visual Thalamus. *Cell*, 165(1), 192–206. Retrieved from <https://doi.org/10.1016/j.cell.2016.02.033>
- Muir-Robinson, G., Hwang, B. J., & Feller, M. B. (2002). Retinogeniculate axons undergo eye-specific segregation in the absence of eye-specific layers. *Journal of Neuroscience*, 22(13), 5259–5264.
- Munivenkatappa, A., & Agrawal, A. (2016). Role of Thalamus in Recovery of Traumatic Brain Injury. *Journal of Neurosciences in Rural Practice*, 07(S 01), S076–S079. Retrieved from <https://doi.org/10.4103/0976-3147.196468>
- Murray, G. D., Butcher, I., McHugh, G. S., Lu, J., Mushkudiani, N. A., Maas, A., ... Steyerberg, E. W. (2007). Multivariable Prognostic Analysis in Traumatic Brain Injury: Results from The IMPACT Study. *Journal of Neurotrauma*, 24(2). Retrieved from <https://doi.org/10.1089/neu.2006.0035>
- Nakagawa, S., Brennan, C., Johnson, K. G., Shewan, D., Harris, W. A., & Holt, C. E. (2000). Ephrin-B Regulates the Ipsilateral Routing of Retinal Axons at the Optic Chiasm. *Neuron*, 25(3), 599–610. Retrieved from [https://doi.org/10.1016/s0896-6273\(00\)81063-6](https://doi.org/10.1016/s0896-6273(00)81063-6)
- Nassi, J. J., & Callaway, E. M. (2009). Parallel processing strategies of the primate visual system. *Nature Reviews. Neuroscience*, 10(5), 360–72. Retrieved from <https://doi.org/10.1038/nrn2619>
- Nudo, R. J. (2013). Recovery after brain injury: mechanisms and principles. *Frontiers in human neuroscience*, 7, 887.
- Oppenheimer, D. R. (1968). Microscopic lesions in the brain following head injury. *Journal of Neurology, Neurosurgery & Psychiatry*, 31(4), 299–306. Retrieved from <https://doi.org/10.1136/jnnp.31.4.299>
- Osterhout, J. A., El-Danaf, R. N., Nguyen, P. L., & Huberman, A. D. (2014). Birthdate and outgrowth timing predict cellular mechanisms of axon target matching in the developing visual pathway. *Cell Reports*, 8(4), 1006–17. Retrieved from <https://doi.org/10.1016/j.celrep.2014.06.063>
- Padula, W. V., Argyris, S., & Ray, J. (1994). Visual evoked potentials (VEP) evaluating treatment for post-trauma vision syndrome (PTVS) in patients with traumatic brain injuries (TBI). *Brain Injury*, 8(2), 125–133. Retrieved from <https://doi.org/10.3109/02699059409150964>
- Papathanasopoulos, P., Konstantinou, D., Flaburiari, K., Bezerianos, A., Papadakis, N., & Papapetropoulos, T. (2008). Pattern Reversal Visual Evoked Potentials in Minor Head Injury. *European Neurology*, 34(5), 268–271. Retrieved from <https://doi.org/10.1159/000117054>

- Park, K. K., Liu, K., Hu, Y., Smith, P. D., Wang, C., Cai, B., ... & He, Z. (2008). Promoting axon regeneration in the adult CNS by modulation of the PTEN/mTOR pathway. *Science*, 322(5903), 963-966.
- Patel, V. C., Jurgens, C. W., Krahe, T. E., & Povlishock, J. T. (2016). Adaptive reorganization of retinogeniculate axon terminals in dorsal lateral geniculate nucleus following experimental mild traumatic brain injury. *Experimental Neurology*, 289, 85–95. Retrieved from <https://doi.org/10.1016/j.expneurol.2016.12.012>
- Pfeiffenberger, C., Cutforth, T., Woods, G., Yamada, J., Rentería, R. C., Copenhagen, D. R., ... & Feldheim, D. A. (2005). Ephrin-As and neural activity are required for eye-specific patterning during retinogeniculate mapping. *Nature neuroscience*, 8(8), 1022-1027.
- Pfeiffenberger, C., Yamada, J., & Feldheim, D. A. (2006). Ephrin-As and Patterned Retinal Activity Act Together in the Development of Topographic Maps in the Primary Visual System. *The Journal of Neuroscience*, 26(50), 12873–12884. Retrieved from <https://doi.org/10.1523/jneurosci.3595-06.2006>
- Piscopo, D. M., El-Danaf, R. N., Huberman, A. D., & Niell, C. M. (2013). Diverse visual features encoded in mouse lateral geniculate nucleus. *Journal of Neuroscience*, 33(11), 4642–4656. Retrieved from <https://doi.org/10.1523/JNEUROSCI.5187-12.2013>
- Pons, T. P., Garraghty, P. E., Ommaya, A. K., Kaas, J. H., Taub, E., & Mishkin, M. (1991). Massive cortical reorganization after sensory deafferentation in adult macaques. *Science*, 252(5014), 1857-1860.
- Povlishock, J. T. (1992). Traumatically induced axonal injury: pathogenesis and pathobiological implications. *Brain pathology (Zurich, Switzerland)*, 2(1), 1-12.
- Povlishock, J. T. (1993). Pathobiology of traumatically induced axonal injury in animals and man. *Annals of emergency medicine*, 22(6), 980-986.
- Povlishock, J., Becker, D., Cheng, C., & Vaughan, G. (1983). Axonal Change in Minor Head Injury. *Journal of Neuropathology & Experimental Neurology*, 42(3), 225. Retrieved from <https://doi.org/10.1097/00005072-198305000-00002>
- Povlishock, J., & Christman, C. (1995). The pathobiology of traumatically induced axonal injury in animals and humans: a review of current thoughts. Retrieved from <https://doi.org/10.1089/neu.1995.12.555>
- Povlishock, John T, & Katz, D. I. (2005). Update of Neuropathology and Neurological Recovery After Traumatic Brain Injury. *The Journal of Head Trauma Rehabilitation*. Retrieved from <https://doi.org/10.1097/00001199-200501000-00008>

- Povlishock, J T, & Becker, D. P. (1985). Fate of reactive axonal swellings induced by head injury. *Laboratory Investigation; a Journal of Technical Methods and Pathology*, 52(5), 540–52.
- Rasmusson, D. D., Turnbull, B. G., & Leech, C. K. (1985). Unexpected reorganization of somatosensory cortex in a raccoon with extensive forelimb loss. *Neuroscience letters*, 55(2), 167-172.
- Richards, L. G., Stewart, K. C., Woodbury, M. L., Senesac, C., & Cauraugh, J. H. (2008). Movement-dependent stroke recovery: A systematic review and meta-analysis of TMS and fMRI evidence. *Neuropsychologia*, 46(1), 3–11. Retrieved from <https://doi.org/10.1016/j.neuropsychologia.2007.08.013>
- Rimel, R. W., Giordani, B., Barth, J. T., Boll, T. J., & Jane, J. A. (1981). Disability caused by minor head injury. *Neurosurgery*, 9(3), 221-228.
- Rivlin-Etzion, M., Zhou, K., Wei, W., Elstrott, J., Nguyen, P. L., Barres, B. A., ... Feller, M. B. (2011). Transgenic mice reveal unexpected diversity of on-off direction-selective retinal ganglion cell subtypes and brain structures involved in motion processing. *The Journal of Neuroscience : The Official Journal of the Society for Neuroscience*, 31(24), 8760–9. Retrieved from <https://doi.org/10.1523/JNEUROSCI.0564-11.2011>
- Robertson, C. S., Valadka, A. B., Hannay, H. J., Contant, C. F., Gopinath, S. P., Cormio, M., ... & Grossman, R. G. (1999). Prevention of secondary ischemic insults after severe head injury. *Critical care medicine*, 27(10), 2086-2095.
- Roland, P. E., Meyer, E., Shibasaki, T., Yamamoto, Y. L., & Thompson, C. J. (1982). Regional cerebral blood flow changes in cortex and basal ganglia during voluntary movements in normal human volunteers. *Journal of Neurophysiology*, 48(2), 467–480. Retrieved from <https://doi.org/10.1152/jn.1982.48.2.467>
- Romero, J., Babikian, V. L., Katz, D. I., & Finklestein, S. P. (2006). Neuroprotection and Stroke Rehabilitation: Modulation and Enhancement of Recovery. *Behavioural Neurology*, 17(1), 17–24. Retrieved from <https://doi.org/10.1155/2006/137532>
- Roozenbeek, B., Maas, A., & Menon, D. (2013). Changing patterns in the epidemiology of traumatic brain injury. Retrieved from <https://doi.org/10.1038/nrneurol.2013.22>
- Rosenbaum, S. B., & Lipton, M. L. (2012). Embracing chaos: the scope and importance of clinical and pathological heterogeneity in mTBI. *Brain Imaging and Behavior*, 6(2), 255–282. Retrieved from <https://doi.org/10.1007/s11682-012-9162-7>
- Rose, T., & Bonhoeffer, T. (2018). Experience-dependent plasticity in the lateral geniculate nucleus. *Current Opinion in Neurobiology*, 53, 22–28. Retrieved from <https://doi.org/10.1016/j.conb.2018.04.016>

- Rossini, P. M., & Pauri, F. (2000). Neuromagnetic integrated methods tracking human brain mechanisms of sensorimotor areas 'plastic' reorganisation. *Brain Research Reviews*, 33(2–3), 131–154. Retrieved from [https://doi.org/10.1016/s0169-328x\(00\)00090-5](https://doi.org/10.1016/s0169-328x(00)00090-5)
- Salottolo, K., Carrick, M., Levy, A., & Morgan, B. (2017). The epidemiology, prognosis, and trends of severe traumatic brain injury with presenting Glasgow Coma Scale of 3.
- Sanes, J. R., & Masland, R. H. (2015). The Types of Retinal Ganglion Cells: Current Status and Implications for Neuronal Classification. *Annual Review of Neuroscience*. Retrieved from <https://doi.org/10.1146/annurev-neuro-071714-034120>
- Sanes, J., Suner, S., & Donoghue, J. (1990). Dynamic organization of primary motor cortex output to target muscles in adult rats I. Long-term patterns of reorganization following motor or mixed peripheral nerve lesions. *Experimental Brain Research*, 79(3), 479–491. Retrieved from <https://doi.org/10.1007/bf00229318>
- Sanes, J., Suner, S., Lando, J., & Donoghue, J. (1988). Rapid reorganization of adult rat motor cortex somatic representation patterns after motor nerve injury. *Proceedings of the National Academy of Sciences*, 85(6), 2003–2007. Retrieved from <https://doi.org/10.1073/pnas.85.6.2003>
- Scheid, R., Walther, K., Guthke, T., Preul, C., & Cramon, Y. D. von. (2006). Cognitive Sequelae of Diffuse Axonal Injury. *Archives of Neurology*, 63(3), 418–424. Retrieved from <https://doi.org/10.1001/archneur.63.3.418>
- Schlageter, K., Gray, B., Hall, K., Shaw, R., & Sammet, R. (1993). Incidence and treatment of visual dysfunction in traumatic brain injury. *Brain Injury*, 7(5), 439–448. Retrieved from <https://doi.org/10.3109/02699059309029687>
- Schneider, K. J., Iverson, G. L., Emery, C. A., McCrory, P., Herring, S. A., & Meeuwisse, W. H. (2013). The effects of rest and treatment following sport-related concussion: a systematic review of the literature. *British Journal of Sports Medicine*, 47(5), 304. Retrieved from <https://doi.org/10.1136/bjsports-2013-092190>
- Schuettauf, F., Naskar, R., Vorwerk, C. K., Zurakowski, D., & Dreyer, E. B. (2000). Ganglion cell loss after optic nerve crush mediated through AMPA-kainate and NMDA receptors. *Investigative ophthalmology & visual science*, 41(13), 4313–4316.
- Schüz, A., & Palm, G. (1989). Density of neurons and synapses in the cerebral cortex of the mouse. *Journal of Comparative Neurology*, 286(4), 442–455. Retrieved from <https://doi.org/10.1002/cne.902860404>
- Sabet, A. A., Christoforou, E., Zatlin, B., Genin, G. M., & Bayly, P. V. (2008). Deformation of the human brain induced by mild angular head acceleration. *Journal of biomechanics*, 41(2), 307–315.

- Sharp, D. J., Scott, G., & Leech, R. (2014). Network dysfunction after traumatic brain injury. *Nature Reviews Neurology*, 10(3), 156. Retrieved from <https://doi.org/10.1038/nrneurol.2014.15>
- Shenton, M., Hamoda, H., Schneiderman, J., Bouix, S., Pasternak, O., Rathi, Y., ... Zafonte, R. (2012). A review of magnetic resonance imaging and diffusion tensor imaging findings in mild traumatic brain injury. *Brain Imaging and Behavior*, 6(2), 137–192. Retrieved from <https://doi.org/10.1007/s11682-012-9156-5>
- Slobounov, S., Tutwiler, R., Sebastianelli, W., & Slobounov, E. (2006). ALTERATION OF POSTURAL RESPONSES TO VISUAL FIELD MOTION IN MILD TRAUMATIC BRAIN INJURY. *Neurosurgery*, 59(1), 134. Retrieved from <https://doi.org/10.1227/01.neu.0000243292.38695.2d>
- Smith, D. H., Hicks, R., & Povlishock, J. T. (2013). Therapy development for diffuse axonal injury. *Journal of Neurotrauma*, 30(5), 307–23. Retrieved from <https://doi.org/10.1089/neu.2012.2825>
- Smith, D. H., & Meaney, D. F. (2000). Axonal Damage in Traumatic Brain Injury. *The Neuroscientist*, 6(6), 483–495. Retrieved from <https://doi.org/10.1177/107385840000600611>
- Spiegel, D. P., Reynaud, A., Ruiz, T., Laguë-Beauvais, M., Hess, R., & Farivar, R. (2016). First- and second-order contrast sensitivity functions reveal disrupted visual processing following mild traumatic brain injury. *Vision Research*, 122, 43–50. Retrieved from <https://doi.org/10.1016/j.visres.2016.03.004>
- Stone, J., Singleton, R., & Povlishock, J. (2001). Intra-axonal neurofilament compaction does not evoke local axonal swelling in all traumatically injured axons. *Experimental Neurology*, 172(2), 320–31. Retrieved from <https://doi.org/10.1006/exnr.2001.7818>
- Strebel, S., Lam, A. M., Matta, B. F., & Newell, D. W. (1997). Impaired cerebral autoregulation after mild brain injury. *Surgical Neurology*, 47(2), 128–131. Retrieved from [https://doi.org/10.1016/s0090-3019\(96\)00459-4](https://doi.org/10.1016/s0090-3019(96)00459-4)
- Sugiyama, K., Kondo, T., Higano, S., Endo, M., Watanabe, H., Shindo, K., & Izumi, S.-I. (2007). Diffusion tensor imaging fiber tractography for evaluating diffuse axonal injury. *Brain Injury*, 21(4), 413–419. Retrieved from <https://doi.org/10.1080/02699050701311042>
- Sun, F., Park, K. K., Belin, S., Wang, D., Lu, T., Chen, G., ... & He, Z. (2011). Sustained axon regeneration induced by co-deletion of PTEN and SOCS3. *Nature*, 480(7377), 372–375.
- Thomas, T., Hinzman, J. M., Gerhardt, G. A., & Lifshitz, J. (2012). Hypersensitive Glutamate Signaling Correlates with the Development of Late-Onset Behavioral Morbidity in Diffuse Brain-Injured Circuitry. *Journal of Neurotrauma*, 29(2), 187–200. Retrieved from <https://doi.org/10.1089/neu.2011.2091>

- Thompson, H., & McCormick, W. (2006). Traumatic brain injury in older adults: epidemiology, outcomes, and future implications. Retrieved from <https://doi.org/10.1111/j.1532-5415.2006.00894.x>
- Thurman, D., Alverson, C., & Dunn, K. (1999). Traumatic brain injury in the United States: a public health perspective.
- Tierney, D. (1988). Visual dysfunction in closed head injury.
- Torborg, C. L., & Feller, M. B. (2004). Unbiased analysis of bulk axonal segregation patterns. *Journal of Neuroscience Methods*, 135(1–2), 17–26.
- Tzekov, R., Dawson, C., Orlando, M., Mouzon, B., Reed, J., Evans, J., ... & Crawford, F. (2016). Sub-chronic neuropathological and biochemical changes in mouse visual system after repetitive mild traumatic brain injury. *PloS one*, 11(4), e0153608.
- Tzekov, R., Quezada, A., Gautier, M., Biggins, D., Frances, C., Mouzon, B., ... Crawford, F. (2014). Repetitive mild traumatic brain injury causes optic nerve and retinal damage in a mouse model. *Journal of Neuropathology and Experimental Neurology*, 73(4), 345–61. Retrieved from <https://doi.org/10.1097/nen.000000000000059>
- Uesaka, N., Ruthazer, E. S., & Yamamoto, N. (2006). The role of neural activity in cortical axon branching. *The Neuroscientist*, 12(2), 102–106.
- Vascak, M., Jin, X., Jacobs, K. M., & Povlishock, J. T. (2017). Mild Traumatic Brain Injury Induces Structural and Functional Disconnection of Local Neocortical Inhibitory Networks via Parvalbumin Interneuron Diffuse Axonal Injury. *Cerebral Cortex (New York, N.Y. : 1991)*, 1–20. Retrieved from <https://doi.org/10.1093/cercor/bhx058>
- Vascak, M., Sun, J., Baer, M., Jacobs, K. M., & Povlishock, J. T. (2017). Mild Traumatic Brain Injury Evokes Pyramidal Neuron Axon Initial Segment Plasticity and Diffuse Presynaptic Inhibitory Terminal Loss. *Frontiers in Cellular Neuroscience*, 11, 157. Retrieved from <https://doi.org/10.3389/fncel.2017.00157>
- Vay, S. L., Wiesel, T. N., & Hubel, D. H. (1980). The development of ocular dominance columns in normal and visually deprived monkeys. *The Journal of Comparative Neurology*, 191(1), 1–51. Retrieved from <https://doi.org/10.1002/cne.901910102>
- Ventura, R. E., Balcer, L. J., & Galetta, S. L. (2014). The neuro-ophthalmology of head trauma. *The Lancet Neurology*, 13(10), 1006–1016. Retrieved from [https://doi.org/10.1016/s1474-4422\(14\)70111-5](https://doi.org/10.1016/s1474-4422(14)70111-5)
- Vos, P., Battistin, L., & Birbamer, G. (2002). EFNS guideline on mild traumatic brain injury: report of an EFNS task force. Retrieved from <https://doi.org/10.1046/j.1468-1331.2002.00407.x>

- Wang, H., & Zhang, Z. (2008). A critical window for experience-dependent plasticity at whisker sensory relay synapse in the thalamus. *The Journal of Neuroscience : The Official Journal of the Society for Neuroscience*, 28(50), 13621–8. Retrieved from <https://doi.org/10.1523/jneurosci.4785-08.2008>
- Wang, J., Fox, M. A., & Povlishock, J. T. (2013). Diffuse traumatic axonal injury in the optic nerve does not elicit retinal ganglion cell loss. *Journal of Neuropathology and Experimental Neurology*, 72(8), 768–81. Retrieved from <https://doi.org/10.1097/NEN.0b013e31829d8d9d>
- Wang, J., Hamm, R. J., & Povlishock, J. T. (2011). Traumatic Axonal Injury in the Optic Nerve: Evidence for Axonal Swelling, Disconnection, Dieback, and Reorganization. *Journal of Neurotrauma*, 28(7), 1185–1198. Retrieved from <https://doi.org/10.1089/neu.2011.1756>
- Weber, A. J., Viswanáthan, S., Ramanathan, C., & Harman, C. D. (2010). Combined application of BDNF to the eye and brain enhances ganglion cell survival and function in the cat after optic nerve injury. *Investigative ophthalmology & visual science*, 51(1), 327-334.
- Whitt, J., Petrus, E., & Neuropharmacology, L.-H. (2014). Experience-dependent homeostatic synaptic plasticity in neocortex.
- Wiegert, J. S., & Oertner, T. G. (2013). Long-term depression triggers the selective elimination of weakly integrated synapses. *Proceedings of the National Academy of Sciences*, 110(47), E4510-E4519.
- Wilkinson, F., James, T. W., Wilson, H. R., Gati, J. S., Menon, R. S., & Goodale, M. A. (2000). An fMRI study of the selective activation of human extrastriate form vision areas by radial and concentric gratings. *Current Biology*, 10(22), 1455–1458.
- Wolf, J. A., & Koch, P. F. (2016). Disruption of Network Synchrony and Cognitive Dysfunction After Traumatic Brain Injury. *Frontiers in Systems Neuroscience*, 10, 43. Retrieved from <https://doi.org/10.3389/fnsys.2016.00043>
- Wolf, J. A., Stys, P. K., Lusardi, T., Meaney, D., & Smith, D. H. (2001). Traumatic axonal injury induces calcium influx modulated by tetrodotoxin-sensitive sodium channels. *Journal of Neuroscience*, 21(6), 1923–1930.
- Wozniak, J. R., Krach, L., Ward, E., Mueller, B. A., Muetzel, R., Schnoebelen, S., ... & Lim, K. O. (2007). Neurocognitive and neuroimaging correlates of pediatric traumatic brain injury: a diffusion tensor imaging (DTI) study. *Archives of Clinical Neuropsychology*, 22(5), 555-568. Retrieved from <https://doi.org/10.1016/j.acn.2007.03.004>
- Wu, C., & Kaas, J. H. (1999). Reorganization in Primary Motor Cortex of Primates with Long-Standing Therapeutic Amputations. *Journal of Neuroscience*, 19(17), 7679–7697. Retrieved from <https://doi.org/10.1523/jneurosci.19-17-07679.1999>

- Xu, X., Ichida, J. M., Allison, J. D., Boyd, J. D., Bonds, A. B., & Casagrande, V. A. (2001). A comparison of koniocellular, magnocellular and parvocellular receptive field properties in the lateral geniculate nucleus of the owl monkey (*Aotus trivirgatus*). *The Journal of Physiology*, 531(1), 203–218. Retrieved from <https://doi.org/10.1111/j.1469-7793.2001.0203j.x>
- Yadav, N. K., & Ciuffreda, K. J. (2014). Objective assessment of visual attention in mild traumatic brain injury (mTBI) using visual-evoked potentials (VEP). *Brain Injury*, 29(3), 352–365. Retrieved from <https://doi.org/10.3109/02699052.2014.979229>
- Yadav, N. K., Thiagarajan, P., & Ciuffreda, K. J. (2014). Effect of oculomotor vision rehabilitation on the visual-evoked potential and visual attention in mild traumatic brain injury. *Brain Injury*, 28(7), 922–929. Retrieved from <https://doi.org/10.3109/02699052.2014.887227>
- Yadav, N., Thiagarajan, P., & Ciuffreda, K. (n.d.). Effect of Oculomotor Vision Rehabilitation (OVR) on Visual Evoked Potential (VEP) Responses and Visual Attention in Mild Traumatic Brain Injury (mTBI).
- Yamahachi, H., Marik, S. A., McManus, J. N. J., Denk, W., & Gilbert, C. D. (2009). Rapid axonal sprouting and pruning accompany functional reorganization in primary visual cortex. *Neuron*, 64(5), 719–29. Retrieved from <https://doi.org/10.1016/j.neuron.2009.11.026>
- Yoles, E., & Schwartz, M. (1998). Degeneration of spared axons following partial white matter lesion: implications for optic nerve neuropathies. *Experimental neurology*, 153(1), 1-7.
- Young, T. R., Bourke, M., Zhou, X., Oohashi, T., Sawatari, A., Fässler, R., & Leamey, C. A. (2013). Ten-m2 is required for the generation of binocular visual circuits. *The Journal of Neuroscience : The Official Journal of the Society for Neuroscience*, 33(30), 12490–509. Retrieved from <https://doi.org/10.1523/JNEUROSCI.4708-12.2013>
- Zeneroli, M., Pinelli, G., Gollini, G., Penne, A., Messori, E., Zani, G., & Ventura, E. (1984). Visual evoked potential: a diagnostic tool for the assessment of hepatic encephalopathy. *Gut*, 25(3), 291–9.
- Zenke, F., & Gerstner, W. (2017). Hebbian plasticity requires compensatory processes on multiple timescales. *Philosophical Transactions of the Royal Society B: Biological Sciences*, 372(1715), 20160259.
- Zhang, K., Johnson, B., Pennell, D., Ray, W., Sebastianelli, W., & Slobounov, S. (2010). Are functional deficits in concussed individuals consistent with white matter structural alterations: combined FMRI & DTI study. *Experimental Brain Research*, 204(1), 57–70. Retrieved from <https://doi.org/10.1007/s00221-010-2294-3>
- Ziburkus, J., & Guido, W. (2006). Loss of binocular responses and reduced retinal convergence during the period of retinogeniculate axon segregation. *Journal of neurophysiology*, 96(5), 2775-2784.



Ziemann, U., Hallett, M., & Cohen, L. (1998). Mechanisms of deafferentation-induced plasticity in human motor cortex.

Zucker, R. S., & Regehr, W. G. (2002). SHORT-TERM SYNAPTIC PLASTICITY. *Annual Review of Physiology*, 64(1), 355–405. Retrieved from <https://doi.org/10.1146/annurev.physiol.64.092501.114547>